

WL-TR-93-2041

AD-A271 932



2

ADVANCED SURVIVABLE RADIATOR  
DEVELOPMENT PROGRAM



R.E.DRUBKA, J.B.BLACKMAN, G.W.GLOVER,  
D.L.JOHNSON, J.KIRBY

MCDONNELL DOUGLAS AEROSPACE  
5301 BOLSA AVE.  
HUNTINGTON BEACH CA 92647

MAR 1993

FINAL REPORT

APPROVED FOR PUBLIC RELEASE; DISTRIBUTION IS UNLIMITED.



AEROPROPULSION AND POWER DIRECTORATE  
WRIGHT LABORATORY  
AIR FORCE MATERIEL COMMAND  
WRIGHT PATTERSON AFB OH 45433-7650

93-26606



102-71

93 11 2 032


**Best  
Available  
Copy**

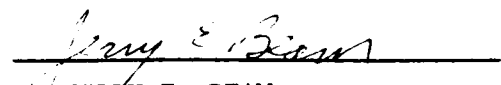
## NOTICE

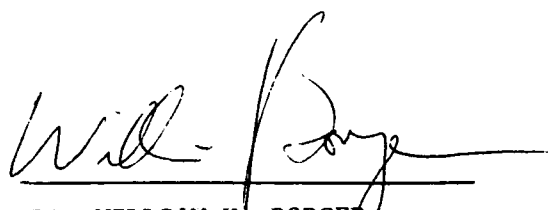
When Government drawings, specifications, or other data are used for any purpose other than in connection with a definitely Government-related procurement, the United States Government incurs no responsibility or any obligation whatsoever. The fact that the government may have formulated or in any way supplied the said drawings, specifications, or other data, is not to be regarded by implication, or otherwise in any manner construed, as licensing the holder, or any other person or corporation; or as conveying any rights or permission to manufacture, use, or sell any patented invention that may in any way be related thereto.

This report is releasable to the National Technical Information Service (NTIS). At NTIS, it will be available to the general public, including foreign nations.

This technical report has been reviewed and is approved for publication.

  
MICHEAL J. MORGAN  
Thermal Technology Section  
Power Technology Branch

  
JERRY E. BEAM  
Section Chief, Thermal Tech Section  
Power Technology Branch

  
DR. WILLIAM U. BORGER  
Division Chief  
Aerospace Power Division

If your address has changed, if you wish to be removed from our mailing list, or if the addressee is no longer employed by your organization please notify WL/POOS, WPAFB, OH 45433- 7251 to help us maintain a current mailing list.

Copies of this report should not be returned unless return is required by security considerations, contractual obligations, or notice on a specific document.

REPORT DOCUMENTATION PAGE			Form Approved OMB No. 0704-0188	
<small>1. This report is the collection of information estimated to average 1 hour per response, including the time for reviewing instructions, searching existing data sources, gathering the data needed, and completing and reviewing this collection of information. Send comments regarding this burden estimate or any other aspect of this collection of information, including suggestions for reducing this burden, to Washington Headquarters Services, Directorate for Information Operations and Reports, 1215 Jefferson Davis Highway, Suite 1204, Arlington, VA 22202-4302, and to the Office of Management and Budget, Paperwork Reduction Project (0704-0188), Washington, DC 20503.</small>				
1. AGENCY USE ONLY (Leave blank)		2. REPORT DATE March 1993		3. REPORT TYPE AND DATES COVERED Final Feb 90 - Mar 93
4. TITLE AND SUBTITLE  Advanced Survivable Radiator Development Program			5. FUNDING NUMBERS  C-F33615-90-C-2044 PE-63218C PR-L215 TA-00 WU-11	
6. AUTHOR(S) Dr. R.E. Drubka, Dr. J.B. Blackman G.W. Glover, D.L. Johnson, Dr. J. Kirby				
7. PERFORMING ORGANIZATION NAME(S) AND ADDRESS(ES) McDonnell Douglas Aerospace 5301 Bolsa Ave. Huntington Beach CA 92647			8. PERFORMING ORGANIZATION REPORT NUMBER	
9. SPONSORING / MONITORING AGENCY NAME(S) AND ADDRESS(ES) Aero Propulsion and Power Directorate Wright Laboratory Air Force Materiel Command Wright Patterson AFB OH 45433-7650			10. SPONSORING / MONITORING AGENCY REPORT NUMBER  WL-TR-93-2041	
11. SUPPLEMENTARY NOTES				
12a. DISTRIBUTION / AVAILABILITY STATEMENT  Approved for Public Release; distribution is unlimited.			12b. DISTRIBUTION CODE	
13. ABSTRACT (Maximum 200 words)  <p>The objective of the program was to analyze, develop, and test an advanced space radiator which would reject waste heat and also survive both the natural environment and the environments for multiple hostile threats.</p> <p>This program defined two phases of work consisting of six tasks in Phase 1 and eight tasks in Phase 2. The purpose of Phase 1 was to assess the feasibility of the ASR approach. Phase 1 planned to evaluate and develop design options through an iterative process of design, analysis, and test. The purpose of Phase 2 was to design, fabricate, and test prototype radiators consisting of heat pipes integrated into the ASR concept. This phase planned to conduct thermal performance and survivability tests on these prototypes to establish the suitability of the ASR for application to near term AF and SDI systems.</p> <p>Because of funding limitations, all activities were terminated following the first task of Phase 1. This task consisted of the analysis and design tradeoff efforts required to determine performance requirements for the ASR. MDSS successfully completed these efforts.</p>				
14. SUBJECT TERMS  Radiator, heat pipe, survivable, hardening, threat, thermal			15. NUMBER OF PAGES 99	
			16. PRICE CODE	
17. SECURITY CLASSIFICATION OF REPORT  UNCLASSIFIED	18. SECURITY CLASSIFICATION OF THIS PAGE  UNCLASSIFIED	19. SECURITY CLASSIFICATION OF ABSTRACT  UNCLASSIFIED	20. LIMITATION OF ABSTRACT  UL	

---

## **TABLE OF CONTENTS**

---

<b>Section</b>	<b>Page</b>
List of Figures .....	iv
List of Tables .....	vi
Forward .....	vii
<b>1 INTRODUCTION</b>	
1.1 Background .....	1-1
1.2 ASR Concept .....	1-1
1.3 ASR Program .....	1-6
<b>2 BACKGROUND</b>	
2.1 System Description .....	2-1
2.1.1 Requirements For SDIO Satellite Hardening .....	2-2
2.1.2 Brilliant Pebbles Design .....	2-3
2.1.3 Brilliant Eyes Design .....	2-6
2.2 Natural Environments .....	2-10
2.3 Functional Description of Radiators .....	2-13
<b>3 ANALYSIS TOOLS</b>	
3.1 Model Assumptions and Capabilities .....	3-1
3.2 Modeling Details .....	3-2
3.2.1 Monte-Carlo Simulation .....	3-3
3.2.2 Fiber Temperature Profile .....	3-7
3.2.3 System Heat Balance .....	3-8
3.3 Model Verification .....	3-9
<b>4 RESULTS</b>	
4.1 ASR Surface Geometry .....	4-1
4.2 Requirements .....	4-2
4.3 Thermal Performance .....	4-3
4.4 Performance Under Direct Irradiation .....	4-7
4.5 Response to a Laser Threat .....	4-16
4.6 Nuclear Environment .....	4-22
4.7 Fiber Options .....	4-22
4.8 The ASR Feasibility Design Space .....	4-24
<b>5 CONCLUSIONS</b> .....	5-1
<b>6 REFERENCES</b> .....	6-1
Appendix A - Program Statement of Work .....	A-1
Appendix B - Fiber Data Sheets .....	B-1

## **TABLE OF CONTENTS**

<b>Section</b>	<b>Page</b>
Glossary .....	GL-1
1-1 Nylon ASR Sample Fielded In Recent Underground	
Test Demonstrates Low $\alpha\epsilon$ .....	1-2
1-2 The Advanced Survivable Radiator (ASR) Concept .....	1-3
1-3 The ASR Program Plan .....	1-7
2-1 Brilliant Pebbles and Brilliant Eyes Provide	
Cost Effective Difference .....	2-2
2-2 Schematic of Brilliant Pebbles Satellite .....	2-4
2-3 Radiator Plate Showing Locations of Attached	
Heat Dissipating Components .....	2-5
2-4 Brilliant Eyes .....	2-7
2-5 Sensor Isometric View .....	2-8
2-6 Scatter From Particulates Dominates Clean Mirror	
Scatter in the IR. ....	2-8
2-7 Particle Blowoff Increases Stray Light Power .....	2-9
3-1 Simplified Flow Chart of the FURRAD .....	3-3
3-2 Monte-Carlo Geometric Concepts .....	3-4
3-3 Monte-Carlo Computational Cell. ....	3-4
3-4 Calculated Energy Absorption Profile of the ASR	
Carpet for a Hemispherical Source. ....	3-5
3-5 Volume Scattering Model Using Escape Probability	
Function for Current Photon Path. ....	3-7
3-6 ASR System Net Heat Balance. ....	3-9
3-7 Representative Test Coupons .....	3-10
3-8 FURRAD Prediction Compared to Test Data	
for Gold Pins with White Base Material .....	3-11
4-1 Fiber Geometry Characteristics .....	4-1
4-2 Contour Plots Showing ASR Effective Emissivity	
for Thermal Conductivities of 100 W/m-k. For both plots	
the radiator base temperature is 400K. ....	4-4
4-3 Contour Plots Showing ASR Effective Emissivity	
Changes for Thermal Conductivities of 1 W/m-k (top) and	
0.1 W/m-k (bottom) .....	4-5

## LIST OF FIGURES

<u>Number</u>	<u>Title</u>	<u>Page</u>
4-4	Plot of FURRAD Results Showing the Scaling Law for Emissivity Enhancement .....	4-7
4-5	Effect of ASR Absorptivity and Operating Temperature on Radiator Area .....	4-8
4-6	Contour Plots Showing the Effect of Solar Flux on ASR Performance .....	4-9
4-7	Emissivity and Absorptivity of ASR System Relative to that of Standard Radiator .....	4-11
4-8	Plots Showing that as the Material Emissivity is Increased, the Effects of Surface Geometry Tend to Diminish the Overall Emissivity .....	4-12
4-9	Effect of Fiber Density and Base Temperature on the Ratio of Heat Rejected by the ASR Relative To A Standard Radiator .....	4-13
4-10	Area Enhancement As A Function Of ASR Geometry .....	4-14
4-11	Effects Of Fiber Conductivity on Both the Temperature Profile and the Emissivity Enhancement Ratio .....	4-15
4-12	Effect of Partially Transmissive Fiber Bundles on ASR Absorptance .....	4-16
4-13	Laser Response Model .....	4-17
4-14	Impact of Laser Intensity on Radiator Temperature .....	4-18
4-15	Fiber Material Options .....	4-19
4-16	Qualitative ASR Feasibility Design Space .....	4-24

THIS QUALITY INSPECTED 5

Accession For	
NTIS GRA&I	<input checked="" type="checkbox"/>
DTIC TAB	<input type="checkbox"/>
Unannounced	<input type="checkbox"/>
Justification	
By	
Distribution/	
Availability Codes	
Dist	Avail and/or Special
A-1	

---

## ***LIST OF FIGURES***

---

<b><u>Number</u></b>	<b><u>Title</u></b>	<b><u>Page</u></b>
2-1	The Space Environment has a Number of Negative. . . . . Effects on Spacecraft Materials	2-11
2-2	Experience in Spacecraft Design Provides Guidelines. . . . . for the Use of Materials	2-13
4-1	ASR Operating Requirements . . . . .	4-2
4-2	Viable Fiber Options Which Meet the SUPER . . . . . Laser Requirements	4-23



## **FOREWORD**

The McDonnell Douglas Space Systems Company (MDSSC) has assembled this report, prepared under contract F33615-90-C-2044, with the Aero Propulsion and Power Directorate, Wright Laboratory as the sponsoring agency. Members of the Advanced Power Group of the Engineering and Technology Center carried out the work. This final report is prepared in accordance with Contract Data Requirements List (CDRL) Sequence Number 6.

The objective of the program was to analyze, develop, and test an advanced space radiator which would reject waste heat and also survive both the natural environment and the environments for multiple hostile threats.

This program defined two phases of work consisting of six tasks in Phase 1 and eight tasks in Phase 2. The purpose of Phase 1 was to assess the feasibility of the ASR approach. Phase 1 planned to evaluate and develop design options through an iterative process of design, analysis, and test. The purpose of Phase 2 was to design, fabricate, and test prototype radiators consisting of heat pipes integrated into the ASR concept. This phase planned to conduct thermal performance and survivability tests on these prototypes to establish the suitability of the ASR for application to near term AF and SDI systems.

Because of funding limitations, all activities were terminated following the first task of Phase 1 and the current Brilliant Eyes architecture and design is not accurately reflected in this report. This task consisted of the analysis and design tradeoff efforts required to determine performance requirements for the ASR. MDSS successfully completed these efforts.

MDSSC technical personnel contributing to the ASR program include Dr. R. E. Drubka, Dr. J. B. Blackmon, G. W. Glover, D. L. Johnson, Dr. J. Kirby, S. M. Kusek, and O. K. Salmassy.



## **1. INTRODUCTION**

### **1.1 Background**

Near term Air Force and Strategic Defense Initiative (SDI) systems must reject thermal loads up to 100 kW at temperatures of 300 K to 400 K. Because of the nature of their mission, these systems must survive both natural and hostile threats. The natural threats include radiation and space debris effects while hostile threats include ground based and space based lasers, nuclear effects, and various kinetic energy weapons. Efficient radiators, which can reject these thermal loads, survive these threats, and are low mass, are required.

Efficient heat rejection requires that the radiator have good thermal coupling with the space sink environment, which implies the radiator should have high infrared emissivity, low solar absorptivity, and high thermal conductance throughout. Additionally, the radiator must be highly reliable (no single point failures), have a low stowage volume for launch, withstand high g launch loads and maneuvers, and satisfy specific platform interface requirements. Current radiator designs for the power levels of interest use either pumped loops or heat pipe radiators to achieve a uniform radiator temperature. Pumped loop radiators are simpler and may be less massive, but for long duration missions, the inherent redundancy of a heat pipe radiator makes it more reliable.

### **1.2 ASR Concept**

The Advanced Survivable Material (ASM) concept refers to an external surface fabricated in a brush or carpet configuration using a range of fiber material options and fabrication techniques. An example of this surface is highlighted in Figure 1-1. Recent underground tests demonstrated that special features associated with the ASM approach were responsible for unprecedented reduction in blow off impulse from x-rays. Work performed under MDSSC IRAD evaluated the survivability mechanisms associated with the ASM approach. The ASM geometry also provides a standoff distance for hypervelocity impact of micrometeoroids and small space debris/dust



Figure 1-1. Nylon ASR Sample Fielded In Recent Underground Test Demonstrates Low  $\alpha/e$

particles and enhances compliance and attenuation of impulse loads generated from particle impacts. ASM configurations employing fibers with protective metal coatings offers enhanced protection to atomic oxygen attack, as well as enhanced nuclear and laser survivability. As part of this effort, potential system applications of the ASM concept were identified: hardened radiators and optical baffles. Use of the ASM to create a hardened radiator is denoted ASR (advanced survivable radiator). Initial analyses indicated that this material not only offered high inherent survivability, but also effective thermal performance. The high survivability of this material, coupled with its effective thermal transport characteristics, could offer a significantly lower overall radiator system mass than a conventional shielded radiator system designed for the same threat levels.

The basic concept of the ASR involves the use of the ASM as an outer protective covering for a radiating surface. The ASR concept uses a brush or carpet configuration and can be constructed from a range of materials. Material options and typical radiator configurations using the ASR are described in Figure 1-2. The ASR material can either be retrofitted to a standard radiator surface or can be integrated

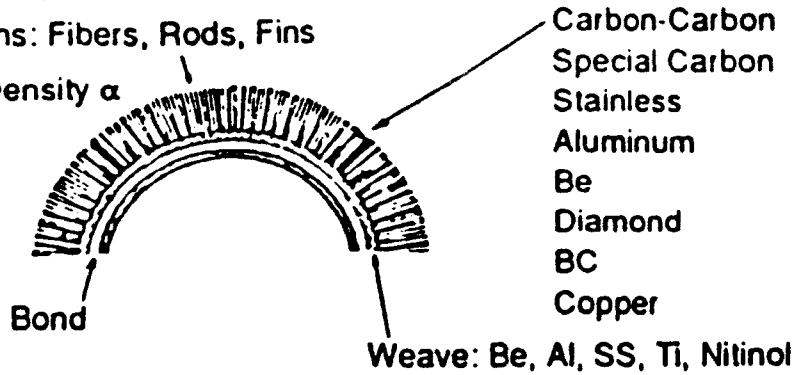
### Material Choices

Numerous ASR material options exist:

Optimum choice dependent on mission, operational requirements, and threat environment

Configurations: Fibers, Rods, Fins

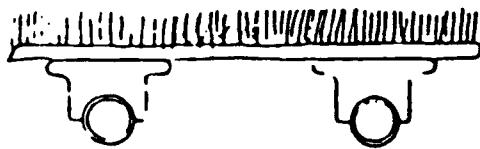
Fiber Area Density  $\alpha$



Configurations: Low Z or High Z, depending on survivability level and type of hostile threat

### Typical Heat Pipe Radiator Configuration Options

Armored Heat Pipe/Fin With ASR



- Easy to retro-fit onto typical armored heat pipe designs to enhance performance

Clustered Heat Pipes With ASR



- Emissivity increased by fiber geometry
- High emissivity retained with substantial loss or damage to fibers

Finned Heat Pipes With ASR



Figure 1-2. The Advanced Survivable Radiator (ASR) Concept

directly with a radiator surface, for example, with the heat pipe itself. In the first approach, the material backing is simply brazed or bonded to the radiating surface with the fibers facing outward. The integral approach offers increased fiber packing density and lower overall system mass.

The feasibility of using ASR as a survivable radiator covering depends not only on its survivability capabilities, but also its impact on radiator thermal performance. An optimal ASR configuration is one which meets anticipated survivability requirements and maintains or enhances radiator thermal performance while minimizing radiator mass. Our precontract efforts indicated that proper selection and application of ASR enhanced radiator thermal performance under normal operating conditions. From this model, the ratio of heat transfer from a radiator with and without ASR is approximated by:

$$\frac{Q_{ASR}}{Q} = \frac{\epsilon_{ASR}}{\epsilon} f(\text{geometry}) \eta \left[ 1 - \frac{\delta T}{T} \right]^4$$

where  $\epsilon_{ASR}$  is the effective emissivity of the ASR surface,  $\epsilon$  is the emissivity of the bare radiator surface,  $\eta$  is an effective fin efficiency of the ASR fibers, and  $\delta T$  is an effective temperature drop from the radiator surface to the base of the fibers.

Four factors govern the impact of ASR on thermal performance: emissivity ratio, geometric effects, effective fin efficiency of the fibers, and thermal characteristics of the ASR weave material and attachment technique. The first two factors act to enhance radiator thermal performance while the latter two act to degrade performance. The net effect on radiator thermal performance can be estimated qualitatively prior to a detailed thermal analysis by closer examinations of each of these factors and bracketing their anticipated range.

The ASR surface can be considered to be comprised of numerous small cavities. Multiple reflections within a cavity act to enhance the emissive power of the cavity relative to that of a plane surface of identical temperature and emittance stretched across its opening. For the fiber densities, fiber materials, and fiber length to diameter ratios under consideration, effective ASR emissivities near unity should be achievable using materials of substantially lower intrinsic emissivity. This gives rise to an effective

emissivity ratio in Equation (1), larger than one and indicates increased thermal performance. Under precontract IRAD activities, effective ASR emissivities near unity were measured for various carbon fiber and steel fiber samples.

Spacecraft are designed to have the solar absorptivity and infrared emissivity of their thermal control surfaces in a specific range. For radiator applications where it is important to radiate as much heat as possible to space while absorbing as little solar radiation as possible, a low  $\alpha/\epsilon$  ratio, on the order of 0.2 or less, is desirable. Higher values of  $\alpha/\epsilon$  are acceptable as the radiator temperature increases.

The geometric effects observed in the above equation arise from an increase in effective radiation area when ASR is applied to nonplanar surfaces. For example, the effective increase in heat transport for a cylindrical geometry is :

$$f(\text{geometry}) = (1 + 2L/D)$$

where L is the fiber length and D is the cylinder diameter. For a 1-inch diameter heat pipe covered with a 1/2-inch layer of ASR,  $f(\text{geometry}) = 2$ . This improvement is reduced when the radiation view factor between pipes is high. Future detailed thermal models will include these geometric effects.

Fiber fin efficiency and bonding resistance act to decrease ASR thermal efficiency. The functional dependence of fin efficiency will result from a detailed ASR thermal model. However, from simple extended fin radiator studies, efficiency can be maximized with high-conductivity fibers, optimized fiber lengths, and low to moderate radiator temperatures.

An important issue will be to minimize the thermal resistance between the radiator surface and the base of the fibers. This includes the contact resistance associated with the attachment technique along with the conduction through the weave material. This factor is particularly important because of the fourth-power dependency of the effective temperature drop across the ASR radiator interface.

### **1.3 ASR Program**

The objective of this program is to develop and test a prototype survivable radiator based on the unique properties of the ASR surface material concept, starting with system level requirements on thermal performance, nuclear survivability, laser survivability, KEW survivability, and natural environments survivability. This program attempts to push survivability, reliability, and performance goals to the highest level. All aspects of this program were to include direct coordination between the potential users within the SDI Space Programs Office, WRDC, and the senior technical personnel directly involved with this contract. The ASR heat pipe radiator concept to be developed on this program could protect near term SDI systems to unprecedented levels of multiple hostile threats while at the same time improve the thermal performance of the radiator.

The program plan, discussed in Appendix A and shown schematically in Figure 1-3, defines the two phase effort to develop the ASR. In Phase 1, the feasibility of the ASR was established. Design options were evaluated and developed through an iterative process of design, analysis, and test. During Phase 2, prototype radiators consisting of heat pipes integrated into the ASR concept were designed, fabricated, and tested. Final detailed designs were developed, and several prototype radiators fabricated. Thermal performance and survivability tests on these prototypes were conducted to establish the suitability of the ASR for application to near term AF and SDI systems. The program was terminated prior to completion of the Phase 1 effort due to funding limitations. At the time of termination, Task 1.1 (Trade Studies) was completed and Task 1.2 (Characterization Tests) was initiated. The results of this activity are described in Section 4.



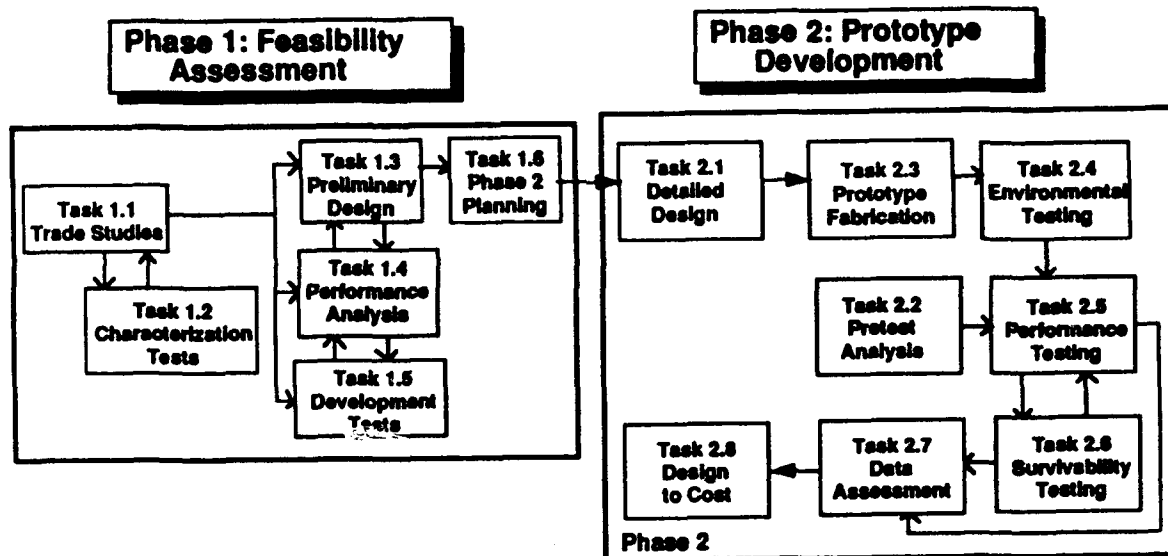


Figure 1-3. The ASR Program Plan

## **2. BACKGROUND**

An understanding of system and component level requirements is needed to guide the development of concepts based on the ASR surface coating. This chapter presents a system that is the most likely user of this technology and the requirements imposed from a system level.

### **2.1 System Description**

In order to counter ICBM and SLBM threats, SDIO is evolving a defense system based upon four major satellite types: a geosynchronous orbiting satellite for launch detection, a communications satellite for control and command of the entire system, a low Earth orbit surveillance/interception (Brilliant Pebbles) satellite, and low Earth orbit discriminator (Brilliant Eyes) satellite, see Figure 2-1. The system is credible because it reduces threat leakage to low enough levels to deter a first-strike threat. Using the benefits of mass production of lightweight, low-cost satellites, the system is also affordable.

The launch of an attack is first detected by the ground-launch detection satellite in geosynchronous orbit. Using sensors that stare directly down, the launch of any rocket booster is detected as soon as it cleared any cloud cover. The launch information is transferred to the command authority and the Brilliant Pebble satellites through a relay communications satellite. In addition to the launch detection capability of the geosynchronous satellite, a portion of the Brilliant Pebble satellites performs ground surveillance. If the decision is made that the launch is part of an attack, the command is sent to the Brilliant Pebbles satellites to intercept and destroy the boosters. The kill rate is expected to be high because of the large number of Brilliant Pebble satellites deployed. Although many of the launch boosters are destroyed during boost phase, some survive if a massive launch scheme is used or countermeasures against Brilliant Pebbles are employed.

Any booster not destroyed during boost phase presents a problem to Brilliant Pebbles. The sensors employed by Brilliant Pebbles are adequate to view any object. But any reasonable threat would include decoys, against which the Brilliant Pebbles could not discriminate. To assist the Brilliant Pebble interceptor in the midcourse and terminal defense phase, the final

set of satellites, i.e., Brilliant Eyes, is used to determine which objects are decoys and which are armed reentry vehicles. The technology required to discriminate such targets is currently under development and most likely employ a cooled IR sensor similar to that now being developed by MDSS.

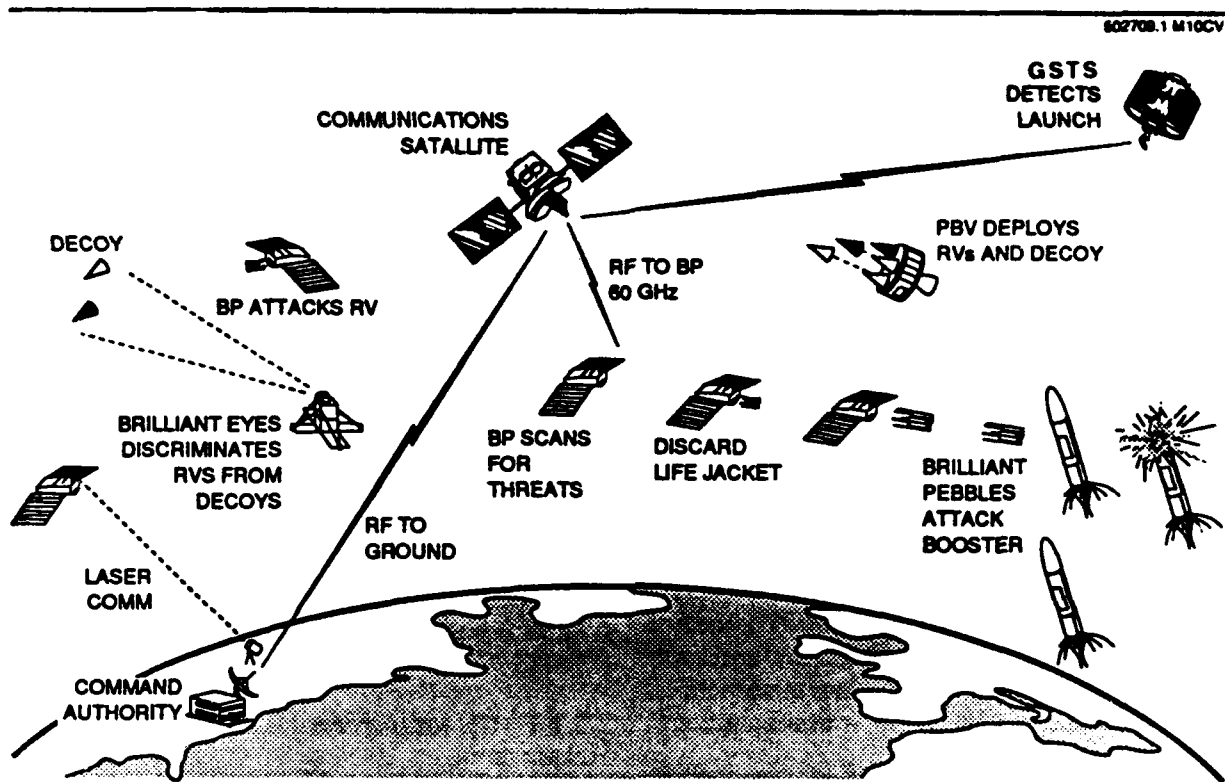


Figure 2-1. Brilliant Pebbles and Brilliant Eyes Provide Cost Effective Deterrence

### 2.1.1 Requirements for SDIO Satellite Hardening

A potential threat to the space-based defense system is the employment of weapons by the offense. The most credible threats to the space-based defense include nuclear weapons, which are attractive because of their relatively low cost and very large kill radius. ASATs and ground-based lasers could also be employed, but the cost effectiveness of ASAT (i.e., use of a single, expensive booster to kill a single low-cost satellite) is questionable. Because the sensors on low-orbital satellites do not stare directly down, a ground-based photon weapon would not directly illuminate the sensitive detectors with sufficient energy to cause damage. The ground based threat could illuminate part of the sunshade/baffle of the telescope. The required hardness levels of a geosynchronous satellite might not be significantly different from

current generation satellites. It would take a long time for a ground-based nuclear or ASAT weapon to reach the geosynchronous satellite. Decoys and other countermeasures could be employed to defeat these threats. Due to the long distance to geosynchronous altitude, the irradiance levels produced by a ground-based laser would be low, i.e., on the order of irradiance levels for which SMATH and ASSH have already demonstrated hardening techniques.

Survivability for the low-Earth orbiting satellites is achieved through two main techniques; total number of satellites deployed and passive countermeasures. Destruction of a single Brilliant Pebble satellite would reduce overall system effectiveness by only a small amount. The effectiveness of 1-on-1 kill is reduced because of the low-deployment cost of a Brilliant Pebble satellite, estimated at \$1,000,000 per deployed satellite. Because of the large number of satellites, measures to passively countermeasure the threat through hardening and use of intrinsically harder components are worth pursuing to deny a 2-on-1 or higher kill ratio. Since there are fewer Brilliant Eyes satellites and the sensor cost is high, the hardness requirement for this class of satellites is also expected to be higher. In both cases, the hardness levels for both nuclear and ground-based laser threats are significantly higher than for current systems.

### **2.1.2 Brilliant Pebbles Design**

To determine achievable hardness level, a detailed description of the systems is required. Figure 2-2 shows a schematic for the Brilliant Pebble satellite. To achieve a low deployment cost, the design uses minimum weight techniques. The satellite consists of two parts: the interceptor, which contains only those items necessary to attack its target, and a life jacket, which contains all other components. The list of components on the interceptor include:

- Stage rocket with associated fuel tanks
- Computer for guidance
- Sensors needed for guidance - UV, IR, star tracker, and Lidar(U) The mass of the interceptor is kept low in order to maximize the velocity achieved by the interceptor. All functions not needed for guidance to target impact are jettisoned with the life jacket. These components include:
  - Periscope assembly to allow use of the UV and IR sensors on interceptors for surveillance
  - A cryogenic cooler to allow use of the interceptor IR sensors for surveillance
  - Solar power panels
  - System radiator
  - Laser communications
  - RF communications

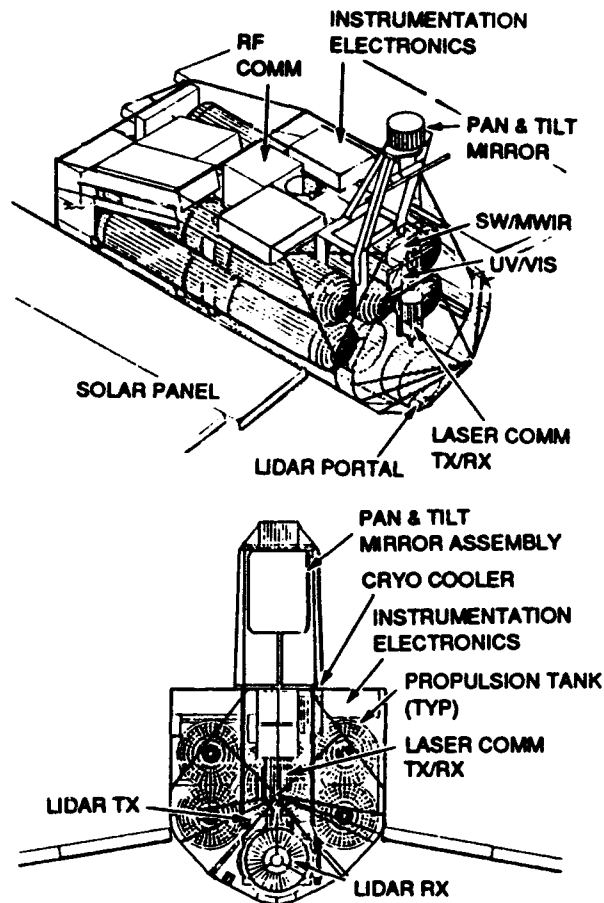


**Figure 2-2 Schematic of Brilliant Pebbles Satellite**

To reduce weight, save cost and simplify the operation, the external mirror is not baffled. The shroud provides some threat protection for all internal components and launch handling. The star tracker, the tilt and pan mirror, and the radiators on top of the shroud are directly susceptible to nuclear threats. Their placement at the top of the Brilliant Pebble precludes their attack by a ground-based laser threat.

There is one radiator for Brilliant Pebbles, see Figure 2-3. It is designed to dissipate the heat generated by the electronic components. The design technique is to simply mount all of the electronics on a common plate that would also serve as the radiator. The power dissipation needs of the electronics are small, and the weight tradeoffs might show that this simple

technique is both cost and weight effective, as shown in the figure. A separate cryo cooler is used to keep the helium cooled to cryogenic temperatures. This cryo cooler is also mounted on the cold plate radiator. Analysis of the thermal response of the entire system shows that

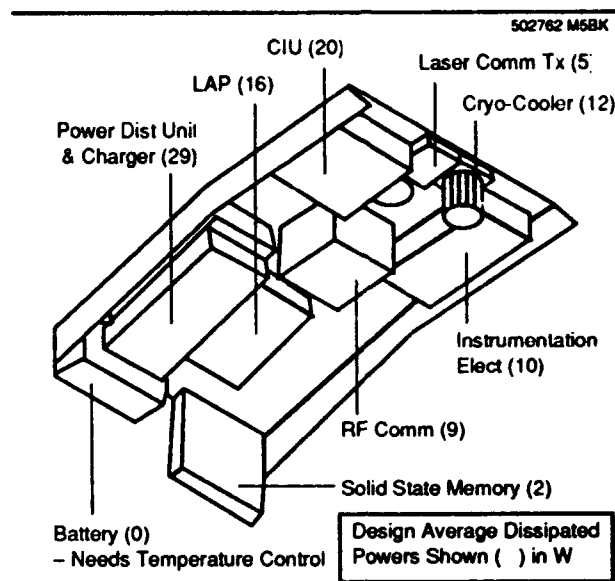


**Figure 2-3. Radiator Plate, Showing Locations of Attached Heat Dissipating Components**

this simple design can keep the system temperatures within 0 to 40 °C (270 K to 310 K). This is achieved by using a controlled emissivity coating and using the thermal mass of the propellant as a heat sink. Changes in the emissivity of the radiator by removal of the coating could allow the system to exceed thermal limits for many of the electronic components.

The key elements of Brilliant Pebbles that need hardening are:

**External Mirror.** This is judged to be the most critical element.

**Radiator.** Loss of the coating will change system response and could cause failure by allowing overall system temperature to exceed limits for an internal component.

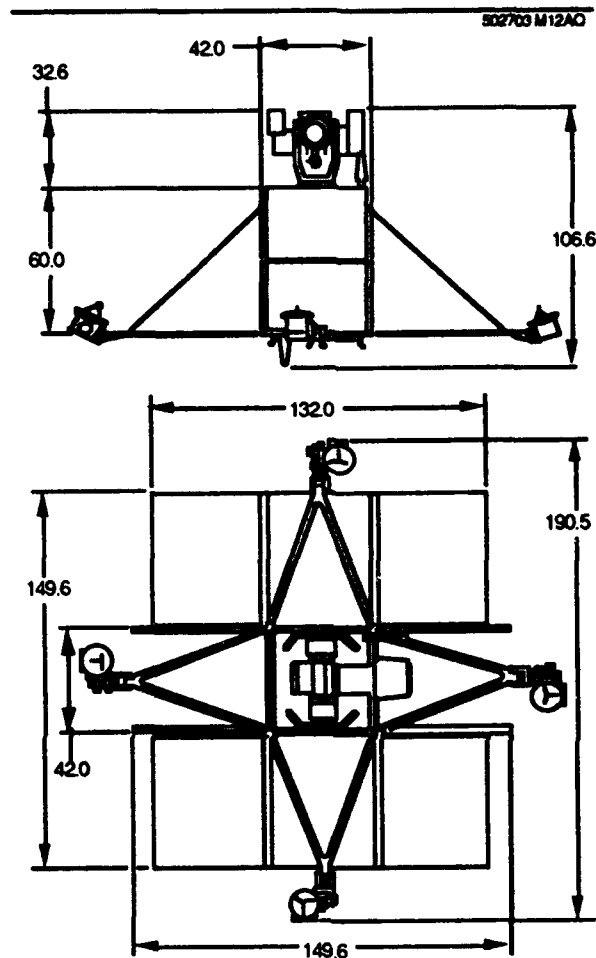
In summary, the radiator is a key element of overall system hardness. Increasing the intrinsic hardness of the radiator has significant payoff in terms of overall system survivability, effectiveness, and cost.

### 2.1.3. Brilliant Eyes Design

The design of the Brilliant Eyes satellite is not as well established as Brilliant Pebbles. Figure 2-4 shows one concept of the design. Other designs exist, but a common component on all designs is the existence of the sensor. Because of the need to discriminate threat RVs from decoys, Brilliant Eyes is expected to employ an optical system that is functionally similar to that being developed by MDSSC for the Ground Based Surveillance and Tracking System (GSTS). A possible configuration of the Brilliant Eyes sensor is shown in Figure 2-5. The system employs a three-mirror system with a scanning mirror to focus light onto an IR focal plane. The sensor is particularly susceptible to nuclear threats. To distinguish threat RVs from decoys, it must scan for a considerable amount of time. Successful intercepts of a discriminated RV could cause the threat RV to salvage fuze, creating a severe nuclear environment, in the Brilliant Eyes field of view. A nuclear threat to the Brilliant Eyes sensor is not only credible but a very distinct possibility.

The sensor and telescope must be designed to withstand nuclear threats. To limit stray light from entering the optical train, the design employs absorptive baffles. The baffles face the same threat as the primary mirror and optical bench. The conventional methods of designing diffuse baffles, use of a black coating over a solid plate, are extremely susceptible to damage. This damage mode causes three problems: reduction in baffle effectiveness, potential coating of mirror surfaces by the particles, and an increase in the scattering of stray light into the optical train by the particles in the field of view. The latter two problems are of main concern. Mirror cleanliness is a major concern for overall system performance as shown in Figure 2-6. Since the mirrors operate at cryogenic temperatures, they become ideal dust "collectors". Particles like to freeze to them. The figure shows that coating of the mirror with baffle particles will increase the BRDF function for the design. The particles in the field of view can degrade the system performance because they are small hot objects competing with real threats for discrimination. Although the particles are expected to cool down quickly, because of their large surface area in relation to their mass, they present another problem. Scattering of light from the particles degrades performance. Figure 2-7 shows the effect of particles in the field of view on stray light power, which is the ratio of stray light scattered onto the detector to the incident light from the viewed object. The allowable stray light power level is expected to be below 0.001, requiring the use of a baffle material with extremely low mass loss in a nuclear

encounter. This is an extremely low allowable, leading to a requirement for a 300 dust level<sup>1</sup> or lower.



Dimensions in Inches

**Figure 2-4. Brilliant Eyes**

In Figure 2-5, the sensor for Brilliant Eyes is expected to employ radiators. The same arguments applied to the Brilliant Pebbles radiator apply here. However, unlike Brilliant Pebbles, damage to the radiator coating has greater system consequences.

<sup>1</sup> (U) The relationship between particle size and number of particles for a given cleanliness level is given by the relationship:  $\log n = 0.9260 (\log^2 X_1 - \log^2 X)$ , where  $n$  is the number of particles,  $X$  is the particle size, and  $X_1$  is the cleanliness level.



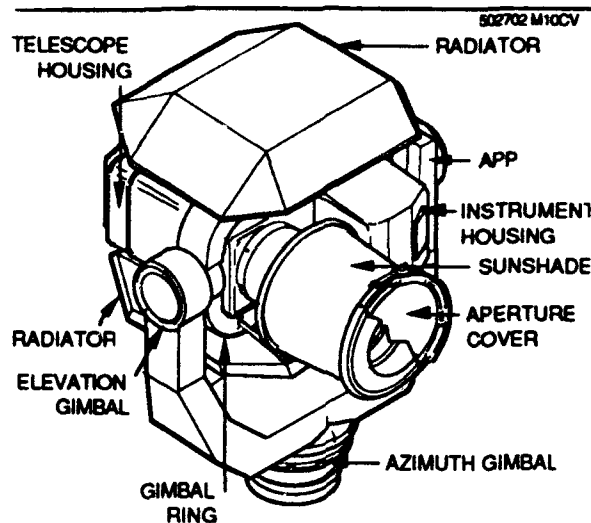


Figure 2-5. Sensor Isometric View

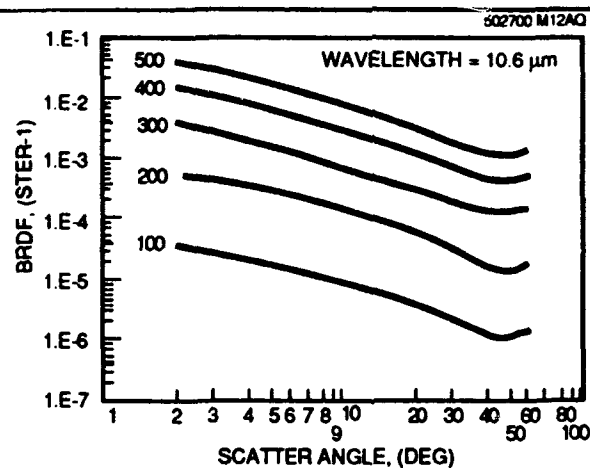


Figure 2-6. Scatter From Particulates Dominat Clean Mirror Scatter In The IR

Nuclear threats are not the only concern. Unlike Brilliant Pebbles, it is not clear that the design and operation of the Brilliant Eyes satellite could yield a design that is self-shielded from a ground-based laser threat. Even though the telescope never looks down, the baffle and sunshade, which are in the telescope barrel, are expected to be at risk from a ground-based laser.

Space-based lasers also impose hardening requirements on the radiators and baffles. The major damage mode expected from a continuous wave laser is related to the induced thermal effects, e.g., radiator overheating or baffle ablation. Pulsed lasers are not expected to cause thermal soak damage; rather, their damage mode is expected to be coating removal.

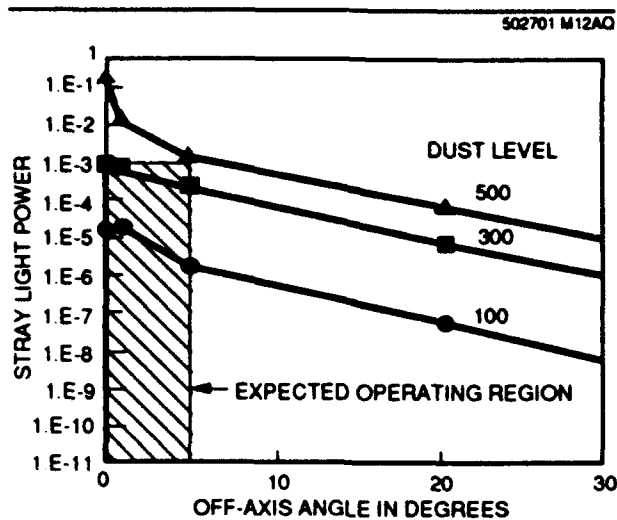


Figure 2-7 . Particle Blowoff Increases Stray Light Power

In summary, both Brilliant Pebbles and Brilliant Eyes contain radiators that will have to be hardened to nuclear and laser threats. Brilliant Eyes will have a sunshade/baffle that will have to be hardened against the threats. Brilliant Pebbles may have a shroud over the external mirror to protect it from nuclear threats, if the intrinsic hardness of the mirror cannot meet system requirements. The hardness levels of these components could determine overall system hardness and, therefore, cost and effectiveness. The payoff for finding low-cost, higher intrinsic hardness coatings for these components is large. Expected worst case damage modes from nuclear threats for both radiators and baffles are coating removal. In some cases, the worst case damage mode from CW lasers is expected to be radiator overheating and burnthrough of baffles. Coating removal in the presence of sensors is also of major concern for CW laser threats. Damage modes from pulsed lasers are expected to be coating removal with the subsequent secondary problems associated with particle formation. Although other damage modes may occur, these are the ones of greatest concern to system designers at this time.

## 2.2 Natural Environments

In addition to the threat environments, the radiator coating and baffle material selection must take into account the natural environments. Many candidate materials perform poorly in a space environment. To understand how this environment affects hardening materials, MDA-SS provides material samples to the Aerospace Corporation and to WL for flight test evaluation

as part of the LDEF flight. Samples provided by MDA-SS to the Aerospace experiments are now undergoing examination at the Aerospace Corporation.

Because MDA-SS is one of the major space station contractors, the space environment is of great concern to us. In addition to the LDEF samples we contributed to the Aerospace trays, we are now analyzing the radiator panels flown on LDEF by McDonnell Douglas. Figure 2-8 shows one of the panels we are evaluating. The panels were covered by a Teflon coated silver. The silver was 1200 Angstroms thick and was plated on 700 Angstroms of Inconel. The whole thermal control coating was bonded to an 0.125-inch-thick aluminum base plate with a pressure sensitive adhesive. A narrow strip at the top was covered by the attachment mechanism and shows the preflight condition of this radiator. The radiator has changed in appearance significantly. The exposed surface is more diffuse, having lost approximately 15 percent of its reflectivity. The teflon was eroded by 0.0013 inch of its total thickness of 0.005 inch. The adhesion between the Inconel layer and pressure sensitive adhesive was reduced to the point that it was easily peeled off. When the material was peeled away up to the area protected by the attachment method, the adhesion was sufficient to result in material failure instead.

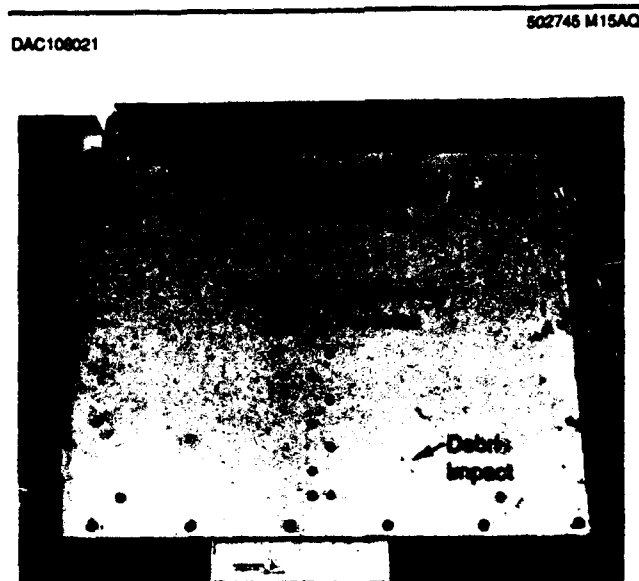


**Figure 2-8. LDEF Radiator Sample**

---

The sample experienced significant debris impact. A total of 29 significant hits were recorded. All of the impacts penetrated the thermal control coating, but none penetrated the aluminum base plate. Loss of thermal control area was minor, i.e., less than 0.06 percent.

Spacecraft in low Earth orbit (LEO) are exposed to a variety of environments which can affect the operation of the spacecraft. These environments and their major effects are summarized in Table 2-1. From a materials standpoint, the most serious effects are caused by solar ultraviolet (UV) radiation, atomic oxygen, and ionizing radiation. Impacts from micrometeoroids and debris also affect material and structural performance. Vehicle charging is a problem for low-altitude spacecraft such as Brilliant Pebbles. Experience gained from the design and operation of spacecraft and from ground testing has revealed which classes of materials are most susceptible to these environments. The primary design solution is to avoid using materials which may be adversely affected. When materials which are known to have problems must be used, it is often possible to coat them with a compatible material or to locate them within the spacecraft.

Table 2-1. The Space Environment has a Number of Negative Effects on Spacecraft Materials.

Environment	Materials Effects/ Issues	Test Techniques/ Facilities
<ul style="list-style-type: none"> <li>• Solar radiation (UV/Visible)</li> <li>• Atomic oxygen attack</li> <li>• Ionizing radiation</li> <li>• Micrometeoroids and space debris</li> </ul>	<ul style="list-style-type: none"> <li>• Thermal control</li> <li>• UV breakdown of coatings, insulators, etc.</li> <li>• Erosion of materials</li> <li>• Degradation of surface properties</li> <li>• Physical damage</li> </ul>	<ul style="list-style-type: none"> <li>• Solar simulators</li> <li>• Neutral atom beam</li> <li>• Cobalt-60 sources</li> <li>• Hypervelocity guns</li> </ul>

Ground test facilities are available to conduct tests for most of the effects induced by the space environment, although the combined effects of two or more environments (e.g., UV and atomic oxygen) are difficult to test.

**UV Radiation** - Degradation by ultraviolet radiation is due primarily to cross-linking of polymers, and polymeric films, coatings, and resins are most susceptible to this effect. The ultimate effects are mainly embrittlement and changes in optical properties. Exposure to UV radiation depends on the amount of exposure to sunlight (which depends on the orbital altitude and inclination), and the sun angle. Instruments and surfaces which rarely look near the sun are therefore relatively unaffected.

**Atomic Oxygen** - The flux of atomic oxygen to which a surface is exposed depends strongly on altitude, local time, solar activity, and the orientation relative to the spacecraft ram direction. Attack by atomic oxygen is primarily due to oxidation, and the ultimate result is erosion of the surface. The effect is particularly bad for organic materials, including carbon. Most metals, such as glass and ceramics, tend to be inert to atomic oxygen attack, although some metals, such as silver, are highly susceptible. Several neutral atom beam facilities were built to test materials for atomic oxygen effects. These can be used to verify the performance of materials which have not yet been used in space. MDA-SSC has developed an atomic oxygen test facility. It is routinely used to analyze materials being considered for Space Station Freedom. The facility is described in the management document.

**Ionizing Radiation** - The natural radiation environment in space has several sources. These include solar and galactic cosmic rays, and protons and electrons from the trapped radiation belts. The particle spectra from these sources depend strongly on altitude and geomagnetic latitude, as well as on solar activity. The optical and thermal properties of material surfaces and coatings can be degraded by electron dose. Beyond a few tens of miles from the surface, proton dose can degrade material properties. Cobalt-60 testing provides an adequate and relatively inexpensive method of testing for ionizing radiation effects.

**Micrometeoroids and Debris** - The LEO environment is constantly bombarded by micrometeoroids, and orbital debris is an increasing problem. Impacts can occur from the orbital velocity of about 7 km/sec up to over 40 km/sec. Damage can range from degradation of surface properties to penetration of the material. Hypervelocity guns are available to test for damage. MDA-SSC has tested in the UDRI and the Delco test facility, now moved to Tullahoma TN. These tests were conducted to validate MDA-SSC analytic methods and our understanding of methods to shield against hypervelocity impact. The results of these tests and the correlation with predictions are contained in our IRAD reports.

**Materials Selection.** - As stated above, the preferred approach is to avoid using materials which are known to be adversely affected by the space environment. Ground testing and experience in operating spacecraft have resulted in guidelines for using materials for various applications. Table 2-2 summarizes some of these guidelines. A (+) in a column indicates that the material has been shown to be compatible with the corresponding environment, a - indicates that the material has been shown to be incompatible, and an 0 indicates that the material is in between.

Table 2-2. Experience in Spacecraft Design Provides Guidelines for the Use of Materials.

Material	UV Radiation	Atomic Oxygen	Ionizing Radiation
Metals (in general)	+	+	+
Silver	+	-	+
Glass	+	+	+
Carbon	+	-	+
Organic resins	-	-	0
Teflon	+	+	-

## 2.3 Functional Description of Radiators

Efficient heat rejection requires that the radiator have good thermal coupling with the space sink environment, which implies that the radiator should have high infrared emissivity, low solar absorptivity, and high thermal conductance throughout. Additionally, the radiator must be highly reliable (there should be no single point failures), have a low stowage volume for launch, withstand high g launch loads and maneuvers, and satisfy specific platform interface requirements.

Current radiators for power levels of interest use three basic types of designs: cold plate radiators, as being considered for Brilliant Pebbles; pumped loops, in which a fluid or other heat transfer mechanism is used to take heat to the radiating elements; and heat pipes, in which the heat is carried out to the radiating elements by a warm gas, which condenses and is transpired back to the heat exchanger through a wick. Pumped loop radiators are simpler and may be less massive, but for long duration missions, the inherent redundancy of a heat pipe radiator (the radiator consists of many redundant pipes) makes it more reliable.

Another consideration in the design of the radiator is its operating temperature. The radiator for Brilliant Pebbles is designed essentially for room temperature operation. Cryogenic cooling for the IR sensor is handled by a separate cryo cooler, essentially a refrigerator to allow efficient operation at room temperatures. Such radiators can be designed to operate in the solar environment by using a low  $\alpha/\epsilon$  ratio, which is the solar absorptance,  $\alpha$ , divided by the infrared emissivity,  $\epsilon$ . For higher temperature radiators, even visibly black materials, such as carbon-carbon can be considered without a significant penalty on overall radiator operation. Emissivity control on conventional radiators is achieved by thin coatings, chosen for their overall  $\alpha/\epsilon$  ratio.

Unacceptable damage modes for all radiators can now be determined. These damage modes are those that exist in addition to the system synergistic damage modes, e.g., the generation of particles that could coat optics or scatter stray light into the optical system. For all radiators, the change in emissivity of the radiator is of concern, the level of concern being inversely proportional to the operational temperature of the radiator. For pumped loop and heat pipe radiators, there is also concern about loss of the fluid integrity of the radiator. If the wall of the heat pipe or pump loop is punctured, loss of the operating fluid would cause radiator loss. But, it is also possible to damage the radiator at lower levels of heat input. If the heat input is sufficient to dry out the wick, its operation could be stopped. In addition, external radiation could overheat portions of the radiator and entire system. These values would be design dependent.

### **3. ANALYSIS TOOLS**

As described in Chapters 1 and 2, the ASR geometry is a highly complex three-dimensional structure which requires sophisticated analyses techniques to adequately predict its thermal performance. The effectiveness of trade studies is therefore closely linked to the ability to assess performance under various configurational and environmental constraints. As part of ongoing IRAD activities, prior to the initiation of this contract, MDSS developed and verified sophisticated analysis tools to predict the optical and the thermal performance of a generic three-dimensional fibrous material. This has been applied both to the radiative surfaces and also to battle technology. Because this tool played an important part in the trade studies discussed in Chapter 4, an overview of its assumptions and capabilities is described in the following discussion. The reader is referred to more detailed information in Reference 1.

The overall model, called FURRAD, employs a three-dimensional Monte Carlo analysis technique to determine the radiative heat transfer characteristics of a predefined fibrous geometry. The fiber pattern on the base material can be either a square or hexagonal array with the fibers being modeled as cylinders of given diameter, length and spacing. Specular or diffuse reflection from fiber surfaces, as well as the ability to define multiple incoming diffuse or directed radiation sources, has been incorporated into the model.

#### **3.1 Model Assumptions and Capabilities**

A number of assumptions were made with respect to the modeling efforts. These assumptions ensured that trade study critical effects were incorporated while secondary effects were neglected. A few of the key assumptions are described below:

- Wavelength dependent material properties of the fiber and base materials are input parameters, e.g.,  $\rho$ , reflectivity mode (specular, diffuse, or scattering) and fiber material density.
- Fiber bundles are represented as cylindrical surfaces in either square or hexagonal arrays normal to the base material.



- **Diffraction of incoming energy is neglected.** This assumes that the fiber diameter is large compared to the wavelength of incident energy.
- **Method of images is used to model the entire array of fibers by a single fiber placed in a rectangular cell with perfectly reflecting walls**

The models developed using the above assumptions have the following capabilities:

- **Fiber surfaces can be modeled as either diffusely reflective, specularly reflective, or partially "translucent" to a wavelength allowing energy to enter the fiber volume and scatter.**
- **Specular surfaces can have a surface reflectivity that depends on the angle of the incoming radiation.**
- **The effective emissivity ( $\epsilon$ ), transmissivity ( $\tau$ ), and reflectivity ( $\rho$ ) as well as the weight per unit area, and an energy absorption profile is determined. The fiber temperature profile and overall heat balance to determine the net heat flow from the radiator are also determined.**
- **Multiple sources of incident energy can be added in the forms of hemispherical (earth albedo) or directional sources (solar radiation, laser, etc.).**

### **3.2 Modeling Details**

A simplified flow chart representing the major sections of the FURRAD code is highlighted in Figure 3-1. The input definition section encodes material geometry and physical characteristics, optical properties, and external source characteristics over a specified wavelength range of interest. A Monte-Carlo simulation is then used to evaluate the radiation heat transfer characteristics within the complex three-dimensional geometry. Once the radiation characteristics are known, temperature profiles within the material and overall heat transfer balances are determined. The following sections provide additional details on the Monte-Carlo simulation, determination of the fiber temperature profile and the system heat balance.

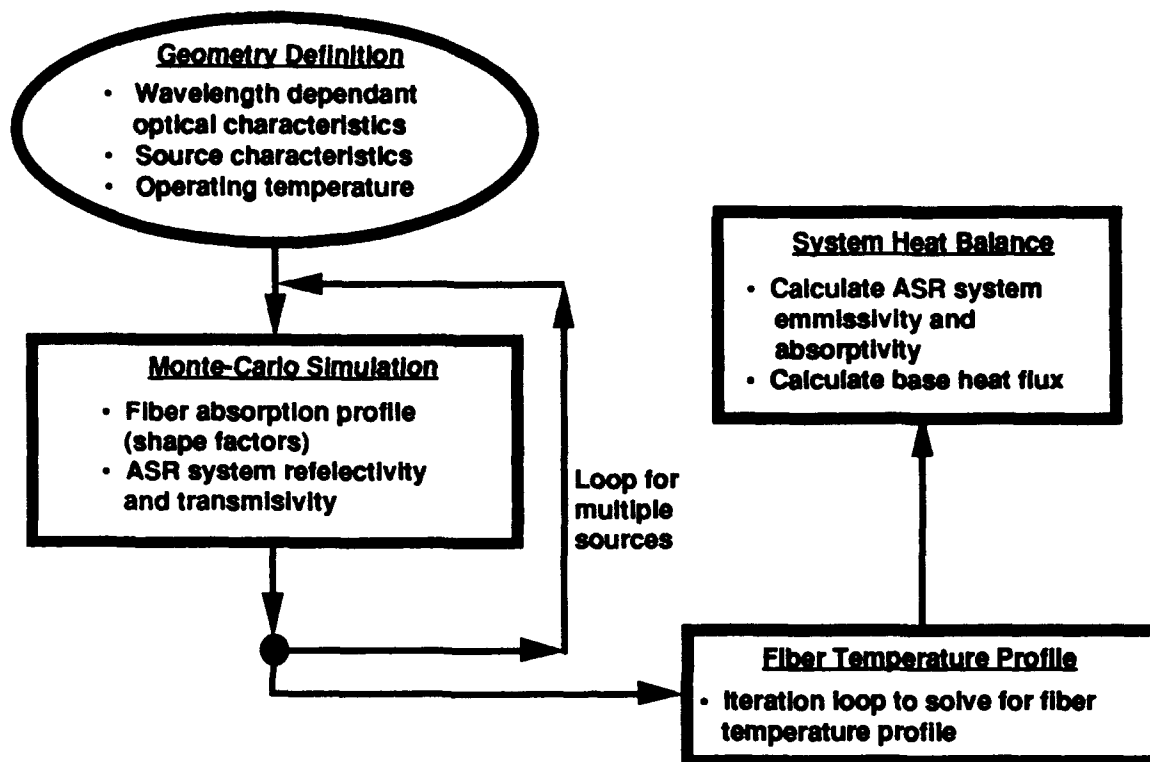


Figure 3-1. Simplified Flow Chart of the FURRAD Analysis Process

### 3.2.1 Monte-Carlo Simulation

A 3-D Monte-Carlo simulation technique is used to model the radiation heat transfer characteristics of the ASR carpet by injecting "photon" particles into the fiber geometry as shown in Figure 3-2 and tracking their progress as they reflect down into the carpet. Using the method of images, a computational cell with perfectly reflecting walls containing a single fiber at the center is used to represent the entire array of fibers (Figure 3-3). As a photon enters the top of the computational cell, regardless of angle, it will either hit the fiber or reflect off the inside of the cell until it impacts the fiber or the base. Since the cell walls are perfectly reflecting, the photon will impact the single fiber (or the base) in the same location it would have hit another fiber if a full array of fibers was modeled. The use of a single computational cell then results in the average absorption profile of the entire ASR carpet. To track exactly how each



photon is absorbed, the fiber length is segmented into many smaller sections and the impacts on each section are tabulated. When the photon enters the computational cell it has a normalized "energy" value of one. When the photon impacts the fiber (or base) a portion of its energy is absorbed by the fiber. The absorbed energy is based on the wavelength dependent optical properties of the material. The photon's normalized energy is decremented by the fiber absorption and reflected back out into the cell either diffusely or specularly, depending on the chosen option. This process continues until the normalized energy remaining in the photon particle is below a small arbitrarily chosen energy value or has escaped the cell. The user has control over how many photon particles to use in the simulation as well as how finely to segment the fiber length. Our experience has shown that 5000 photon particles and 50 length divisions provide accurate results. A representative absorption profile is shown in Figure 3-4 for high-reflectivity fibers having moderate tip reflectivity.

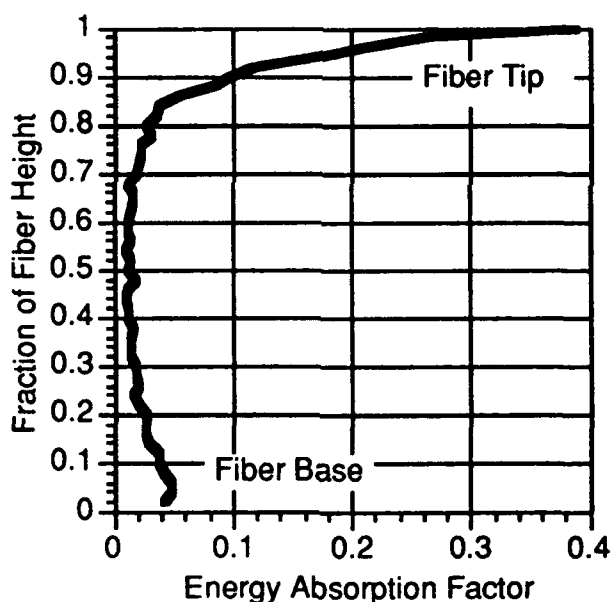


Figure 3-4 - Calculated Energy Absorption Profile of the ASR Carpet for a Hemispherical Source ( $P/D = 2.5$ ,  $L/D = 15$ ,  $\rho = .8$ )

To simulate the behavior of fiber materials that may be partially translucent to an incoming wavelength of energy, a volume scattering model is used in the FURRAD code. This model takes the place of the reflective models used in FURRAD when this option is selected. The volume scattering model is based on the principal that a photon

can enter and scatter within the fiber volume, releasing energy until it escapes the fiber or releases its energy. The relevant input parameters in this case are the albedo for single scatter ( $\omega$ ) and the optical depth ( $T_d$ ). The value of  $\omega$  represents how much energy is scattered without being absorbed into the material. Therefore, if  $\omega$  is near 1.0 then most of the energy is reflected and the material would appear "white" to a particular wavelength. If  $\omega$  is near zero, then most of the incident energy would be absorbed and the material would appear black to the respective wavelength ( $\omega$  is somewhat like a reflectivity value). The value of  $T_d$  represents how far a photon could penetrate into the fiber before being scattered. For values of  $T_d$  less than 1, the fiber material is more transparent; conversely, large values of  $T_d$  indicate that the material is opaque.  $T_d$  can be estimated for a fiber constructed by winding smaller filaments together using the following formulas:

$$T_d = \frac{A_d}{V} l \quad (3-1)$$

Where:

$$A_d = \left( \frac{N}{V} \right) A_f \quad (3-2)$$

$V$  = Volume of a fiber bundle

$l$  = Length of fiber

$N$  = Number of filaments counted across the fiber diameter

$A_f$  = Cross-sectional area of filament

To determine whether the photon continues to be scattered inside the fiber volume or escapes, an escape probability is calculated and compared to a random number. For these scattering applications, the escape probability varies with the negative exponential of the optical depth. If the escape probability is higher than the random number then the photon escapes along its current path, otherwise the photon has been scattered and its energy is decreased using the  $\omega$  factor and a new direction is calculated. When the photon is scattered, its location within the length of the fiber is determined and the absorbed energy is tabulated in the correct discrete volume element along the fiber length, as shown in Figure 3-5.

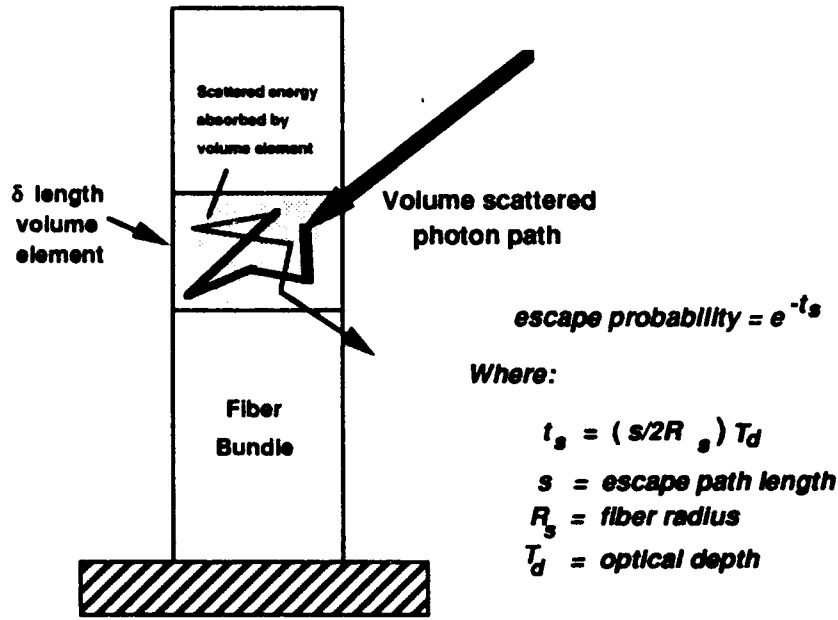


Figure 3-5. Volume Scattering Model using Escape Probability Function for Current Photon Path

### 3.2.2 Fiber Temperature Profile

Using the previously described absorption and emission profiles calculated by the Monte-Carlo simulation techniques, the fiber temperature profile can be obtained through a one-dimensional heat conduction equation governing the ASR system. Starting with an initial guess for the fiber-tip temperature, the differential heat conduction equation is numerically solved to calculate the fiber base temperature. This calculated base temperature is compared with the inputted radiator base temperature and the process iterates until the assumed tip temperature results in the correct base temperature. The result of this entire process is the temperature profile along the fiber length.

$$\frac{KA_0}{\pi D} \frac{d^2 T_i}{dz^2} = \epsilon_i (\sigma T_0^4 - \sigma T_i^4) - \sum_{j=1}^n \alpha_i G_j + 4\epsilon_i \sigma T_0^3 (T_i - T_0) \quad (3-3)$$

Where:

$$\alpha_i = \frac{(A - A_0) F_i^e}{\pi D \Delta z} \quad , \quad \text{External Absorption} \quad (3-4)$$

$$\epsilon_i = \frac{(A - A_0) F_i}{\pi D \Delta z} \quad , \quad \text{External Emission} \quad (3-5)$$

And:

$A$	=	Cross-sectional area of computational cell
$A_0$	=	Cross-sectional area of fiber
$F_i^*$	=	Absorption profile for external sources
$F_i$	=	Absorption profile for external sources
$D$	=	Diameter of fiber
$\Delta z$	=	Length of discrete fiber element
$K$	=	Thermal conductivity of fiber material
$s$	=	Stephan-Boltzman constant
$T_i$	=	Temperature at slice $i$ of the fiber
$T_0$	=	Temperature of the fiber tip
$T_s$	=	Equivalent space temperature
$G_e$	=	External source strength (W/m <sup>2</sup> )
$m$	=	Number of external sources

When the correct fiber temperature profile has been solved for, the effective ASR system emissivity is computed. The effective system emissivity is one of the most important parameters used in the trade studies. The effective emissivity is defined as a fictitious conventional surface that results in the same thermal performance as that of the ASR configuration. In this manner, the thermal performance effects of using an ASR type surface (namely emissivity and absorptivity) can be directly compared to more conventional radiator surfaces.

$$e_{eff} = e_o \frac{A_o}{A} \left( \frac{T_o}{T_b} \right)^4 + \left( 1 - \frac{A_o}{A} \right) \tau + \left( 1 - \frac{A_o}{A} \right) \sum_{i=1}^n F_i \left( \frac{T_i}{T_b} \right)^4 \quad (3-6)$$

Where:

$T_b$	=	Fiber base temperature
$n$	=	Number of fiber lengthwise divisions

### 3.2.3 System Heat Balance

Given the effective emmissivity and the temperature profile of the ASR carpet, FURRAD performs a heat balance to calculate the net heat flow rejected by radiator surface. If  $q_{abs}$  is positive the radiator is absorbing heat from the environment, and if negative the radiator is rejecting heat. Figure 3-6 is a sketch showing the elements considered in the overall heat balance equation.

$$q_{abs} = (1 - \rho) G_{hemi} + \sum_{i=1}^m (1 - \rho_i^*) G_i - \epsilon_{eff} \sigma T_b^4 \quad (3-7)$$

Where:

$\rho$	=	Reflectivity of fiber material in infrared
--------	---	--

$\rho_i^*$  = Reflectivity of fiber material for an external source wavelength  
 $G_{hemu}$  = Strength of external hemispherical source  
 $m$  = Number of external sources

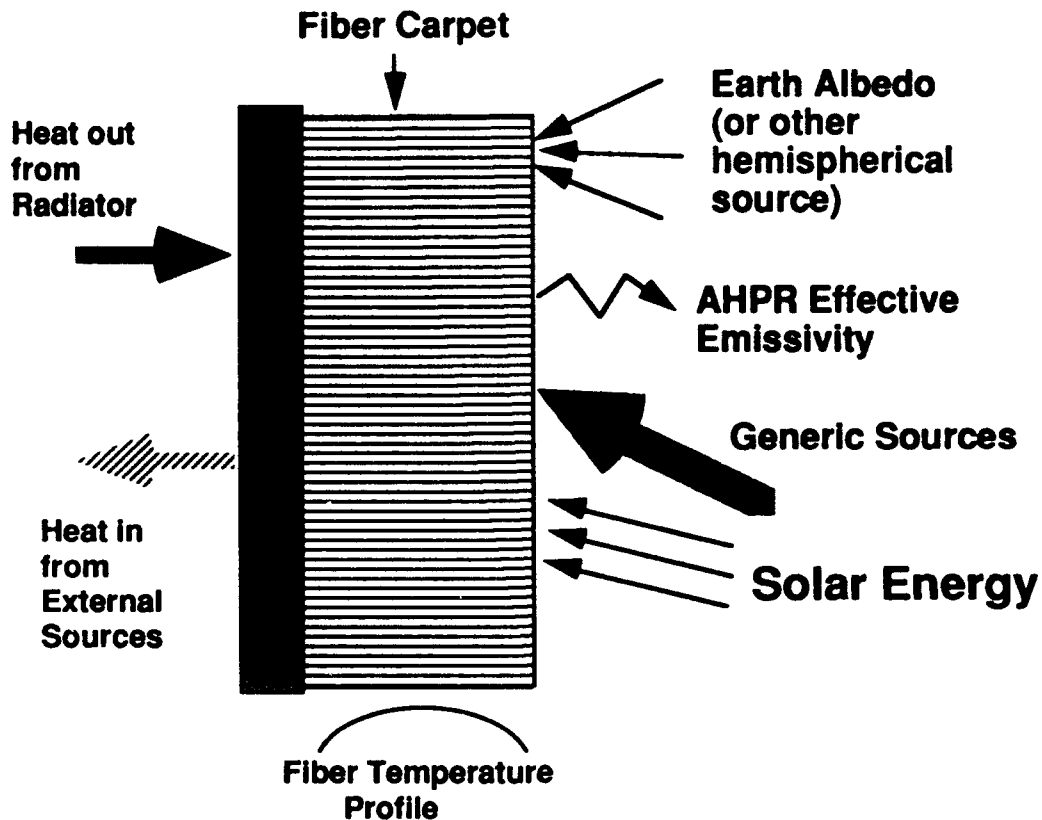


Figure 3-6. ASR System Net Heat Balance

### 3.3 Model Verification

Verification of the FURRAD code was carried out under MDSSC IRAD. The optical performance of small pinned coupons (Figure 3-7) was directly compared to the results predicted by FURRAD. The arrays of pins approximated the geometry of an actual array of ASR fibers in a controlled environment. A number of "simulated ASR" geometry were tested. A portion of the coupons were coated with high-reflectivity white paint while others utilized a gold-plated surface.



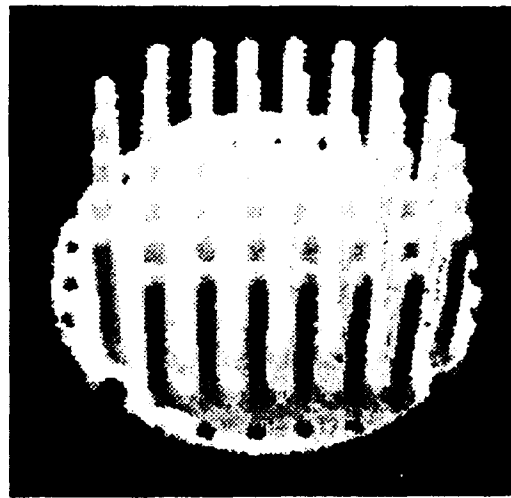
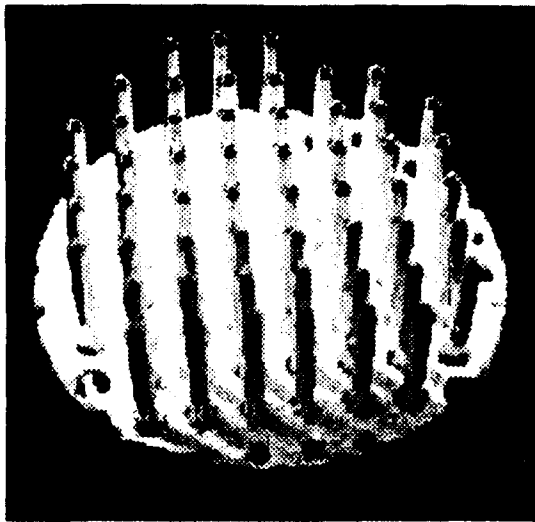


Figure 3-7. Representative Test Coupons

The surface reflectivity of these test coupons, along with various control disks, was measured over a wide spectrum range. The wavelength dependent material properties together with the sample geometry were then input into the FURRAD code and compared to the actual test data. Figure 3-8 shows representative test results together with the FURRAD predictions for one of the test coupons. As can be seen, the correlation is quite good for a wide range of wavelengths. Results indicated that the wavelength integrated emissivity differed less than 5 percent between the FURRAD calculations and the measured results.

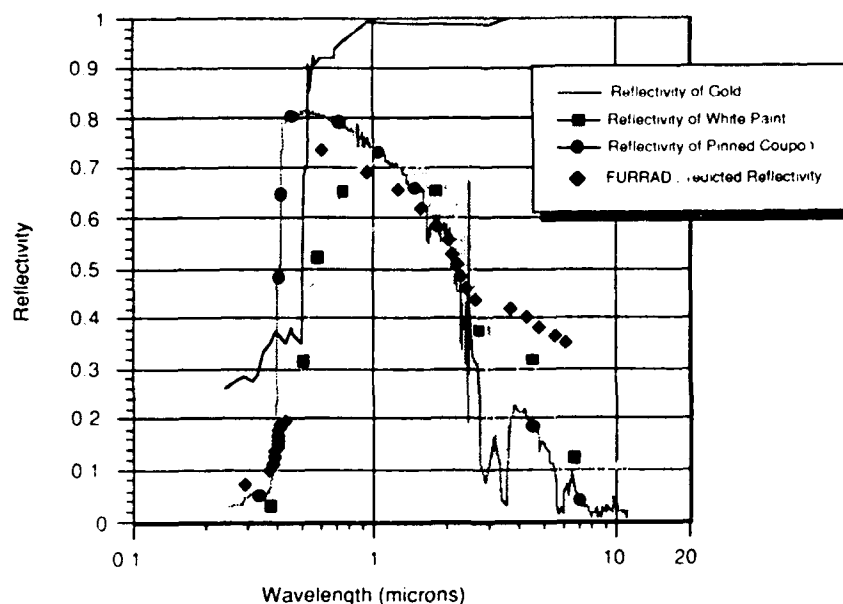
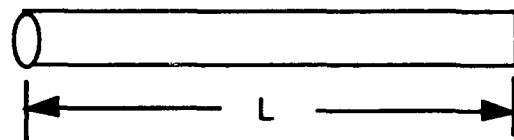
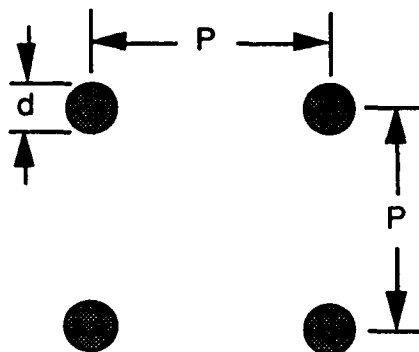


Figure 3-8 FURRAD Prediction Compared to Test Data for Gold Pins with White Base Material

## 4. RESULTS

### 4.1 ASR Surface Geometry

The ASR configuration refers to an external surface fabricated in a brush or carpet configuration using a range of fiber material options and fabrication techniques. In more conventional weaving operations, fiber filaments, on the order of ten microns, are wound together to form larger fiber bundles having diameters on the order of a millimeter. These fiber bundles are quite flexible and extend normal from the weaving mat. As indicated in Figure 4-1, the weaving pattern is normally in a square arrangement. The fiber bundles are assumed to have a diameter  $d$ . Spacing between successive fiber bundles is defined as the pitch,  $p$ . The length of the fiber bundle, measured from the base of the weave material to the fiber bundle tip, is defined as  $L$ .



$$\text{Fiber Area Density} = (\pi / 4)(P / d)^{-2}$$

$$P / D = 1, \text{ Maximum Fiber Density} \approx 78\%$$

$$\text{Mass / Area} = \rho(\pi / 4)(P / d)^{-2} L$$

Figure 4-1. Fiber Geometry Characteristics

For the purposes of initial trade studies, fiber-bundles are initially modeled as solid cylindrical surfaces. This is useful for defining geometric constraints on the ASR covering and assessing the impact of material characteristics on overall thermal performance. However, the method of constructing the fiber bundles can significantly affect thermal performance. The number of filaments per bundle, twist angle, bundle tightness, etc., will impact not only the effective axial thermal conductivity, but also the

bundle optical characteristics. Thus, early trade studies must be complemented by more detailed evaluations using the tools described in Section 3.

As observed in Figure 4-1, the ratio of fiber-bundle pitch to fiber-bundle diameter ( $P/d$ ) will play an important role in the overall thermal performance of the surface. When  $P/d$  is small, the fibers are closely packed, and the surface thermal performance will be dominated by the fiber tips. For large values of  $P/d$ , the fibers are sufficiently separated so that the base material dominates thermal performance.

By proper selection of the fiber geometry and fiber materials, thermal performance can be optimized. The goal of the trade studies is then to identify a minimum mass configuration that maximizes overall thermal performance subject to operational constraints of the natural and hostile threat environments.

## 4.2 Requirements

Operational requirements for the ASR were derived from the mission profiles discussed in Section 2. Hostile threat environments are taken to be the current SUPER goals. These are summarized in Table 4-1.

Table 4-1 ASR Operating Requirements

Operating Temperature	300 K - 400 K
External Source	Direct Solar Irradiation
Natural Environment	Atomic Oxygen Micrometeoroids/Space Debris
Hostile Environment	
Ground Based Laser	$W/cm^2 @ \mu m$
Space Based Laser	$W/cm^2 @ \mu m$
Nuclear Threat - X-rays	$cal/cm^2$
Projectile	$W/cm^2 @ Hz$

We begin by examining the performance of the ASR surface under no threat conditions to define a global feasible design space. The various design constraints will then be added to assess the impact on this design space.

### 4.3 Thermal Performance

We first consider an ASR coated radiator surface operating at 400 K and directed towards deep space. In this case, there is no incident insolation from either the sun or the Earth albedo. The impact of the ASR geometry and fiber thermal conductivity on effective surface emissivity is highlighted in Figures 4-2 and 4-3. Here, it is assumed that the fiber bundles and the base material have diffuse reflectivity of 0.2, characteristic of conventional radiators. Consider first the case of the fiber bundles having a high effective axial thermal conductivity. For values of  $k$  on the order of 100 W/m-K, the fibers will be nearly isothermal. Figure 4-2 (a) highlights the effective surface emissivity as a function of the fiber surface geometry. As the fiber length shrinks to 0, the surface emissivity tends toward that of the material characteristics of 0.8. For a given  $P/d$ , increasing the fiber bundle  $L/d$  increases the effective emissivity of the surface. Consider the case where the fiber  $L/d$  has a value of 15-20. For low values of  $P/d$ , the fibers are bundles close together. In this case, the thermal performance is dominated by the fiber tips. As one would expect, the emissivity is close to that of the characteristic materials. For high values of  $P/d$ , the fibers are separated so that the base material dominates the radiative characteristics of the surface. Once again, the emissivity begins to approach that of the characteristic materials. However, in the range of  $P/d$  from 2.5 to 4.5, a local optimum region exists where the surface emissivity is maximized. In this case, the fiber geometry acts as small optical cavities to increase the effective emissivity of the surface. Thus, use of "fuzzy" surfaces can enhance the emissivity over that of the characteristic materials.

The ASR surface is in effect a three-dimensional fin problem. Thermal conductivity of the fiber bundles will have a significant impact the overall thermal performance of the surface. The impact of thermal conductivity is highlighted in Figures 4-2 (b) and 4-3. As the thermal conductivity is reduced, the fibers become non-isothermal. A thermal gradient along the fibers is established and the fibers are in effect radiating at a lower temperature than that of the base material. As can be seen, the effective emissivity can be significantly reduced over that of the characteristic materials. The question is then to define constraints on the fiber bundles thermal conductivity to ensure surface emissivity enhancement, i.e., emissivity of the ASR surface larger than that of the characteristic materials.

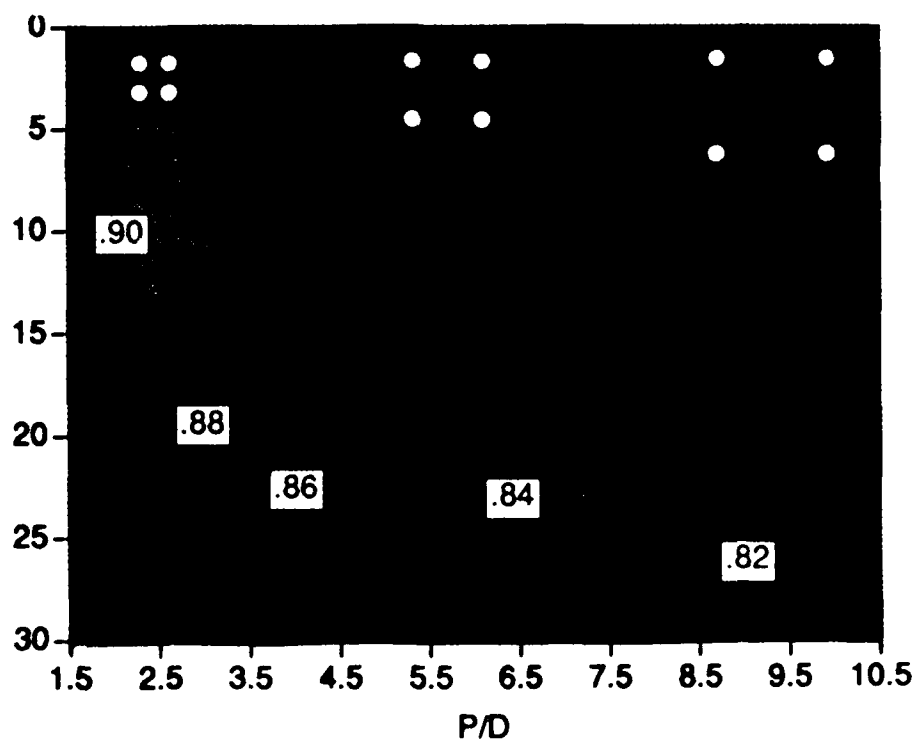
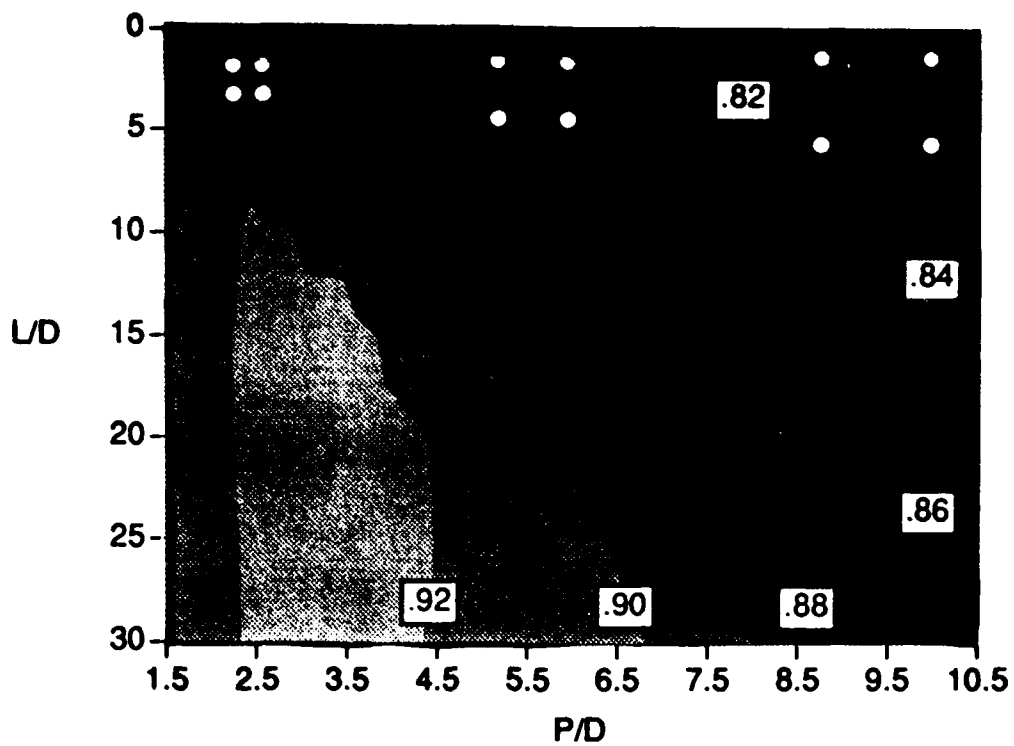


Figure 4-2. a) Contour Plot Showing ASR Effective Emissivity for Thermal Conductivities of 100W/m-K, and 10 W/m-K. For both plots the radiator base temperature is 400K.

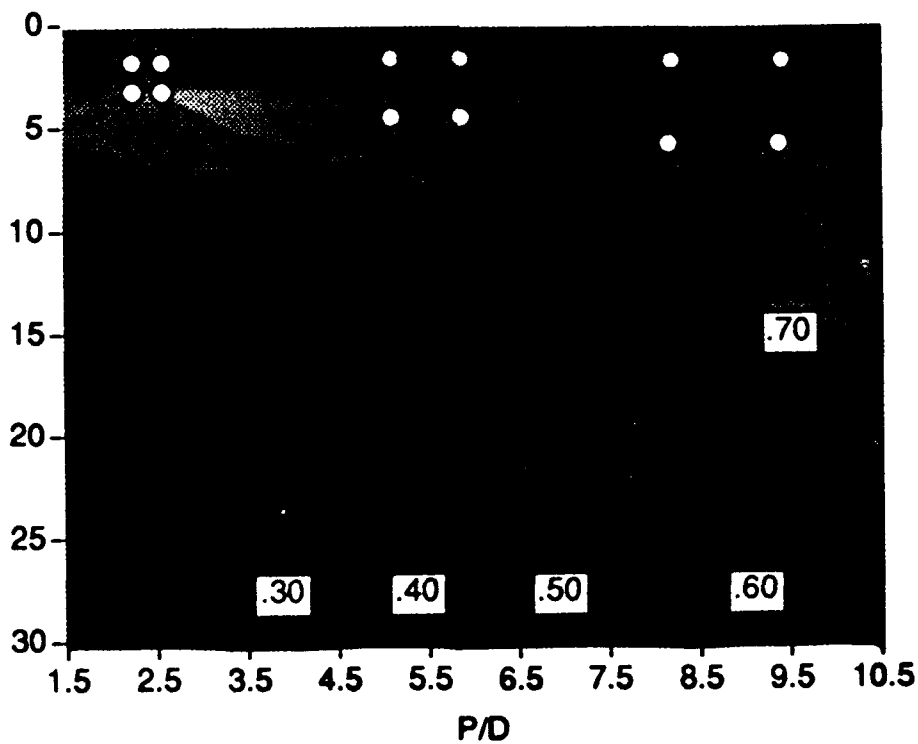
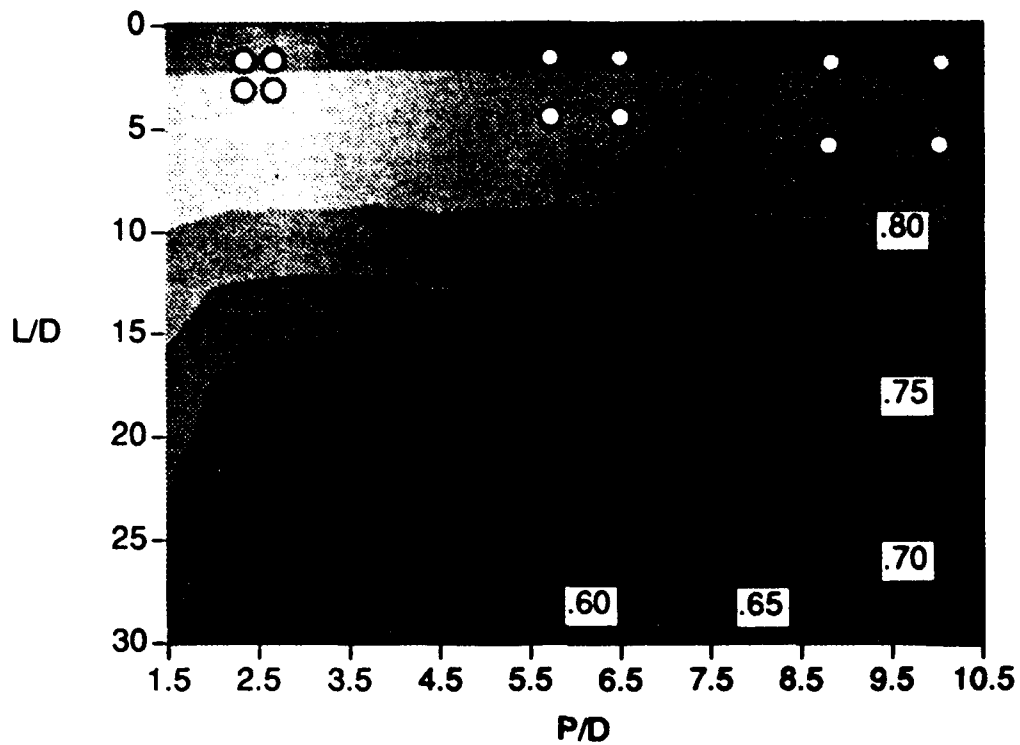


Figure 4-3. Contour Plots Showing ASR Effective Emissivity Changes for Thermal Conductivities of 1 W/m-K (top) and 0.1 W/m-K (bottom)

The thermal conductance of heat flow along the fiber bundle can be written simply as:

$$K_c = (\pi/4) d^2 (k/L)$$

If one assumes that this single fiber bundle is radiating only from its tip at a characteristic temperature  $T$ , then its conductance can be defined as:

$$K_r = \sigma T^3 \epsilon (\pi/4) d^2$$

The ratio of these two conductances ( $N$ ) will then provide an indication of the scaling importance of the thermal conductivity:

$$N = \epsilon \sigma T^3 L / k$$

Though this neglects the effect of fiber to fiber interaction, the scaling should vary as the third power of temperature and vary inversely as the thermal conductivity. The FURRAD code was run over a range of parameters for a prescribed  $P/d$  geometry. A value of  $P/d$  of 3.5, which provided the maximum emissivity enhancement, was selected. Results are shown in Figure 4-4. Data reduction indicated that the scaling for emissivity enhancement was indeed inversely proportional to thermal conductivity and proportional to the third power of temperature. It also depended directly on fiber length and the fiber length to diameter ratio. For values of this parameter, less than 0.2 emissivity enhancement could be expected. Thus, a geometric constraint based on material and operational characteristics can be defined:

$$L^2/D < 0.2 k/(\sigma T^3)$$

The temperature scaling indicates that this effect is much more important at higher temperatures. Using thermal conductivities of characteristic materials, operation at room temperature will not impose significant constraints on fiber geometry.

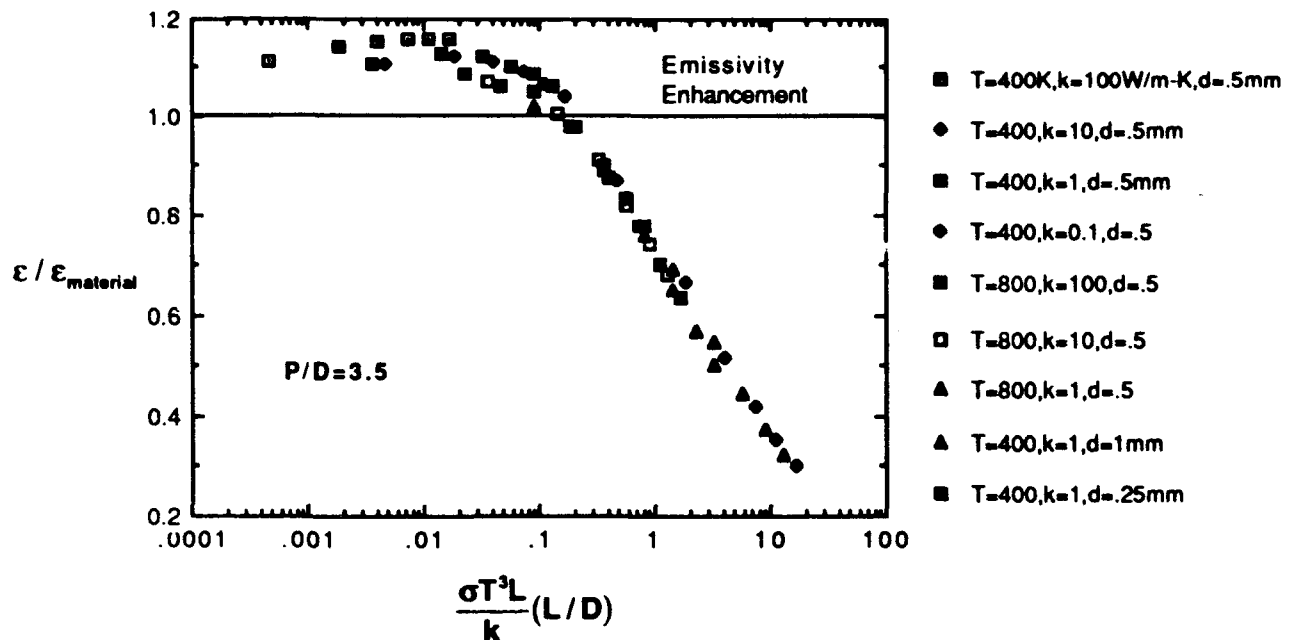


Figure 4-4. Plot of FURRAD Results Showing the Scaling Law for Emissivity Enhancement

#### 4.4 Performance Under Direct Irradiation

Through geometric modification of the surface, it was demonstrated that surface emissivity can be increased over that of the materials used to fabricate the surface. The impact of using surface geometry when operating in direct solar insolation is considered next. Consider first a hypothetical flat radiating surface having an IR emissivity of 0.8 and a solar absorptivity of 0.2 and operating in direct sun. We next fabricate a hypothetical ASR surface having an IR emissivity of 1.0 using this same material. It is assumed that fiber thermal conductivity is high so that the fiber bundles are isothermal. The impact of ASR absorptivity and operating temperature are highlighted in Figure 4-5. In this case, radiator area reduction is used as a comparison of these two hypothetical cases. When the area reduction is less than one, the ASR offers enhanced operation over the conventional radiator. In cases where the area ratio is greater than one, the conventional radiator offers enhanced performance. At higher operating temperatures (600 K), use of the hypothetical ASR radiator provides enhanced performance irrespective of its solar absorptivity. At lower operating



temperatures the ASR offers enhanced thermal performance if the ASR absorptivity is less than 1.5 times the conventional radiator absorptivity. For values larger than this, use of surface geometry hinders thermal performance. Clearly, the manner in which surface absorption is modified by geometry will be critical in operating an ASR in direct insolation.

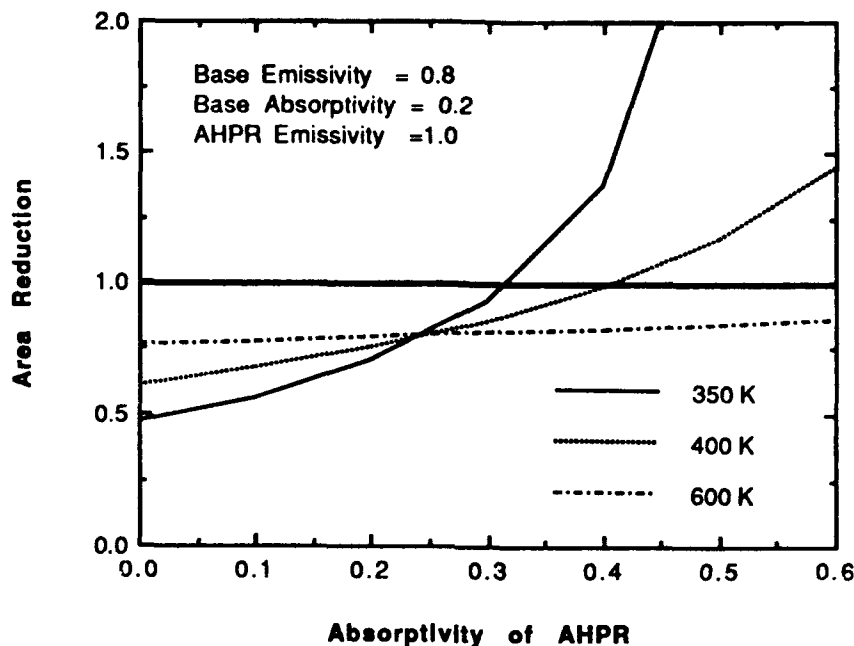


Figure 4-5. Effect of ASR Absorptivity and Operating Temperature on Radiator Area

The effect of direct solar insolation on the performance of the ASR is considered next in Figure 4-6. The thermal performance of the ASR will be referenced to a hypothetical flat radiator surface having an emissivity of 0.8 and an absorptivity of 0.2. For the ASR, we will assume that both the fiber bundles together with the base material exhibit similar optical characteristics to the conventional radiator surface. Assuming an operating temperature of 400 K, the ratio of heat rejection by the ASR covered radiator, to that of the standard radiator, is compared for sun "off" and sun "on" conditions. With the sun "off" conditions, it is observed that using the ASR geometry enhances the net heat rejection by over 15 percent. However, with the sun "on", the ASR radiator does not perform as well as a standard radiator. In fact, the optimal geometry for the sun "off" case leads to a significant degradation in thermal performance with the sun "on".

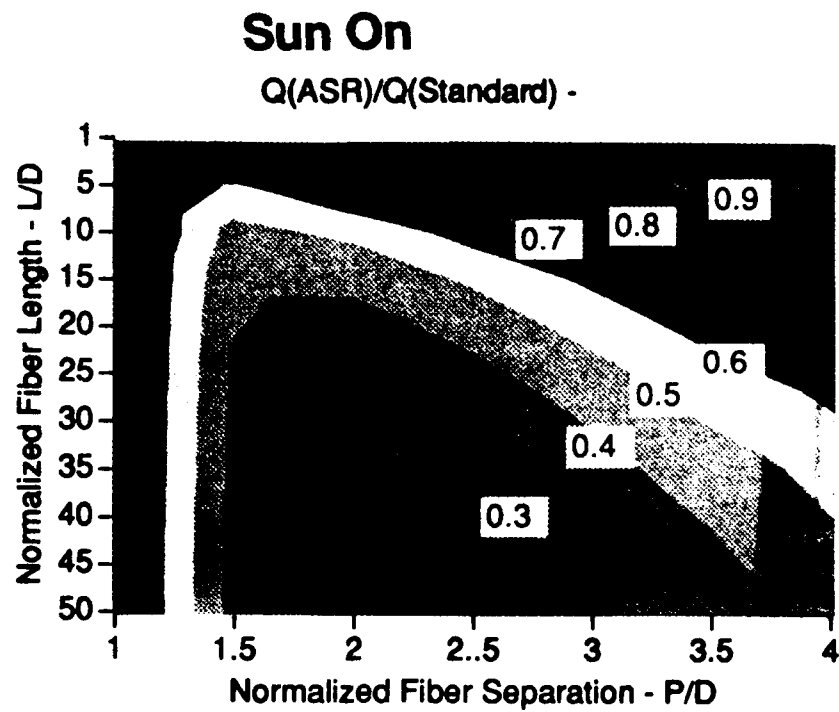
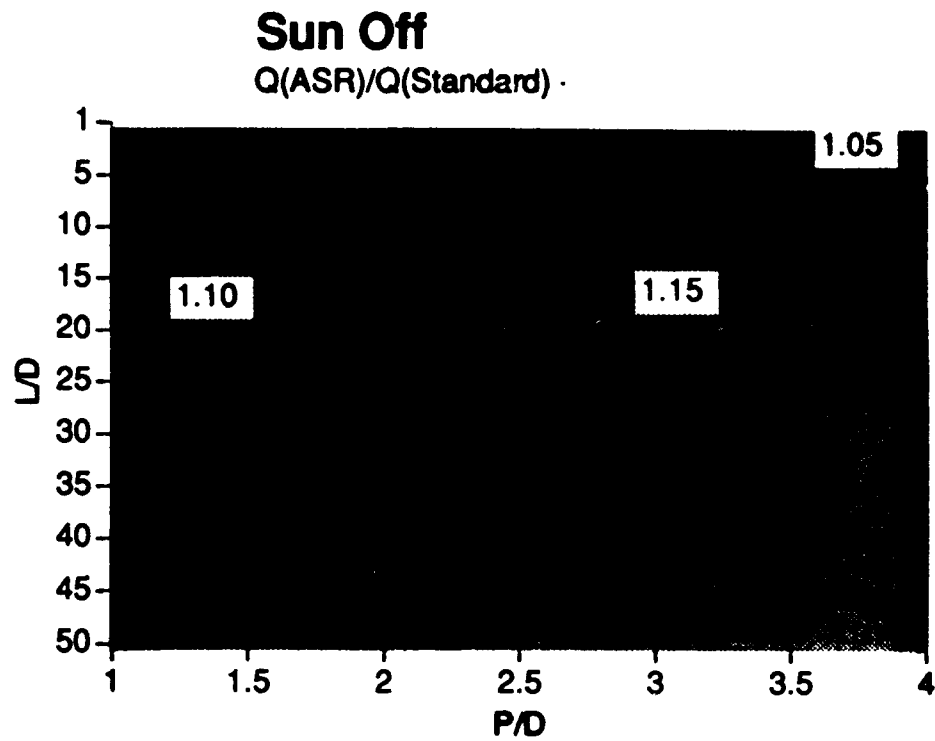


Figure 4-6. Contour Plots Showing the Effect of Solar Flux on ASR Performance

The reason for this behavior can be extracted from the results presented in Figure 4-7. For the same operating conditions used in Figure 4-6, emissivity and absorptivity of the ASR, relative to that of the standard radiator, are shown as a function of fiber  $L/d$  and fiber area density. In the case of the IR emissivity, it is observed that as the fiber bundle  $L/d$  is increased, the emissivity enhancement increases. Depending on the geometry, a gain of 15-20 percent can be attained. On the other hand, the ASR geometry acts to increase absorptivity significantly. Figure 4-7 (b) indicated that the solar absorptivity can increase by more than a factor of 3. Figure 4-5 demonstrated that this large increase in absorptivity will not be conducive to enhanced thermal performance while operating in direct sunlight. Thus, absorption effects dominate ASR performance for long fibers and high fiber-densities. If the ASR is to operate in direct sun, short fibers and/or low-fiber densities will be required.

Even with short fibers for the ASR, the thermal performance in direct sun will be impacted by the optical characteristics of the fiber and base materials. As described in Figure 4-8, as the base emissivity is increased, the effects of surface geometry to enhance overall emissivity are diminished as one would expect. Even with short fibers ( $L/d = 1$ ), the low material absorptivity can lead to substantially higher absorptivity in the ASR.

This is further demonstrated in Figure 4-9. Here, the ratio of heat rejection by the ASR relative to a standard radiator (emissivity = 0.8, absorptivity = 0.2) is examined as a function of operating temperature while operating in direct sun. Two different fiber area densities are highlighted. Operation of the ASR in direct sun within a 300-400 K operating range may not be feasible if fibers are tightly wound and can be characterized as solid surfaces. Because of absorptivity effects in these types of fiber bundles, operation in direct sun must be limited to over 500 K. Though not illustrated, operation of the ASR under the earth's albedo will allow enhanced thermal performance within the 300-400 K operating temperature.

The survivability of the ASR concept for some of the hostile threats is directly related to the increase in surface area provided by the ASR geometry. For convenience, the area enhancement is provided as a function of the ASR geometry in Figure 4-10. From a survivability perspective, certain threats will define a minimum area ratio. If the

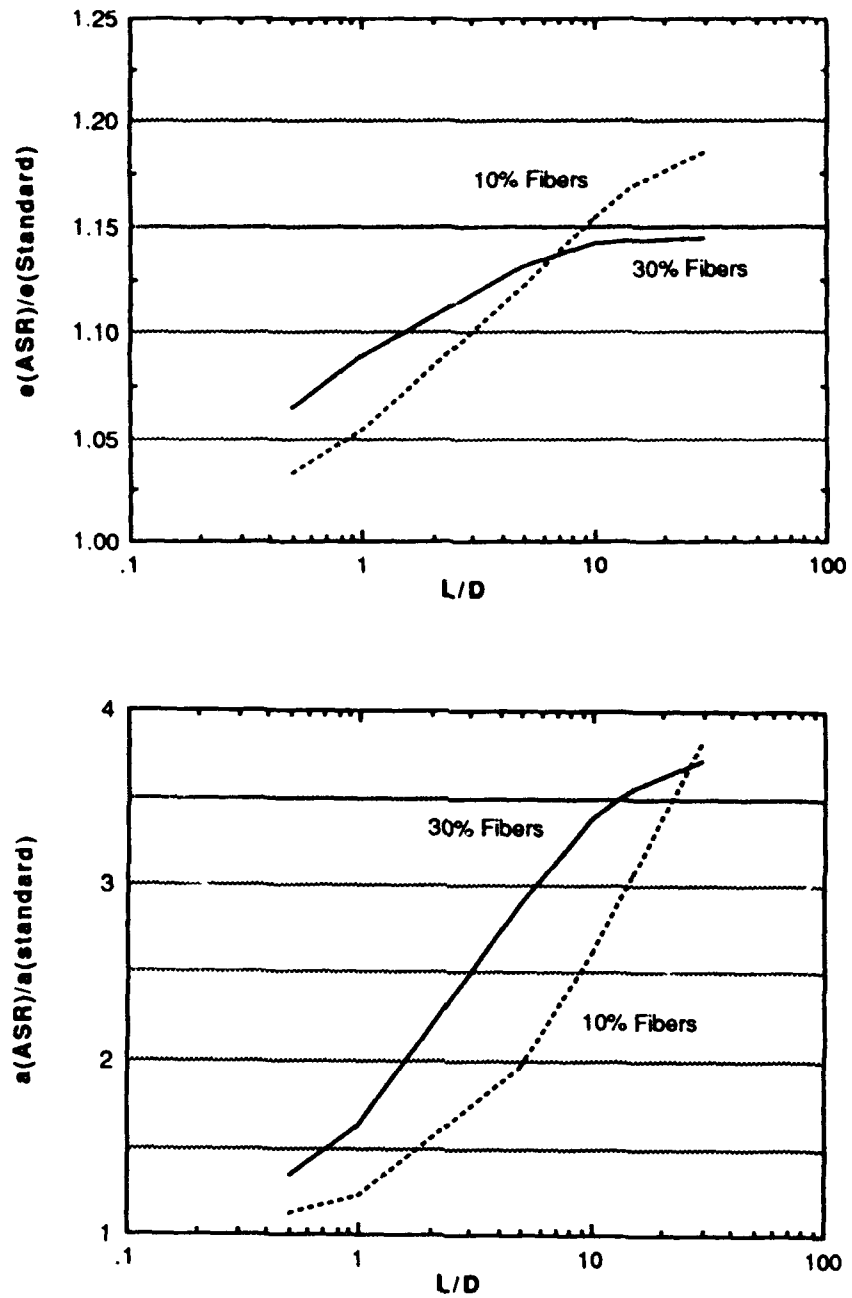


Figure 4-7. Emissivity and Absorptivity of ASR System Relative to that of Standard Radiator

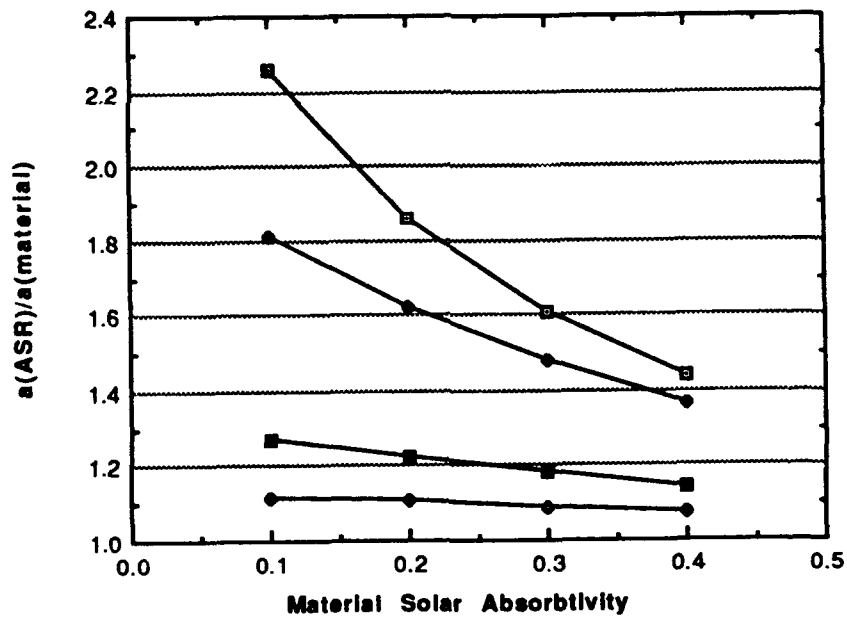
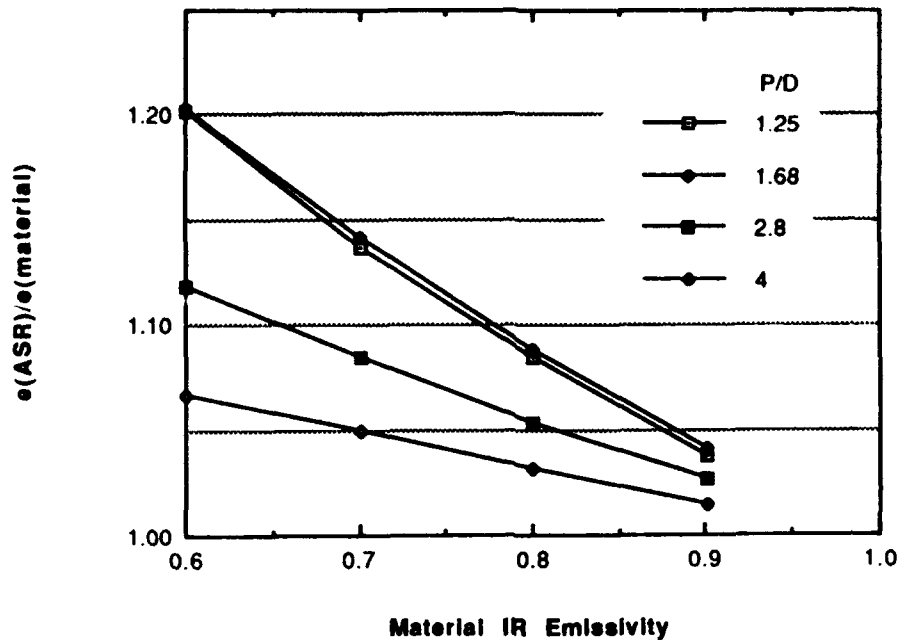


Figure 4-8. Plots Showing that as the Material Emissivity is Increased, the Effects of Surface Geometry Tend to Diminish the Overall Emissivity

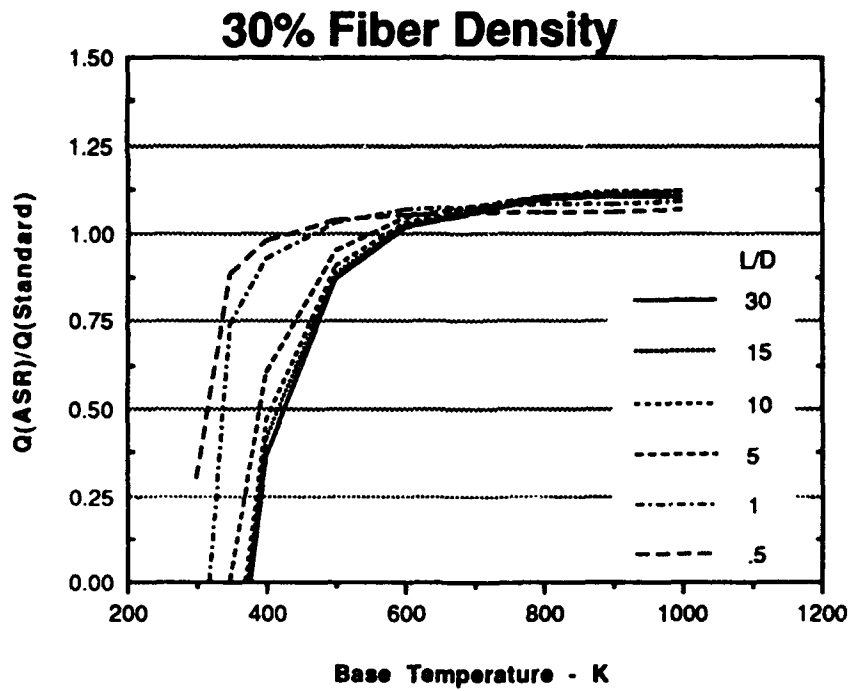
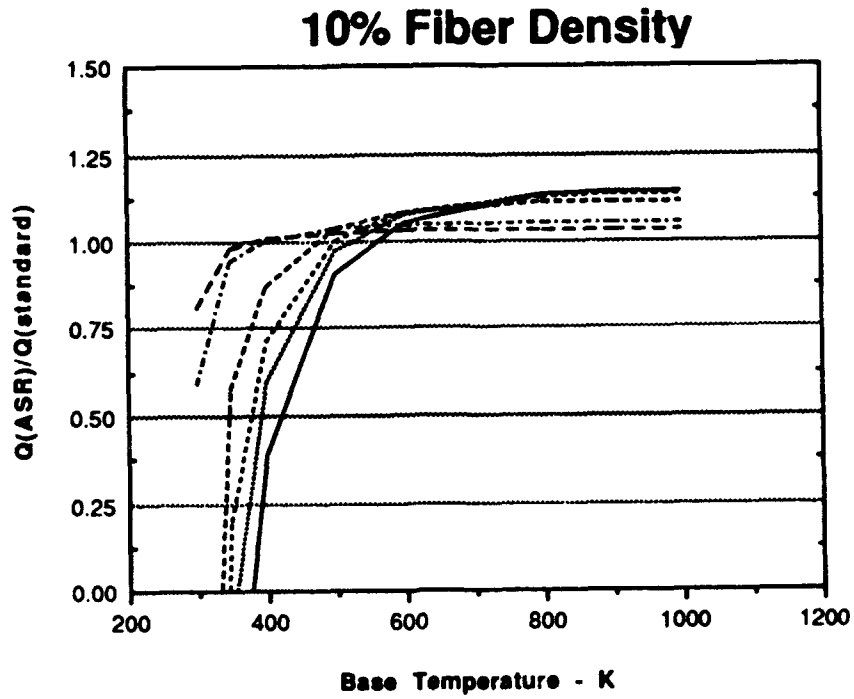


Figure 4-9. Effect of Fiber Density and Base Temperature on the Ratio of Heat Rejected by the ASR Relative to a Standard Radiator ( $\epsilon = 0.8$ ,  $\alpha = 0.2$ )

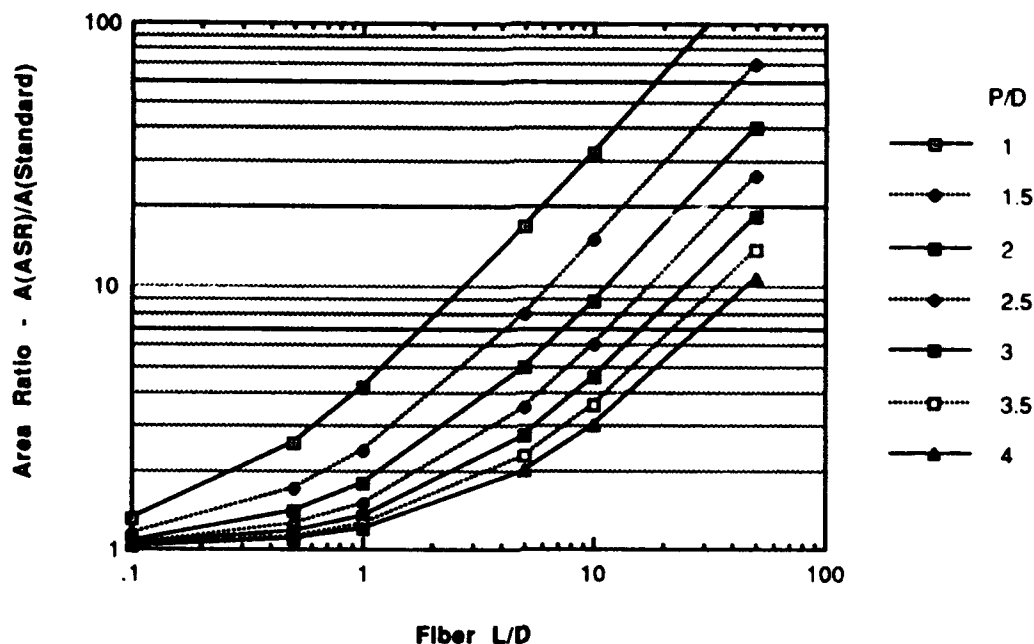


Figure 4-10. Area Enhancement as a Function of ASR Geometry

ASR must operate in direct sun, the move toward shorter fibers will lead to increased fiber density. This, in turn, will lead to a mass penalty over more optimal geometries.

In cases where short fibers are required, thermal conductivity requirements for isothermal fibers will easily be met. Estimates of fiber-temperature profile are highlighted in Figure 4-11 for a relatively short fiber ( $L/d=5$ ) configuration operating at 400 K. As can be seen, thermal conductivities larger than 1 W/m-K will result in nearly isothermal fibers.

As discussed earlier, the construction of fiber bundles can significantly influence the bundle optical characteristics. Bundle twist and bundle tightness can directly control transmissivity and hence bundle absorptivity. Using the volume scattering model described in Section 3, this effect was investigated. Characteristic results are presented in Figure 4-12. The absorptivity ratio is defined as the solar absorptivity of the ASR accounting for volume scattering divided by the solar absorptivity of the same configuration assuming diffuse surface reflectivity. ASR absorptance can be reduced by minimizing optical depth and maximizing single scatter albedo. If we can construct fiber bundles with these characteristics and meet the survivability requirements, we

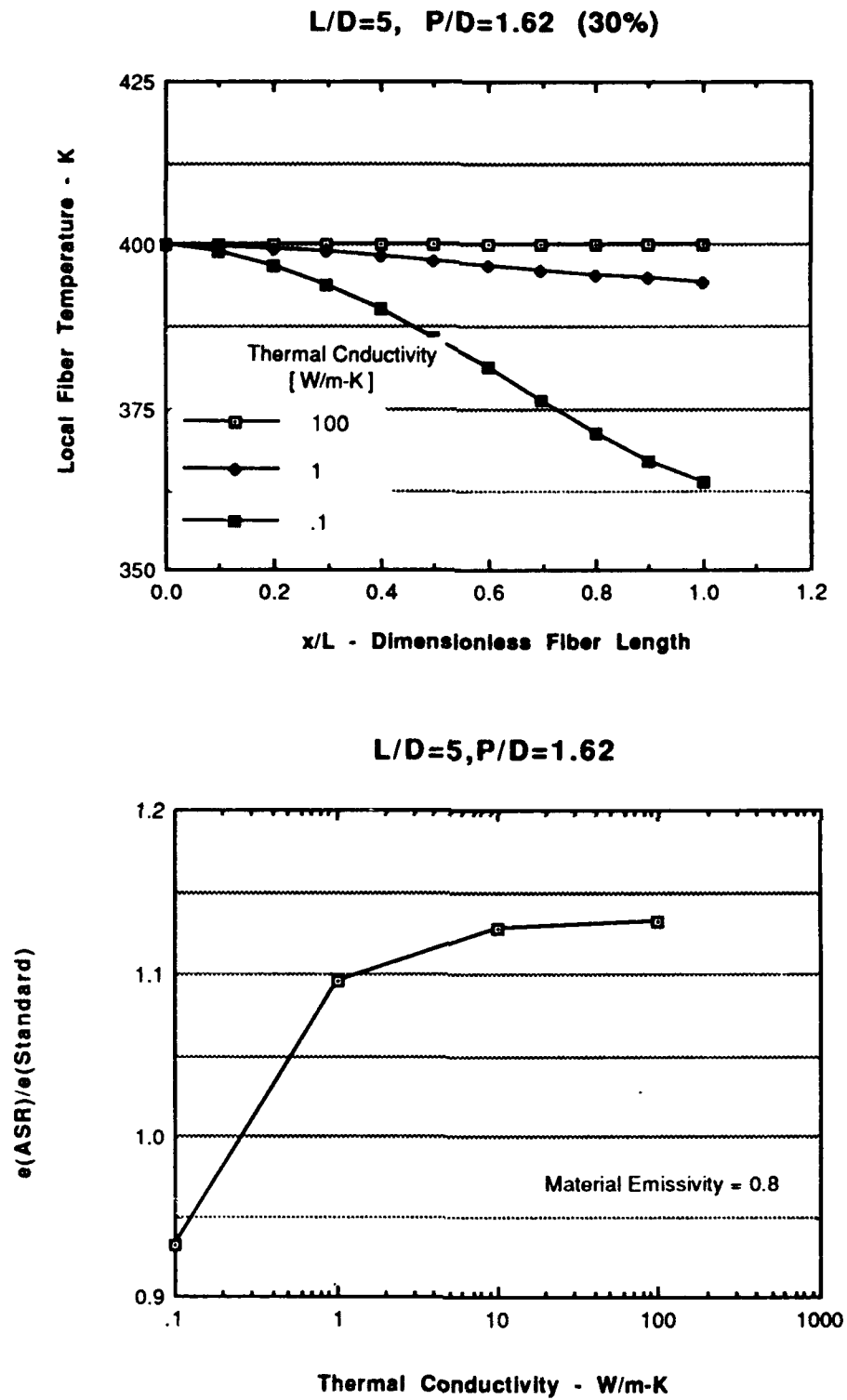


Figure 4-11. Effects of Fiber Conductivity on Both the Temperature Profile and the Emissivity Enhancement Ratio



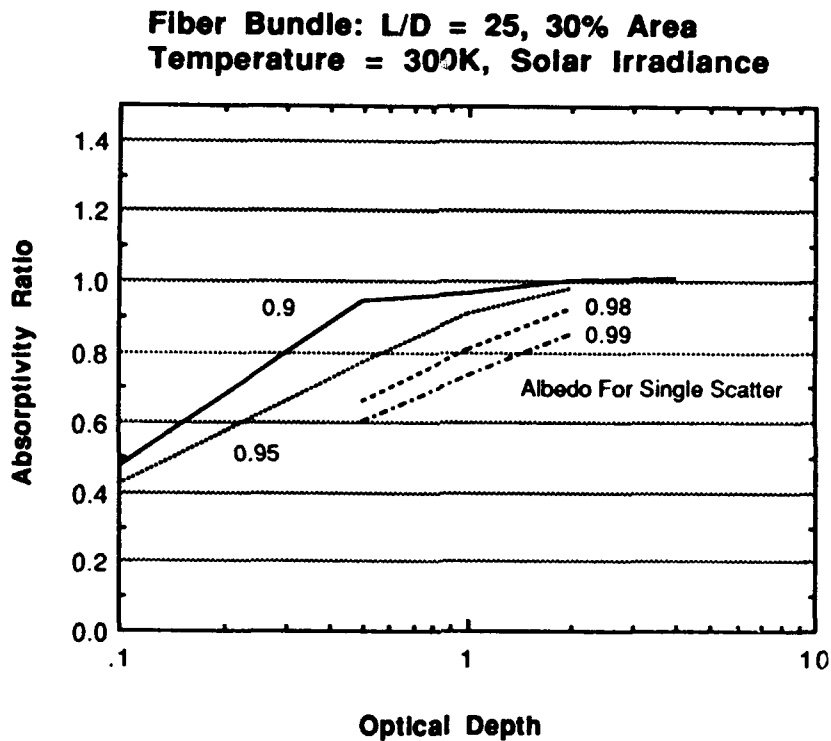


Figure 4-12. Effect of Partially Transmissive Fiber Bundles on ASR Absorptance

can significantly ease or even eliminate the constraints previously identified requiring short L/d fibers. This effect would result in a radiator design which would have enhanced thermal performance over a conventional flat-plate radiator even at temperatures of 300 K. The viability of this approach is tied to the attainability of a fiber bundle with a high single-scatter albedo and a low-optical depth. Because of the analysis difficulty this presents, parameter estimation will require testing of various materials and bundles.

#### 4.5 Response to a Laser Threat

As discussed previously, a significant constraint on the ASR will be its survivability to laser threats. We have performed top level parametrics to identify the impact of laser intensity and surface optical characteristics on the ASR steady-state operating temperatures. In this fashion, once we know temperature limits for viable fiber options, we can directly relate it to a maximum laser survivability. The approach taken is

shown in Figure 4-13. The radiator is assumed to be radiating at a temperature  $T$  on the front side and at a temperature  $pT$  on the backside. The parameter  $p$  varies between 0-1 and is dependent on the design of the radiator. The parameter  $p$  has unique limits: for  $p=1$  the radiator is isothermal and for  $p=0$  the backside of the radiator is effectively insulated. The radiator is uniformly irradiated by a laser of intensity  $I$ . The surface absorptivity to the laser wavelength is  $\alpha$  and the surface emissivity is  $\epsilon$ . A simple heat balance of the system gives rise to the indicated equation in Figure 4-13. Parametrics on the limits of  $p$  are shown in Figure 4-14. Superposition of the SUPER requirements on these figures identifies the maximum surface temperature as a function of surface absorptivity and emissivity. The worst case condition will occur for lasers operating in the IR where  $\alpha = \epsilon$ . For lasers operating in other spectral regions (HF for example) the surface temperature is strongly dependent on the surface absorptivity. Hence, we were able to create a credible model for the effectiveness of ASR in the face of a laser threat.

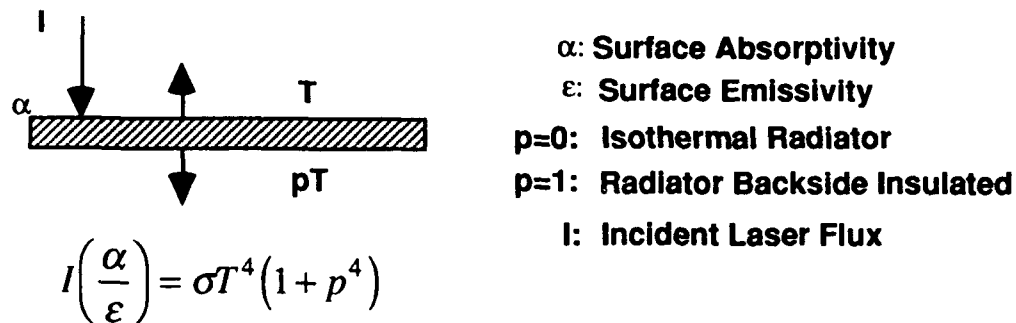


Figure 4-13. Laser Response Model

We assembled a comprehensive list of currently manufactured fiber options. This list, shown in Figure 4-15, incorporates available thermophysical data. We developed the last column from the parametric approach taken above. This column indicates the maximum allowable laser intensity for a given  $(\alpha/\epsilon)$  ratio. The dual numbers in the last column represent two different radiator configurations. The lower of the numbers is representative of radiator configurations for which the backside of the radiator is effectively insulated ( $p=0$ ). The higher number is representative of an isothermal radiator where the backside is radiating to space ( $p=1$ ). For  $\text{CO}_2$  laser threats,  $(\alpha/\epsilon)$  is nearly unity so the last column gives the maximum intensity directly. For other laser threats,  $(\alpha/\epsilon)$  can range from 0.2 to 0.5. In these cases the maximum laser intensity

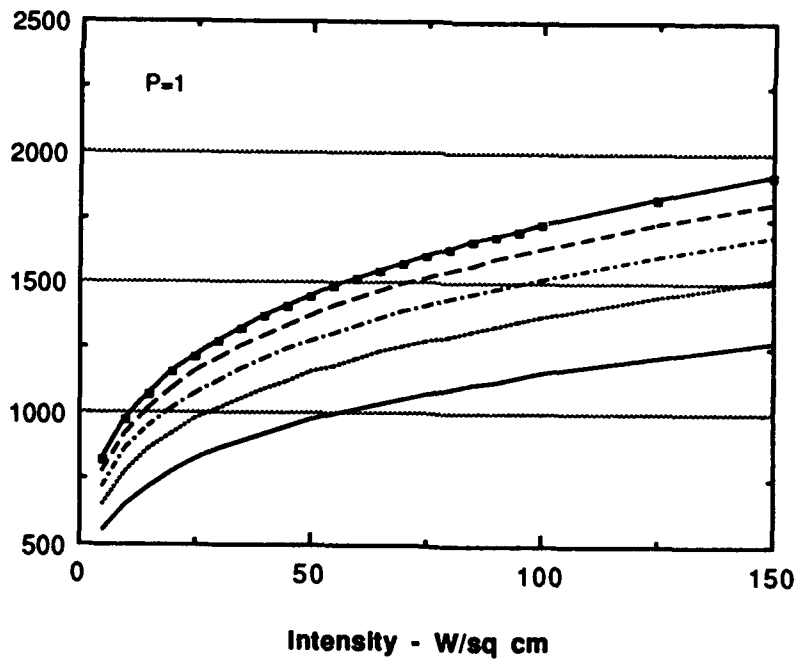
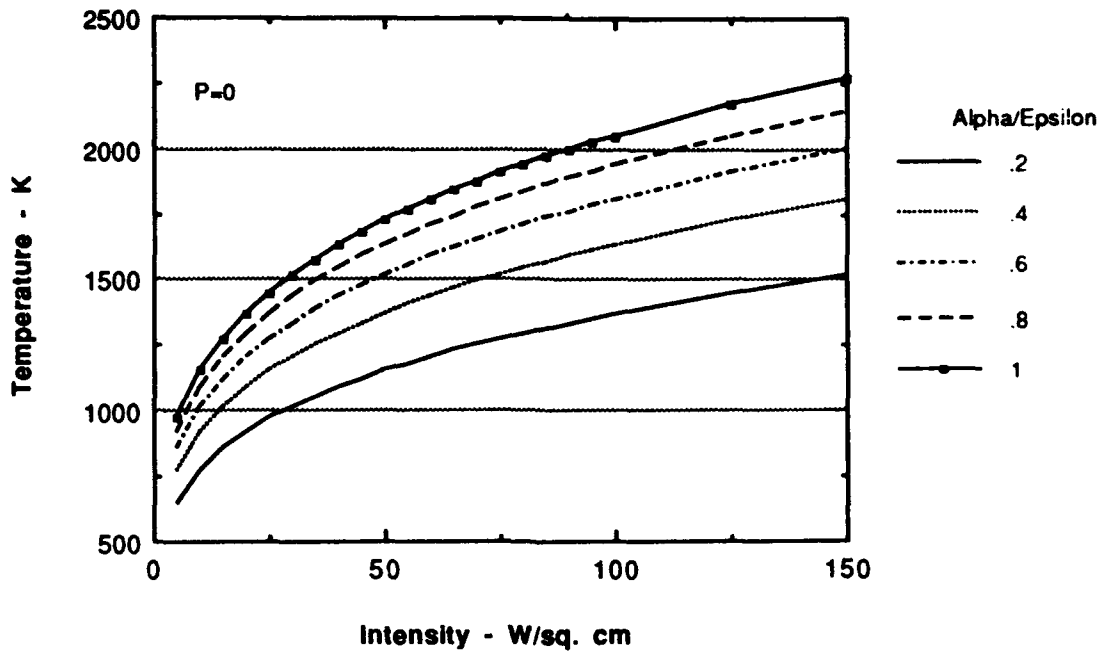


Figure 4-14. Impact of Laser Intensity on Radiator Temperature

Fiber	Category	Form	Max Use Temp (K)	Manufacturer, Product Name	Chemical Composition	Filament Diameter (Microns)	Coeff. Thermal Expansion ppm per degree F	Thermal Conductivity W/m-K	Density, (g/cc)	k(ave) - (W/cm <sup>2</sup> ) 1-side 2-side
S- Glass	Glass	Continuous	616	Owens Corning, S- Glass	65% SiO <sub>2</sub> 25% Al <sub>2</sub> O <sub>3</sub> 10% MgO	7	3.1	approx. 10.0	2.49	0.8 1.6
Quartz	Glass	Continuous	1350 +	JP Stevens, Astroquartz II	99.99% SiO <sub>2</sub>	9	0.3	1.4	2.20	19 38
Carbon	Carbon	Continuous	1900 +	Hercules, AS-4, IM-6,	100 % carbon from polyacrylonitrile (PAN)	8.0 5.5			1.80 1.73	74 148
Carbon	Carbon	Continuous	1900 +	Amoco, T-50, T-300, T-500	100 % carbon from polyacrylonitrile (PAN)	6.5 7.0 7.0	-0.4 -0.3 -0.3	69 8.6 8.6	1.81 1.76 1.79	74 148
Carbon	Carbon	Continuous	1900 +	Amoco, P-55S, P-75S, P100S, P120S	100 % carbon from coal tar pitch	10 10 10 10	-0.70 -0.75 -0.78 -0.8	109 185 519 609	2.0 2.08 2.15 2.18	74 148
Nickel Carbon	Carbon	Continuous	810 +	American Cyanamid, Cycom NCG Nickel Plated Graphite	40 WT % Nickel 60 WT % Carbon	7.6			3.0	2.5 5
Copper Carbon	Carbon	Continuous	810 +	American Cyanamid, Copper Plated Graphite	WT % Copper 26 WT % Carbon	8				2.5 5
Boron over Tungsten	Boron	Continuous	2200	Textron Specialty Materials, Lowell, MA,	Boron, over 12.7 micron Tungsten wire	100 or 140	4.6		2.57 for 100μ 2.50 for 140μ	133 266
Boron over Carbon	Boron	Continuous	2200	Textron Specialty Materials, Lowell, MA,	Boron, over Pitch Based Carbon					133 266

Figure 4-15. Fiber Material Options

Fiber	Category	Form	Max Use Temp (K)	Manufacturer, Product Name	Chemical Composition	Filament Diameter (Microns)	Coeff. Thermal Expansion ppm per degree F	Thermal Conductivity W/m-K	Density, (g/cc)	(a/s) - (W/cm <sup>2</sup> ) 1-side 2-side
Silicon Carbide	Ceramic	Continuous	1350 +	Dow Corning, Nicalon	Impure $\beta$ -SiC using Polymer Precursor	10 to 20		11.6	2.3 to 2.6	19 38
Silicon Carbide	Ceramic	Continuous	1350 +	Dow Corning, Nicalon	Impure $\beta$ -SiC using CVD	140		11.6	3.05	19 38
Alumina	Ceramic	Continuous	1250	DuPont	100% $Al_2O_3$	20		35 (as single crystal)	3.9	14 28
Alumina Boria Silica	Ceramic	Continuous	1650	3 M Co., Nextel 440	70 % $Al_2O_3$ 28 % $SiO_2$ 2 % $B_2O_3$	10 to 12	2.43		3.05	42 84
Alumina Boria Silica	Ceramic	Continuous	1480	3 M Co., Nextel 312	62 % $Al_2O_3$ 24 % $SiO_2$ 14 % $B_2O_3$	10 to 12	1.67		2.7	27 54
Silicon Nitride	Ceramic	Continuous	1480 +		100% $Si_3N_4$ from organic precursor		1.5	14 to 33	< 3.44	27 54
Silicon Nitride Carbide	Ceramic	Continuous	1366	NASA-MSFC, Huntsville, AL	$Si_3N_4C_2$	25 to 100			< 3.44	20 40
Silicon Nitride Carbide	Ceramic	Continuous	1366	Dow Corning, HPZ SiNC	$Si_3N_4C_2$	8 to 15			2.3 to 2.5	20 40
Silicon Titanium Carbon Oxygen	Ceramic	Continuous	1530 +	Textron Specialty Materials, Lowell, MA, Tyranno	$Si_2Ti_3N_2O_1$	8 to 10	1.72		2.3 to 2.5	31 62
PBI	Organic	Continuous	720 (air) 1280 (vacuum)	Hoechst Celanese, Charlotte, NC, PBI	Poly 2,2'-(m-phenylene)-5,5'-bibenzimidazole. $C_{20}H_{12}N_4$	11 to 21		0.35	1.43	vacuum 15 30
LCP	Organic	Continuous	560	Hoechst Celanese, Liquid Crystal Polymer-LCP	Aromatic Copolyester	23			1.4	0.5 1.0

Figure 4-15 (cont.). Fiber Material Options

Fiber	Category	Form	Max Use Temp (K)	Manufacturer, Product Name	Chemical Composition	Filament Diameter (Microns)	Coeff. Thermal Expansion ppm per degree F	Thermal Conductivity $\frac{W}{m-K}$	Density, (g/cc)	$k(a/c) - (W/cm^2)$ 1-side 2-side
PE	Organic	Continuous	380	Allied Signal, Spectra 900, Spectra 1000	Oriented Ultra High Molecular Weight Polyethylene	38 $\mu$ for Spectra 900 and 27 $\mu$ for Sp. 1000		0.33	0.97	0.1 0.2
Aramid	Organic	Continuous	533	DuPont, Kevlar 49	Para-aramid, Highly aromatic Polyamide	12			1.44	0.45 0.90
Aramid	Organic	Continuous	533	DuPont, Nomex	Meta-aramid, Highly aromatic Polyamide	15 to 17	11.0		1.38	0.45 0.90
Nylon 6/6	Organic	Continuous	420	DuPont, Nylon 6/6	$C_{12}H_{10}O_2N_2$	100 to 200	50	0.24	1.14	0.18 0.36
PEK	Organic	Continuous	540	ICI, PEK	Polyether ketone, $C_{13}H_8O_2$	33			1.32	0.5 1.0
PEEK	Organic	Continuous	520	ICI, PEEK	Polyether-etherketone, $C_{18}H_{12}O_3$	33			1.32	0.5 1.0
Stainless Steel	Metal	Continuous	1366	Commercial, 304 Series Stainless	Iron, chromium, nickel, carbon	12	9.56	17	8.0	20 40
Copper	Metal	Continuous	1090 +	Commercial	100% Copper	25 to 250	9.17	391	8.96	8 16
Copper Beryllium Cobalt	Metal	Continuous	1090 +	Commercial	97% Copper 2% Beryllium 1% Cobalt	50 to 250	5.5	105	8.26	8 16
Copper Nickel Beryllium	Metal	Continuous	1090 +	Commercial	58.8% Copper 30% Nickel 1.2% Beryllium	50 to 250	9	30	8.6	8 16
Gold	Metal	Continuous	1090 +	Commercial	100% gold	25 to 250		297	19.3	8 16
Silver	Metal	Continuous	1090 +	Commercial	100% silver	25 to 250		429	10.5	8 16

Figure 4-15 (cont.). Fiber Material Options

would be given by two to five times the values indicated. Comparing these values to the SUPER requirements allows an initial screening of the fiber materials.

We analyzed the ASR fiber option matrix to identify viable fiber options which could meet the SUPER laser requirements. We identified fourteen options which are summarized in Table 4-1. A majority of the options are ceramic fibers (Silicon Nitride, Alumina Boria Silica, etc.) which provide high peak temperatures. Optical characteristics of these nonconductors should include high IR emissivity and low solar absorptivity. Although we identified additional material options, such as Boron Nitride as being promising, they are currently not available in fiber form. We restricted this table to fiber options which were commercially available. Samples of all of the key fibers identified in the above Table were obtained for further characterization tests.

#### **4.6 Nuclear Environment**

Trade studies on the performance of the various fiber materials in a nuclear environment were carried out.

#### **4.7 Fiber Options**

We previously identified potential fiber materials capable of meeting the imposed laser survivability requirements. We examined these options from two additional perspectives, thermal performance and nuclear hardness, in order to develop a finalized set of options capable of meeting the stressing SUPER requirements. Table 2-3 summarizes this list. While all of the materials exhibit high-temperature characteristics required for laser survivability, we discarded a few of the materials because of their thermal performance. The boron-coated fibers are characteristically a dark material and will have high solar absorptivity. Boron over tungsten has the additional problem of a low nuclear hardness. Silicon carbide is another fiber that is characteristically dark in the solar spectrum and will lead to unacceptable solar absorption. The remainder of the materials exhibit a "white" or "gray" appearance in the solar spectrum and "black" in the IR spectrum, and will lead to acceptable thermal performance. Technical data sheets of various fibers are included in Appendix B.

Table 4-2. Viable Fiber Options Which Meet the Super Laser Requirements

Fiber	Category	Form	Max Use Temp (K)	Manufacturer, Product Name	Chemical Composition	Filament Diameter (Microns)	Coeff. Thermal Expansion ppm per degree F	Thermal Conductivity $\frac{W}{m-K}$	Density, (g/cc)
Quartz	Glass	Continuous	1350 +	JP Stevens, Astroquartz II	99.99% SiO <sub>2</sub>	9	0.3	1.4	2.20
Boron over Tungsten	Boron	Continuous	2200	Textron Specialty Materials, Lowell, MA	Boron, over 12.7 micron Tungsten wire	100 or 140	4.6		2.57 for 100 $\mu$ 2.50 for 140 $\mu$
Carbon	Carbon	Continuous	1900 +	Hercules, AS-4, IM-6	100 % carbon from polyacrylonitrile (PAN)	8.0 5.5			1.80 1.73
Boron over Carbon	Boron	Continuous	2200	Textron Specialty Materials, Lowell, MA	Boron, over Pitch Based Carbon				
Silicon Carbide	Ceramic	Continuous	1350 +	Dow Corning, Nicalon	Impure B-SiC using Polymer Precursor	10 to 20		11.6	2.3 to 2.6
Silicon Carbide	Ceramic	Continuous	1350 +	Dow Corning, Nicalon	Impure B-SiC using CVD	140		11.6	3.05
Alumina	Ceramic	Continuous	1250	DuPont	100% Al <sub>2</sub> O <sub>3</sub>	20		35 (as single crystal)	3.9
Alumina Boria Silica	Ceramic	Continuous	1650	3 M Co., Nextel 440	70 % Al <sub>2</sub> O <sub>3</sub> 28 % SiO <sub>2</sub> 2 % B <sub>2</sub> O <sub>3</sub>	10 to 12	2.43		3.05
Alumina Boria Silica	Ceramic	Continuous	1480	3 M Co., Nextel 312	62 % Al <sub>2</sub> O <sub>3</sub> 24 % SiO <sub>2</sub> 14 % B <sub>2</sub> O <sub>3</sub>	10 to 12	1.67		2.7
Silicon Nitride	Ceramic	Continuous	1480 +		100% Si <sub>3</sub> N <sub>4</sub> from organic precursor		1.5	14 to 33	< 3.44
Silicon Nitride Carbide	Ceramic	Continuous	1366	NASA-MSFC, Huntsville, AL	Si <sub>x</sub> N <sub>y</sub> C <sub>z</sub>	25 to 100			< 3.44
Silicon Nitride Carbide	Ceramic	Continuous	1366	Dow Corning, HPZ SiNC	Si <sub>x</sub> N <sub>y</sub> C <sub>z</sub>	8 to 15			2.3 to 2.5
Silicon Titanium Carbon Oxygen	Ceramic	Continuous	1530 +	Textron Specialty Materials, Lowell, MA, Tyranno	Si <sub>x</sub> Ti <sub>y</sub> N <sub>z</sub> O <sub>t</sub>	8 to 10	1.72		2.3 to 2.5
Stainless Steel	Metal	Continuous	1366	Commercial, 304 Series Stainless	Iron, chromium, nickel, carbon	12	9.56	17	8.0



#### 4.8 The ASR Feasibility Design Space.

The initial trade studies were integrated to assess the level of improvement the ASR concept provides over conventional survivable radiator concepts and assess the concept feasibility design space. This approach is conceptually outlined in Figure 4-16. We have defined an ASR feasibility design space which is a function of hardness requirements (laser and nuclear) and operating temperature. This figure shows a cut through this design space for one particular operating temperature.

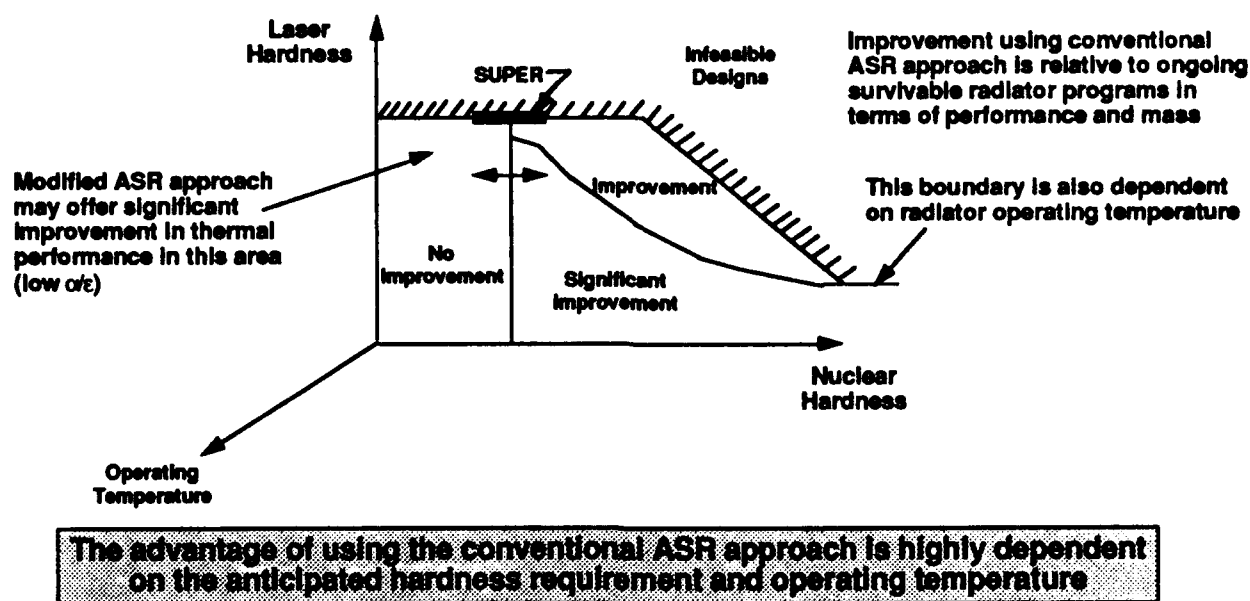


Figure 4-16. Qualitative ASR Feasibility Design Space

The design space is bounded on the vertical axis by the worst case SUPER laser threat. This boundary is limited by material constraints. Depending on the imposed requirements, the ASR concept can offer little or no improvement up to significant improvement. At the lower end of the SUPER nuclear requirements, there are few material effects from the nuclear environment, and so the ASR special features will be of little benefit. At high nuclear levels, the improvement in hardness is a function of not only the ASR special features but also the fiber material selection. At low laser hardness requirements (relative to SUPER) suitable fiber choices are available that lead to unprecedented nuclear hardness. As the laser threat increases at a given nuclear hardness, material selections become constrained to ceramic fibers. These

fibers in combination with the ASR special features still offer enhanced survivability over conventional survivable radiators. The improvement boundary is a function of the radiator operating temperature. This dependence on temperature is due to the fact that the ASR absorptance characteristics are dependent on the ASR geometry. In general, as the operating temperature increases, the region of significant improvement also increases.

## **5. CONCLUSIONS**

Based on the trade studies completed under Task 1.1, the following are conclusions about the feasibility of the ASR concept:

- The thermal performance of the three-dimensional ASR surface geometry has been well characterized for specular, diffuse and transmissive fiber bundles.
- The ASR geometry enhances surface emissivity to near unity values. Optimal fiber pitch and lengths were identified as a function of effective axial thermal conductivity.
- Fiber conductivity scaling parameters and limits were defined to ensure increased emissivity from the geometric surface configuration. These limits were not found to be important for low-temperature radiator applications.
- Geometry induced absorptivity changes are greater than emissivity changes. This presents potential problems for ASR configurations operating in direct insolation.
- Use of transmissive fiber bundles having high single-scatter albedo and low optical depth could alleviate absorptivity issues and allow operation in direct insolation at low-operating temperatures.
- ASR materials and geometries were identified that could withstand repeated SUPER survivability goals. Marginal mass effectiveness at the SUPER threats was identified.
- A feasibility map for the ASR concept was identified. While the ASR met or exceeded SUPER goals, its ultimate effectiveness occurred at higher nuclear threats and lower laser threats. In this case superior mass effectiveness was identified.

## **6. REFERENCES**

1. G.W. Glover, "Modeling the Advanced High Performance Radiator," MDC Report 93H0039, January 1993.

**Appendix A**  
**Program Statement of Work**

This appendix summarizes the ASR program as originally envisaged by the Wright Laboratory. MDSSC completed Task 1.1, Trade Studies, before termination of the program. This appendix will also serve as potential planning material in the event future effort in this technology is revived.

## **A.0 PROGRAM TASK SUMMARY**

The ASR development program consists of a two-phase effort. In Phase 1, MDSSC will assess the feasibility of the ASR approach and will evaluate and develop design options through an iterative process of design, analysis, and test. During Phase 2, MDSSC will design, fabricate, and test prototype radiators consisting of heat pipes integrated into the ASR concept. MDSSC will conduct thermal performance and survivability tests on these prototypes to establish the suitability of the ASR for application to near term AF and SDI systems. The Program Plan tasks presented below are in compliance with the contractual Statement of Work.

### **A.1 (SOW 4.0) PHASE 1 FEASIBILITY DEMONSTRATION**

This effort includes all necessary investigations, parametric analysis, supporting technology assessments, analytical and experimental investigations, conceptual designs, experimental hardware development, and testing to meet the requirements outlined below.

#### **A.1.1 (SOW 4.1) TASK 1.1: TRADE STUDIES**

MDSSC will develop ASR concepts to meet or exceed the SUPER survivability requirements. MDSSC will employ the ASR material approach, as outlined in the technical proposal, to meet these requirements. MDSSC will perform parametric analyses of the thermal performance and the survivability of the radiator concepts. Based on the results of these analyses, MDSSC will select three preferred concepts for further development. MDSSC will develop plans for subsequent analysis, design, and test efforts, and present them to the Air Force for review and approval prior to proceeding past Task 1.2 (SOW 4.2).

#### **A.1.2 (SOW 4.2) TASK 1.2: CHARACTERIZATION TESTS**

MDSSC will measure thermal, mechanical and optical properties of wires, fibers, and carpet materials as required to support parametric analyses conducted under Task 1.1 (SOW 4.1). Measurements will include thermal conductivity, spectral reflectance and transmittance, and thermal expansion coefficient.

#### **A.1.3 (SOW 4.3) TASK 1.3: PROTOTYPE PRELIMINARY DESIGN**

MDSSC will develop preliminary prototype designs for the three ASR concepts developed in Task 1.1 (SOW 4.1). These designs will incorporate results from Task 1.4 (SOW 4.4) and Task 1.5 (SOW 4.5) and will be the basis for the prototype development and testing of Phase 2. The preliminary designs will identify all materials and define preliminary fabrication procedures.

#### **A.1.4 (SOW 4.4) TASK 1.4: PERFORMANCE ANALYSIS**

MDSSC will analyze the thermal performance (SOW 4.4.1 and 4.4.2) of the prototype preliminary designs developed in Task 1.3 (SOW 4.3) as well as their response to relevant natural and hostile threats (SOW 4.4.3).

##### **SUBTASK 1.4.1: HEAT PIPE ANALYSIS (SOW 4.4.1)**

MDSSC will perform the necessary analyses to characterize the performance of the heat pipe designs developed in Task 1.3 (SOW 4.3). These analyses will optimize the design parameters and verify that the designs satisfy all of the performance requirements.

##### **SUBTASK 1.4.2: ASR MATERIAL THERMAL ANALYSIS (SOW 4.4.2)**

MDSSC will analytically characterize the thermal performance of the ASR surface material developed in Task 1.3 (SOW 4.3). MDSSC will use detailed thermal transport models to optimize the design parameters and verify that the designs satisfy all of the performance requirements.

### **SUBTASK 1.4.3: SURVIVABILITY ANALYSIS (SOW 4.4.3)**

MDSSC will analytically determine the survivability performance of the ASR surface material under natural and hostile threats as defined in the SUPER Survivability Specifications.

### **A.1.5 (SOW 4.5) TASK 1.5: DEVELOPMENT TESTS**

MDSSC will, in parallel with the prototype design and analysis efforts, conduct development tests to investigate fabrication techniques, thermal performance, and survivability of the ASR concepts.

#### **SUBTASK 1.5.1: FABRICATION TECHNIQUES (SOW 4.5.1)**

MDSSC will evaluate various ASR surface material fabrication and material attachment techniques. MDSSC will fabricate three ASR surface material configurations and attach them to representative radiation surfaces in sufficient quantity to perform the thermal performance and survivability tests of Subtasks 1.5.2 and 1.5.3 (SOW 4.5.2 and 4.5.3).

#### **SUBTASK 1.5.2: RADIATOR PERFORMANCE (SOW 4.5.2)**

MDSSC will experimentally characterize the thermal performance of three ASR surface material configurations. The configurations will be those identified in Task 1.1 (SOW 4.1) and developed under Task 1.5.1 (SOW 4.5.1). As MDSSC refines the designs to incorporate the results of development tests, MDSSC will conduct additional thermal performance tests.

#### **SUBTASK 1.5.3: SURVIVABILITY TESTS (SOW 4.5.3)**

MDSSC will fabricate and test samples of the ASR surface material in a high energy CW laser environment and under impact by projectiles typical of kinetic energy weapons, micrometeoroids and space debris. The test samples will be representative of the ASR concepts selected for further development in Task 1.1 (SOW 4.1). The tests will include sufficient instrumentation and sufficient range of test conditions to establish survivability levels for the ASR concepts and to verify the accuracy of the analytical models used to predict the ASR performance in Task 1.4 (SOW 4.4). MDSSC will



evaluate the data from these tests, as well as those from Underground Nuclear Tests of the ASR surface material performed on independent programs in terms of their implications to the ASR designs.

#### **A.1.6 (SOW 4.6) TASK 1.6: PHASE 2 PLANNING**

MDSSC will develop a plan for the detailed design, fabrication, and demonstration testing of the selected prototype ASR designs. The plan will include the preliminary prototype designs developed in Task 1.3 (SOW 4.3). It will identify all material suppliers and describe facilities for fabricating the ASR surface material. Plans for testing the prototype thermal performance and survivability to natural and hostile threats as defined by the SUPER Survivability Specifications will include facility descriptions and test conditions. MDSSC will await written approval from the government Program Contracting Officer (PCO) prior to proceeding into Phase 2.

#### **A.2 PHASE 2 PROTOTYPE DEVELOPMENT AND TEST**

Upon written approval from the government PCO, MDSSC will design, fabricate, and test a functional prototype ASR. The prototype ASR will be tested under simulated launch and space environment conditions, and its thermal performance and survivability as defined in the SUPER Survivability Specifications will be demonstrated.

##### **A.2.1 (SOW 4.7.1) TASK 2.1: PROTOTYPE DETAILED DESIGN**

MDSSC will develop detailed designs for the most promising prototype ASR employing the ASR surface material concept. The government contract monitor will determine the most promising prototype ASR. The design will be based on the preliminary prototype designs developed in Task 1.3 (SOW 4.3) and will incorporate the results of Task 2.2 (SOW 4.7.2). The design will be of sufficient detail to permit hardware fabrication of a functional ASR.

##### **A.2.2 (SOW 4.7.2) TASK 2.2: PRETEST ANALYSIS**

MDSSC will analyze the performance of the detailed prototype design developed in Task 2.1 (SOW 4.7.1) and predict its behavior in the thermal performance and survivability tests of Tasks 2.5 (SOW 4.7.5) and 2.6 (SOW 4.7.6). MDSSC will make design recommendations and will identify instrumentation requirements.

### **A.2.3 (SOW 4.7.3) TASK 2.3: PROTOTYPE FABRICATION**

MDSSC will fabricate a functional prototype heat pipe radiator according to the detailed design developed in Task 2.1 (SOW 4.7.1). MDSSC will fabricate and instrument sufficient quantities of the prototype ASR to permit complete characterization of the thermal performance and the survivability of the functional ASR concept in Tasks 2.4 (SOW 4.7.4), 2.5 (SOW 4.7.5), and 2.6 (SOW 4.7.6).

### **A.2.4 (SOW 4.7.4) TASK 2.4: ENVIRONMENTAL TESTING**

MDSSC will perform functional testing with the prototype ASR to simulate acoustic, shock, and vibration conditions during launch as defined by the SUPER Survivability Specifications.

### **A.2.5 (SOW 4.7.5) TASK 2.5: RADIATOR PERFORMANCE TESTING**

MDSSC will plan and conduct tests to establish the heat transport performance of the functional prototype ASR. MDSSC will test 15 functional ASR prototypes before and after exposure to natural and hostile threats.

### **A.2.6 (SOW 4.7.6) TASK 2.6: SURVIVABILITY TESTING**

MDSSC will gear the survivability testing performed during this phase toward concept validation rather than development testing. MDSSC will accomplish three types of testing: Nuclear X-rays, CW Laser, and Hypervelocity projectiles.

### **A.2.7 (SOW 4.7.7) TASK 2.7: DATA ASSESSMENT AND DESIGN IMPLICATIONS**

MDSSC will assess the results of the performance and survivability tests, performed in Tasks 2.5 (SOW 4.7.5), and 2.6 (SOW 4.7.6), and determine the accuracy of the analytical models. MDSSC will modify the models as required. MDSSC will then develop concepts for applying the ASR designs to near term SDI systems, as determined by the government contract monitor, and assess the impact on the system survivability and performance using the validated models.

### **A.2.8 (SOW 4.9) TASK 2.8: RELIABILITY AND MAINTAINABILITY / DESIGN TO COST**

MDSSC will give consideration to the factor of reliability and maintainability. MDSSC will determine a prediction of the degree of reliability and maintainability based on the

techniques used to design and fabricate similar systems. MDSSC will develop and explain estimates of the relative cost of the proposed components.

**Appendix B**  
**Fiber Data Sheets**

# MITSUI MINING COMPANY LIMITED

NEW YORK OFFICE

TOWER 49

12 EAST 49TH STREET

21ST FLOOR

NEW YORK, NY 10017

PHONE: (212) 486-0473

FAX: (212) 486-9594

May, 1991

## ALMAX FIBER INFORMATION

ALMAX, the trade name pending application, is the AL-1000 and AL-1001 fiber manufactured by the Mitsui Mining Company Limited.

U.S. Representative office: Mitsui Mining Company Limited  
12 East 49th Street, 21st Floor  
New York, N.Y. 10017  
Tel. (212) 486-9473  
Fax (212) 486-9594

### COMPOSITION AND PROPERTIES OF ALMAX

Chemical Composition : 99.5 % or more  $\text{Al}_2\text{O}_3$

Sizing Agents : Epoxides, PVA

Microstructure : Polycrystalline

### FILAMENT

Filament Diameter : 10 micrometer

Filament Shape : Round

Filaments per strand : 1,000 filaments per strand

Twist: Not twisted  
(Twisted yarn sample is also available.)

Fiber manufacturing process: Dry spinning and continuous firing process

PRICE : 1991 price \$ 200-300/lb  
Projected Price \$ 60/lb

AVAILABILITY : Developmental, limited availability

CAPACITY : Several metric tons per year

May, 1991

MECHANICAL PROPERTIES

Handleability : Minimum radius of curvature: 5-7 mm.  
 Tensile Modulus :  $4.69 \times 10^7$  psi  
 Tensile Strength :  $2.56 \times 10^5$  psi  
 Elongation at break : 0.5 %  
 Maximum structural use temperature :  $1,400^\circ \text{C}$

## Dielectric Constant of Fiber / Epoxy Resin Matrix

	<u>Dielectric Constant (at room temperature)</u>				
	<u>1MHz</u>	<u>100MHz</u>	<u>500MHz</u>	<u>1GHz</u>	<u>Vf (%)</u>
ALMAX/Resin ( $\text{Al}_2\text{O}_3 = 99.5 \text{ wt\%}$ )	6.5	5.9	4.9	4.3	46

	<u>Tan (at room temperature)</u>				
	<u>1MHz</u>	<u>100MHz</u>	<u>500MHz</u>	<u>1GHz</u>	<u>Vf (%)</u>
ALMAX/Resin ( $\text{Al}_2\text{O}_3 = 99.5 \text{ wt\%}$ )	0.024	0.019	0.0033	0.0021	46

PHYSICAL PROPERTIES

Density :  $0.13 \text{ lbs/in}^3$   
 Crystal Phase :  $\alpha - \text{Al}_2\text{O}_3$

CHEMICAL COMPOSITION  $\text{Al}_2\text{O}_3$  : 99.5 % up

CHEMICAL PROPERTY : Chemically inert, stable for almost all kinds of chemicals, except for hydrofluoric at the elevated temperature

May, 1991

AVAILABLE FORMS:

Continuous Fiber " Yarn "  
Chopped Fiber  
(cut length : 0.5 mm, 1 mm, 3 mm,  
5mm, 6 mm and 10 mm)  
Woven Cloth  
(Plane Weave, 8 harness Stain etc.)  
(Braided Sleeves)  
(Tape)  
(Board)

ANTICIPATED APPLICATIONS:

Non - Composite :      Thermal Insulator  
                             Catalyst Carrier

Composites :

- Organic Composites      Armor plates  
                             Radome  
                             Sporting Goods

- Metal Composites      Automotive parts  
                             Aircraft engine parts  
                             Aerospace structural materials





11/90

## ALTEX FIBER

### PRODUCTS

Textron Specialty Materials is the distributor for Sumitomo's Altex® fibers and woven fabrics. High performance composites containing Altex fibers are used in turbine engines, airframes, cryostats, sporting goods, radomes and other high performance applications.

### FEATURES:

*Sumitomo's Altex Fiber has the following properties:*

- Continuous filaments
- High strength/high modulus
- Electrically insulating
- Stability in molten metals
- Stability at high temperatures in air\*
- Good handleability (can be woven)
- Radar transparent
- No galvanic corrosion

*\*Sumitomo Altex fiber retains 90% of its room temperature strength after heating at 1100 °C (2012 °F) in air for 200 hours.*

### TYPICAL PROPERTIES OF ALTEX FIBER

Chemical Composition	85% Al <sub>2</sub> O <sub>3</sub> , 15% SiO <sub>2</sub>
Density	3.25 g/cm <sup>3</sup> (0.117 lbs/in <sup>3</sup> )
Tensile Strength	1.8 GPa (260 ksi)
Tensile Modulus	210 GPa (30 msi)
Heat Capacity	0.71 kJ/kg K @ 298 K

### FIBER PRODUCTS ARE SPECIFIED USING A CODING SYSTEM:

**SA-BC-D** Example: **SN-10-1K**

- N** = No sizing
- 1** = 15 microns diameter
- 0** = No surface treatment
- 1K** = 1000 filaments per yarn

A	B	C	D
Sizing	Filament Diameter	Surface Treatment	Filaments per yarn
N = None X = Epoxy V = PVA	1 = 15 microns (Standard) 2 = 10 microns (Special) 3 = 22 microns (Special)	0 = None 1 = Organic Matrix 2 = Epoxy Resin Matrix	0.5K = 500 1 K = 1000

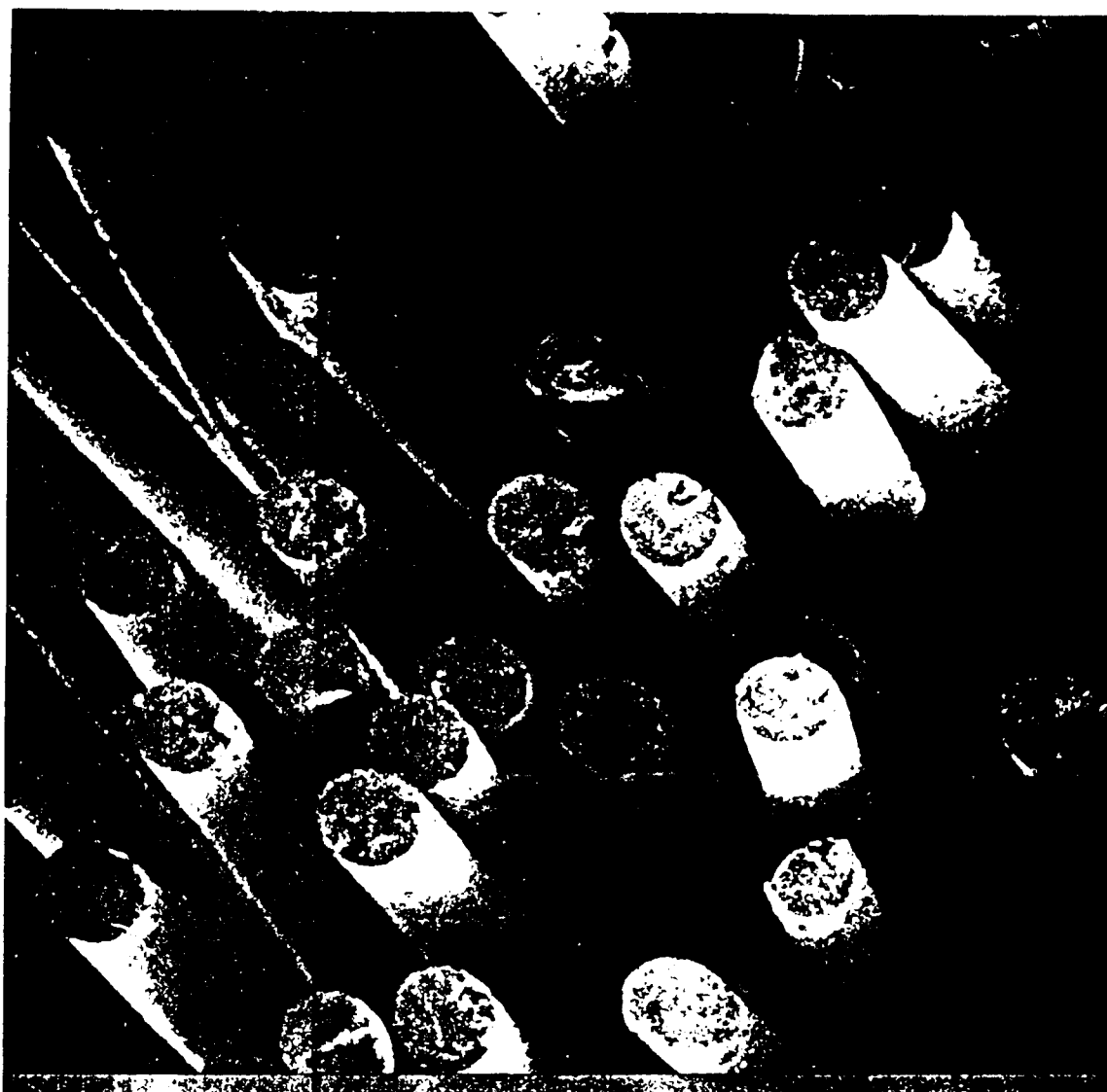
*Plain and Satin weave fabrics are available in various forms*

#### For additional assistance, contact:

Tom Foltz (technical and product form) 508-454-5341  
Mike Corcoran (price and availability) 508-454-5487

Textron Specialty Materials  
2 Industrial Avenue, Lowell, MA 01851  
TEL (508) 452-8961  
FAX (508) 454-5619

## ALTEX FIBER



**TEXTRON** Specialty Materials

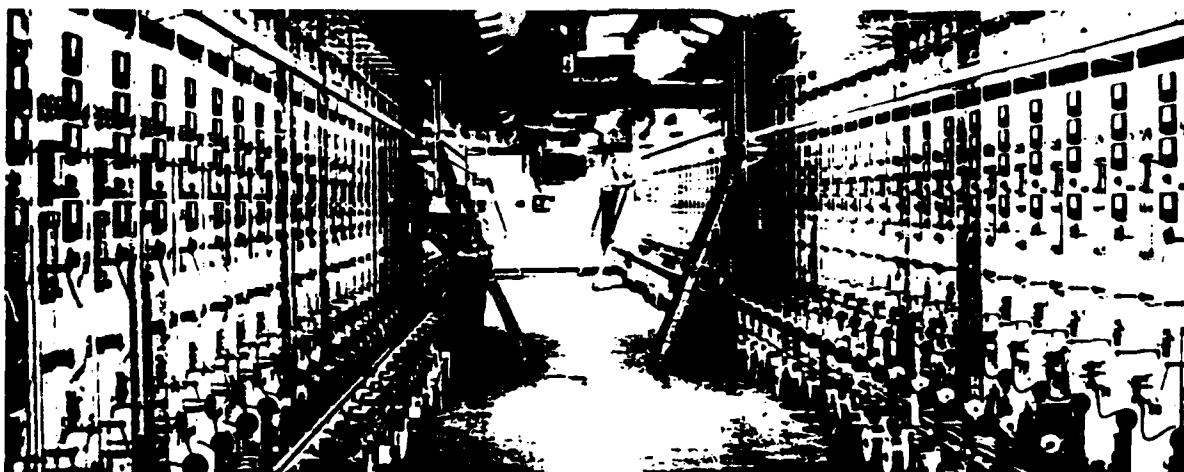


SUMITOMO  
CHEMICAL

## TEXTRON BORON CHARACTERISTICS FOR STRENGTH AND STIFFNESS AT MINIMUM WEIGHT

Continuous production of Textron Boron filament provides uniform, high-quality filament for use in the versatile Textron prepreg tapes, filament-wound structures, metal matrix composites, and reinforced structural elements. Manufacturing procedures are precisely controlled and constantly monitored to assure a consistent standard, reproducible filament in diameters of 4.0 and 5.6 mil (100 and 140  $\mu\text{m}$ ).

Textron Boron filament, acceptable for a wide variety of reinforcing applications, meets all applicable government and industry specifications and is available in production quantities.



Textron's Boron filament production facility is capable of manufacturing 35,000 lbs/yr. of filament and over 50,000 lbs/yr. of Boron/Epoxy tape.

Here, exceptionally strong, lightweight boron filament is being produced by a chemical vapor deposition process using a fine tungsten wire as the substrate and boron trichloride gas as the boron source.

### TEXTRON BORON CHARACTERISTICS

Tensile Strength	520 ksi (3600 MPa)
Modulus	$58 \times 10^6$ psi (400 GPA)
Coefficient of Thermal Expansion	2.5 PPM/°F (4.5 PPM/°C)
Hardness (Knoop)	3200
Density*	0.093 lb/in <sup>3</sup> (2.57 g/cm <sup>3</sup> )

\*Density of 4.0 mil fiber.

Density of 5.6 mil diameter fiber is .090 lbm/in<sup>3</sup> (2.50 g/cm<sup>3</sup>).

## **TEXTRON SILICON CARBIDE FIBER**

Textron has developed a silicon carbide fiber for high performance composites in both metal ceramic and polymer matrix composites.

Silicon carbide offers the advantages of:

- Low cost
- High strength
- High heat resistance (up to 1200°C)
- Low electrical conductivity
- Corrosion resistance/chemical stability
- Wettability for metals
- Compatibility in plastics

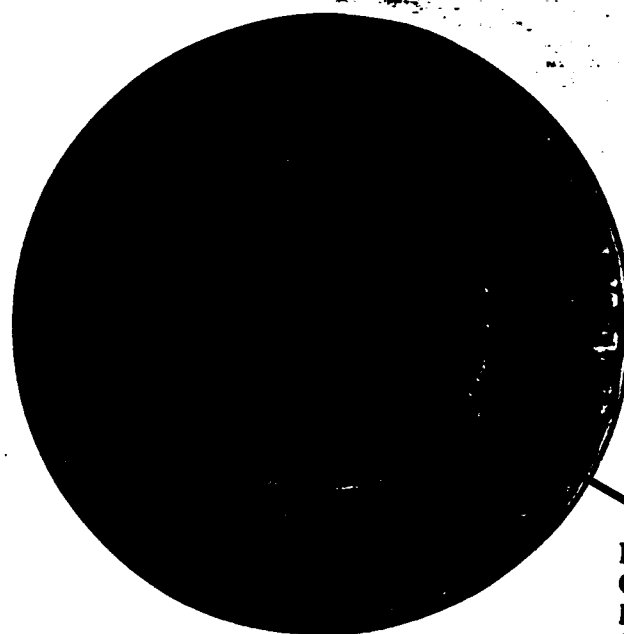
Aluminum composites fabricated by casting and hot molding have full translation of fiber properties. Textron is developing components for aircraft, helicopter, missile, bridge structures, gun barrels and projectile munitions.

Titanium composites are being developed for gas turbine engine fan blades, drive shafts hypervelocity vehicles (NASP), aircraft landing gears and missile structures. Silicon carbide fibers have maintained properties subsequent to the rigorous superplastic forming processes.

Epoxy/silicon carbide composites possess compressive strength twice that of epoxy/graphite.

The excellent wettability and oxidative resistance of silicon carbide makes it an excellent candidate for polyimides, ceramics and magnesium.

# CONTINUOUS SILICON CARBIDE FILAMENT



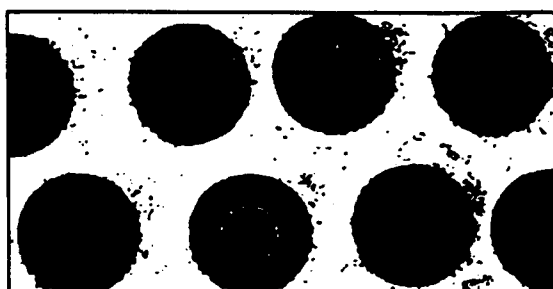
LOW COST  
CARBON  
MONOFILAMENT  
SUBSTRATE

## ■ CVD Silicon Carbide Filament

Textron has developed a Silicon Carbide (SCS) filament for the reinforcement of metal matrix composites. This Silicon Carbide filament is cost effective and is compatible with high temperature processing in aluminum and titanium.

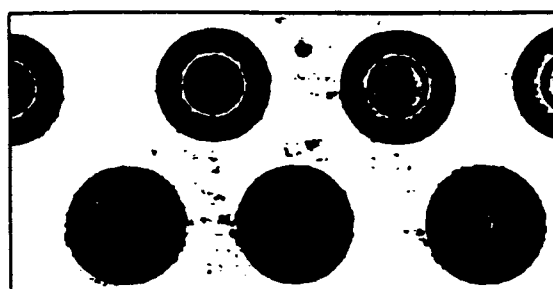
## FILAMENT PROPERTIES

■ Diameter	5.6 mils	140 $\mu$ m
■ Tensile Strength	500 + ksi	3450 MPa
■ Modulus	58 msi	400 GPa
■ Density	.11 lb/in <sup>3</sup>	3.0 gm/cc



### HOT MOLDED SILICON CARBIDE ALUMINUM

■ 48% Fiber Volume
■ 6061 Aluminum
■ Density .103 lb/in <sup>3</sup> 2.84 gm/cc



### HOT PRESSED SILICON CARBIDE TITANIUM

■ 35% Fiber Volume
■ 6AL-4V Titanium
■ Density .14 lb/in <sup>3</sup> 3.86 gm/cc

### R.T., 0°, LAMINATE TYPICAL TEST DATA

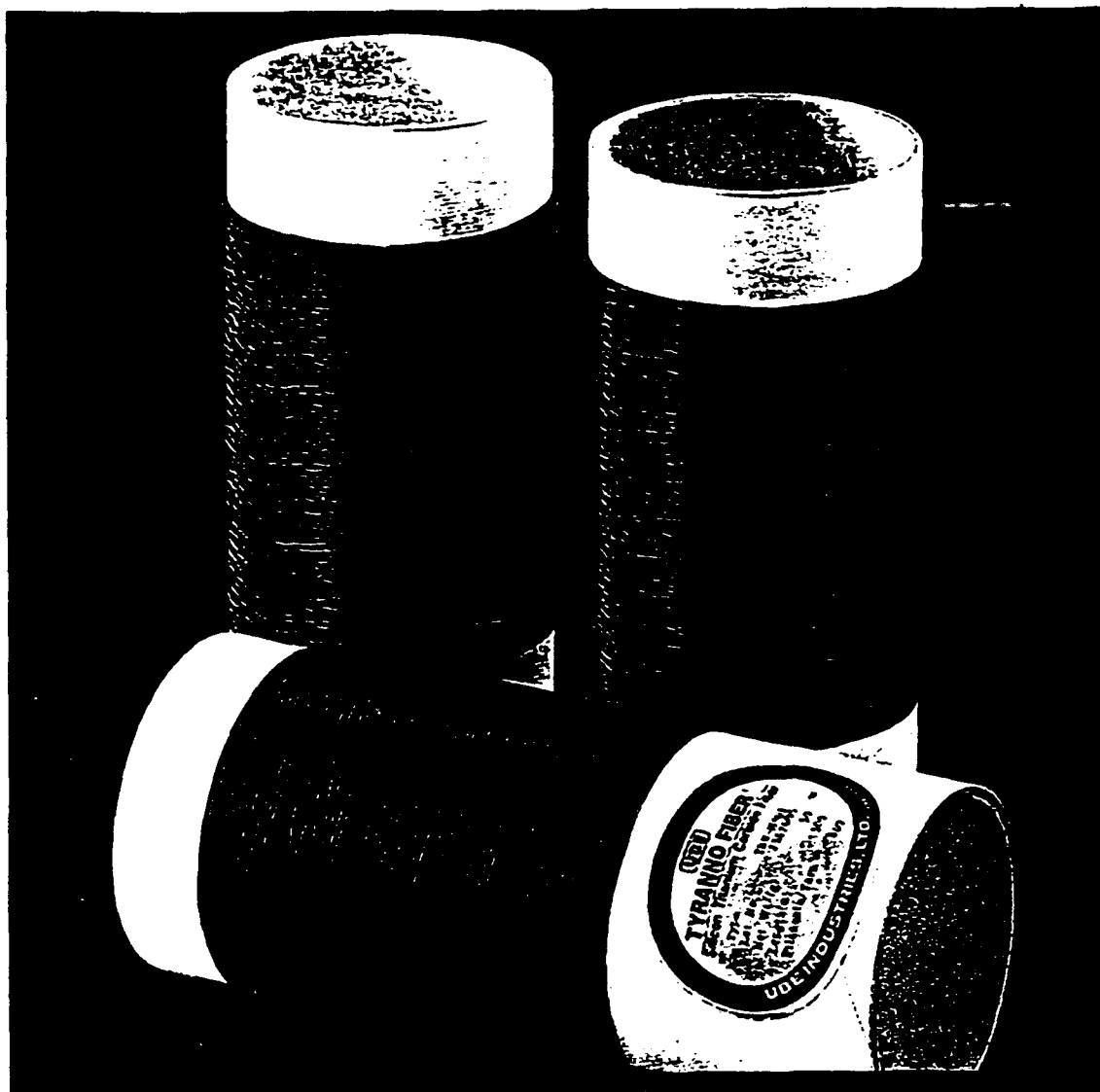
0° Tensile Strength	225 ksi	1550 MPa
0° Tensile Modulus	28 msi	193 GPa
90° Tensile Strength	12 ksi	83 MPa

### R.T., 0°, LAMINATE TYPICAL TEST DATA

0° Tensile Strength	250 ksi	1725 MPa
0° Tensile Modulus	28 msi	193 GPa
90° Tensile Strength	60 ksi	415 MPa

## TYRANNO FIBER®

8/91



■ Textron Specialty Materials is the exclusive distributor of TYRANNO FIBER® developed by Ube Industries, Ltd. of Tokyo, Japan.

Ube's new TYRANNO FIBER is a highly effective reinforcement for plastic, metal, and ceramic matrix composites. This continuous, inorganic fiber is made from organometallic polymers, yielding a composition of silicon, titanium, carbon and oxygen. Because of its high tensile strength, high modulus, and excellent high temperature resistance, it offers tremendous potential for applications in aerospace and sporting goods.

**TEXTRON** Specialty Materials

**UBE**

**TYRANNO FIBER\*****PRODUCTS AVAILABLE****FROM TEXTRON****SPECIALTY****MATERIALS****TYPICAL PROPERTIES OF TYRANNO FIBER**

Filament Diameter	*8.5 ± 0.5 microns, 10.5 ± 0.5 microns
Filaments/Yarn	400, 800, *1600, 3200, 6400
Density	2.37 g/cm <sup>3</sup> (0.086 lbs/in <sup>3</sup> )
Tensile Strength	2.9 GPa (420 ksi)
Tensile Modulus	190 GPa (28 msi)
Tensile Strain to Failure	1.4 to 1.5%
Electrical Resistivity	10 <sup>3</sup> ohm-cm
Thermal Expansion Coefficient (along fiber axis 0-500°C)	3.1 × 10 <sup>-6</sup> /°C
Specific Heat	0.19 cal/deg (60°C), 0.28 cal/deg (400°C)
Heat Resistance (more than 95% strength remains after 6 hours exposure)	1300°C (in N <sub>2</sub> gas), 1000°C (in Air)

\*STANDARD FORM

**FABRICS****FLAT FABRICS****TUBE SHAPED FABRICS****3-D CUBE**

Plain Weave  
Satin Weave  
Braided Tubes, Sleeves, Ropes

270 g/m<sup>2</sup>  
Various densities

1 meter by desired length  
1 meter by desired length  
Special Order

**HYBRID FIBERS**

• FINE CERAMIC  
PULVERIZED  
POWDER  
COMPOSITES



• CERAMIC  
WHISKER  
COMPOSITES

■ Standard Fiber—200 gram spools (1000 meters)

Other Fibers

- Varied Electrical Resistivity Fibers
- Hybrid Fibers
- Chopped Fibers

- High (10<sup>7</sup> ohm-cm) to low (10<sup>9</sup> ohm-cm)
- With whiskers or powders
- Various lengths and electrical resistivities

**For additional assistance, contact:**

Tom Foltz (technical and product form) (508) 454-5341 Mike Corcoran (price and availability) (508) 454-5487

Textron Specialty Materials, 2 Industrial Avenue, Lowell, MA 01851 TEL (508) 452-8961 FAX (508) 454-5619

**NEXTEL 312 CERAMIC FIBERS**  
**TYPICAL PROPERTIES**

**Physical Properties**

Composition	62% Al <sub>2</sub> O <sub>3</sub> , 24% SiO <sub>2</sub> , 14% B <sub>2</sub> O <sub>3</sub>
Color	White
Length	Continuous
Fiber Density	2.7 gm/cc
Fiber Diameter	10-12 micron
Surface Area	<1 m <sup>2</sup> /gm*

**Mechanical Properties**

Tensile Strength	1725 MPa (250,000 psi)
Tensile Modulus	138 GPa (20 x 10 <sup>6</sup> psi)
Elongation	1.2%

**Thermal Properties**

Continuous Use Temperature	1204°C (2200°F)
Short Use Temperature	1371°C (2500°F)
Lineal Shrinkage 2000°F (1093°C)	1.25%
Melting Point	1800°C (3272°F)
Thermal Expansion Coefficient	
25-500°C	3.0 x 10 <sup>-6</sup> ΔL/L/°C
Specific Heat	0.25 BTU/lb/°F or Cal/gm/°C

**Electrical Properties**

Dielectric Constant	5.2 @ 9.375 x 10 <sup>9</sup> hertz
---------------------	-------------------------------------

**Optical Properties**

Refractive Index	1.570
------------------	-------

Above data is based on averages.

\* Inquire about enhanced surface area.



**NEXTEL™ CERAMIC FIBER  
TECHNICAL DATA**

**NEXTEL 440 CERAMIC FIBERS  
TYPICAL PROPERTIES**

**Physical Properties**

Composition	70% Al <sub>2</sub> O <sub>3</sub> , 28% SiO <sub>2</sub> , 2% B <sub>2</sub> O <sub>3</sub>
Color-as supplied	Coral*
-at temperature	White
Length	Continuous
Fiber Density	3.05 gm/cc
Fiber Diameter	10-12 micron
Surface Area	<0.2 m <sup>2</sup> /gm

**Mechanical Properties**

Tensile Strength	2070 MPa (300,000 psi)
Tensile Modulus	186.3 GPa (27 x 10 <sup>6</sup> psi )
Elongation	1.1%

**Thermal Properties**

Continuous Use Temperature	1371°C (2500°F )
Short Use Temperature	1649°C (3000°F)
Lineal Shrinkage 2900°F	< 1%
Melting Point	1800°C (3272°F)
Thermal Expansion Coefficient	
25-500°C	4.38 x 10 <sup>-6</sup> ΔL/L/°C
25-1000°C	4.99 x 10 <sup>-6</sup> ΔL/L/°C
Specific Heat (500°C)	0.27 (Cal/gm°C) or BTU/lb°F)

**Electrical Properties**

Dielectric Constant	5.7 @ 9.375 x 10 <sup>9</sup> hertz
Loss Tangent (10 GHz)	0.015

**Optical Properties**

Refractive Index	1.616
------------------	-------

\*Nextel 440 fibers are color coded in the sizing to distinguish them from Nextel 312 fibers.  
All data is based on averages

# NEW ASTROQUARTZ® II

## A BETTER SOLUTION TO HIGH-HEAT HIGH-STRENGTH PROBLEMS.

**Its strength is in numbers.**

Astroquartz II and original Astroquartz are composed of identical raw materials. Through improved manufacturing and handling techniques, however, Astroquartz II represents a stronger, cleaner product with unparalleled quality, standards and specifications. Such innovation, for which Stevens has long been known, gives new flexibility to your design opportunities.

### Physical and Mechanical Properties

With a tensile strength of 500,000 psi, Astroquartz II has a higher strength-to-weight ratio than virtually all other high temperature materials.

Because of its low coefficient of linear expansion, Astroquartz II offers great dimensional stability. Fibers are flexible, and function well in applications subject to torsion and

PHYSICAL PROPERTIES OF FIBERS	
Filament diameter	
yarn and fabric	0.00035 in. (9 microns)
Filament tensile strength	
at room temperature (psi)	500 x 10 <sup>6</sup>
Specific gravity	2.2
Hardness (Mohs' scale)	5-6
Young's modulus	10 x 10 <sup>6</sup>
Poisson's ratio	0.17

flexing. Astroquartz II is transparent to ultraviolet radiation in the 2,000A and upwards range. It does not form paramagnetic centers, nor does it capture neutrons in high energy applications. Astroquartz II is an excellent electrical insulator, and retains these properties at high temperatures.

### DATA SUMMARY OF PURE FUSED SILICA<sup>(1)(2)</sup>

<b>Mechanical Properties</b>		<b>Thermal Properties</b>		<b>Electrical Properties</b>		<b>Dielectric strength</b>	
Density (grams/cc)	2.20	at 20°C	CGS	Resistivity at 20°C	Ω x cm	at 20°C	kV/cm
Hardness (Mohs' scale)	5-6	Stress point	log η = 14.6	at 800°C	Ω x cm	Loss factor at	250/400
Poisson's ratio	0.17	Annealing point	log η = 13	Dielectric constant	2 x 10 <sup>9</sup> (approx.)	20°C, 1 MHz	1 x 10 <sup>-4</sup>
Young's modulus	daN/cm <sup>2</sup> 6.2 - 7.2 x 10 <sup>6</sup>	Softening point	log η = 7.6	at 20°C, 1 MHz	3.78	Power factor at	2 x 10 <sup>-4</sup>
Breaking stress tensile	daN/cm <sup>2</sup> 500,000					Optical Data	
<b>Thermal Properties</b>						Refractive index at 15°C	n <sub>D</sub> 1.4585
Mean coefficient of linear expansion 0 - 1,000°C per °C	0.54 x 10 <sup>-6</sup>					Dispersion	n <sub>C</sub> - n <sub>F</sub> 0.0067
Mean specific heat, 0 - 500°C	cal/g°C 0.230					Chemical Data	
						SiO <sub>2</sub> content	% 99.99

(1) Cf. Technical leaflet S 1: "Transparent pure fused quartz." (2) The values shown relate to solid test pieces.

### Chemical Properties

Astroquartz II fibers (identical to Astroquartz) are chemically stable. They are water-insoluble, imputrescible and non-hygroscopic. Halogens, common acids in either liquid or gaseous form, have no effect on Astroquartz II with the exception of hydrofluoric and hot phosphoric acids. Astroquartz II should not be used in environments where strong concentrations of alkalis are present.

### TYPICAL CHEMICAL ANALYSIS OF ASTROQUARTZ II

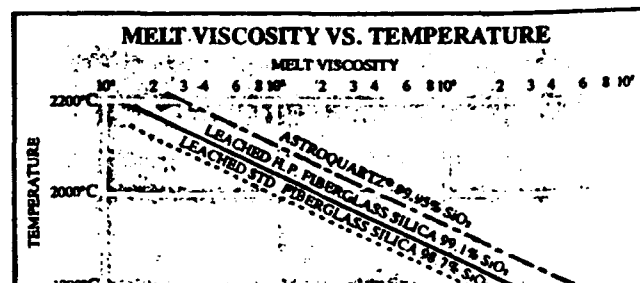
Element	exclusive of binders	
SiO <sub>2</sub>	99.99	
Phosphorous	ppm	3
Sodium	ppm	3.4
Potassium	ppm	2.4
Lithium	ppm	1.2
Boron	ppm	< 5
Calcium	ppm	2.8
Magnesium	ppm	2
SrO <sub>2</sub>	ppm	< 1
Iron	ppm	3.5
Titanium	ppm	< 4
Aluminum	ppm	20-30
Manganese	ppm	2
Copper	ppm	1
Cadmium	ppm	2.2
Antimony	ppm	5
Chromium	ppm	2.5

> GREATER THAN < LESS THAN ≤ LESS THAN OR EQUAL TO

### Thermal Properties

Astroquartz II can be used at temperatures much higher than either "E" glass or "S" glass fiber, up to 1,050°C. Above this temperature slow devitrification or crystallization occurs with the loss of flexible mechanical properties. Repeatedly varied temperatures and various impurities, especially alkalis, may promote devitrification at somewhat lower temperatures.

Astroquartz II fiber softens at approximately 1,300°C but never liquifies. Volatilization begins near 2,000°C. Because of their very high melt viscosity, Astroquartz products are often used in ablative composites.



# STEVENS ASTROQUARTZ® II

## ASTROQUARTZ® II YARN

---

### TECHNICAL DATA

---

#### ASTROQUARTZ® II YARN

ASTROQUARTZ® II yarn is made from high purity, extremely fine continuous filaments of pure fused silica which exhibits excellent refractory properties and is capable of extended exposure to 2000°F. Fiber composition is 99.90% SiO<sub>2</sub> (silica) exclusive of binder.

ASTROQUARTZ® II yarn, with more than five times the yield of high silica leached yarn, has higher tensile strength and abrasion resistance. As a result, high production efficiencies are now possible in the production of high temperature flexible insulation.

ASTROQUARTZ® II yarn, because of its high purity, high temperature resistance, excellent electrical properties and low density, is widely used in the form of braided insulation in thermocouple wire, coaxial cables, space separators, hoop-wire and heating elements. It has proven to be far superior in physical property characteristics when compared to the comparatively thick, low strength high silica leached yarns.

#### ASTROQUARTZ® II YARN PROPERTY DATA

TYPE	APPROXIMATE DIAMETER	APPROXIMATE BREAKING STRENGTH*	APPROXIMATE YIELD
300 2/0	0.008"	3.0 lb.	15,000 yds/lb.
300 2/2	0.012"	6.0 lb.	7,500 yds/lb.
300 2/4	0.018"	10.0 lb.	3,750 yds/lb.
300 2/8	0.020"	24.0 lb.	1,875 yds/lb.

These yarns are available with 9779 binder system which is compatible with phenolic, epoxy, and some polyimide resins.

ALL STATEMENTS HEREIN ARE EXPRESSIONS OF OPINION WHICH WE BELIEVE TO BE ACCURATE AND RELIABLE BUT ARE PRESENTED WITHOUT GUARANTEE OR RESPONSIBILITY ON OUR PART. STATEMENTS CONCERNING POSSIBLE USE OF OUR PRODUCTS ARE NOT INTENDED AS RECOMMENDATIONS FOR THEIR USE IN THE INFRINGEMENT OF ANY PATENT. NO PATENT WARRANTY OF ANY KIND EXPRESS OR IMPLIED IS MADE OR INTENDED.

---

For further information write to: J.P. STEVENS & CO., INC. • INDUSTRIAL PRODUCTS GROUP  
33 STEVENS ST., P.O. BOX 208 • GREENVILLE, S.C. 29602

ASTROQUARTZ® II yarn of heavier counts can also be manufactured. Please consult us for price and delivery.

\* Tested in accordance with ASTM Test Method D-578.

PRICE LIST  
ASTROQUARTZ® II YARN

<u>POUNDS</u>	<u>PRICE PER POUND</u>
1-10	\$105.00
11-99	\$ 91.00
100-999	\$ 82.00
1000-Over	For requirements of 1000 pounds or more, please ask for quote.

NOTE: Above prices are for the standard yarns tabulated under Property Data and finished with 9779 binder. Please consult us for availability and prices for heavier yarns and/or special finishes. Minimum quantity on special finishes will be twenty-two pounds unless the finish is available from stock.

PACKAGE INFORMATION

Yarns are available on standard milk bottle packages for the piled yarns and double flanged packages for the twisted single yarn; with net yarn weights ranging from a minimum of 1 pound to a maximum of 2.5 lb/package.

NOTE: A special braiding package of I.D. 5/8", length 4-1/4" with a straight or pineapple build is available, with a net yarn weight of either 1/8 lb. or 1/4 lb. This package is suitable for both Wardwell and Butt braiders. This special package is available on a "made to order" basis. Please consult us for price and delivery.

ALL SALES OF STEVENS' PRODUCTS ARE SUBJECT TO THE TERMS AND CONDITIONS OF STEVENS' STANDARD CONFIRMATION OF ORDER.  
ALL ORDERS SUBJECT TO ACCEPTANCE AT GREENVILLE OFFICE.

ALL STATEMENTS HEREIN ARE EXPRESSIONS OF OPINION WHICH WE BELIEVE TO BE ACCURATE AND RELIABLE BUT ARE PRESENTED WITHOUT GUARANTEE OR RESPONSIBILITY ON OUR PART. STATEMENTS CONCERNING POSSIBLE USE OF OUR PRODUCTS ARE NOT INTENDED AS RECOMMENDATIONS FOR THEIR USE IN THE INFRINGEMENT OF ANY PATENT. NO PATENT WARRANTY OF ANY KIND, EXPRESS OR IMPLIED, IS MADE OR INTENDED.

For further information write to: J.P. STEVENS & CO., INC. • INDUSTRIAL PRODUCTS GROUP  
33 STEVENS ST., P. O. BOX 206 • GREENVILLE, S.C. 29602  
TELEPHONE (803) 879-9091 OR (803) 239-4828

## ASTROQUARTZ® II FIBER CHARACTERISTICS

### Number of filaments:

1. 300 1/0 - 120 filaments
2. 300 2/0 - 240 filaments
3. 300 2/2 - 480 filaments

### Fiber diameter in microns:

Each filament is 9 microns in diameter  
This is equivalent in diameter to a  
fiberglass G filament.

### TERMS OF SALE

PRICE: All prices shall be subject to change without notice.  
The effective date of a price change shall be the date  
stated on the Corporation's applicable price sheet.

OFFERING: Made subject to general terms and conditions of sale.

TERMS: Net 30 Days

FREIGHT: F.O.B. Slater, S.C.

MINIMUM ORDER: 1 kg or 2.2 lbs + 10% if available from stock  
10 kg + 10% if it is a special order.

ALL SALES OF STEVENS' PRODUCTS ARE SUBJECT TO THE TERMS AND CONDITIONS OF STEVENS' STANDARD CONFIRMATION OF ORDER  
ALL ORDERS SUBJECT TO ACCEPTANCE AT GREENVILLE OFFICE.

ALL STATEMENTS HEREIN ARE EXPRESSIONS OF OPINION WHICH WE BELIEVE TO BE ACCURATE AND RELIABLE BUT ARE PRESENTED WITHOUT GUARANTEE  
OR RESPONSIBILITY ON OUR PART. STATEMENTS CONCERNING POSSIBLE USE OF OUR PRODUCTS ARE NOT INTENDED AS RECOMMENDATIONS FOR THEIR  
USE IN THE INFRINGEMENT OF ANY PATENT. NO PATENT WARRANTY OF ANY KIND, EXPRESS OR IMPLIED, IS MADE OR INTENDED.

For further information write to: **J.P. STEVENS & CO., INC. • INDUSTRIAL PRODUCTS GROUP**  
1/1/85 **33 STEVENS ST., P. O. BOX 208 • GREENVILLE, S.C. 29602**  
2100-32 **TELEPHONE (803) 879-9091 OR (803) 239-4828**

4/91



## Preliminary Technical Data

**TONEN CORPORATION**  
1-1-1 HITOTSUBASHI, CHIYODA-KU,  
TOKYO, 100 JAPAN

### High Purity Silicon Nitride Fiber

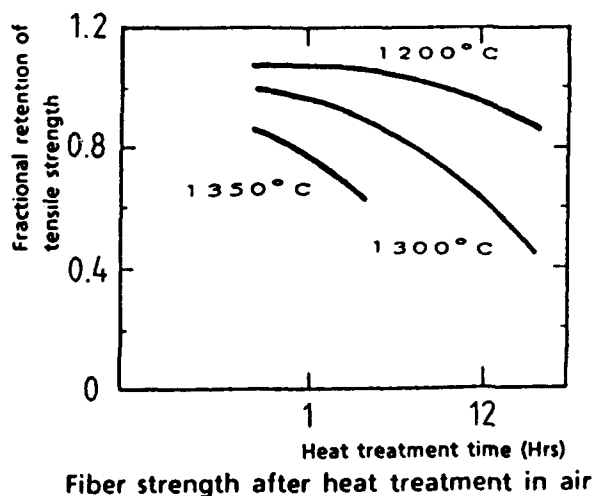
Pure silicon nitride fibers are produced from our polymer material, TONEN polysilazane, through a spinning and pyrolyzing process. The high strength and high modulus continuous fibers, because of their extremely high purity, exhibit superior heat and oxidation resistivity and high corrosion resistance to molten metal.

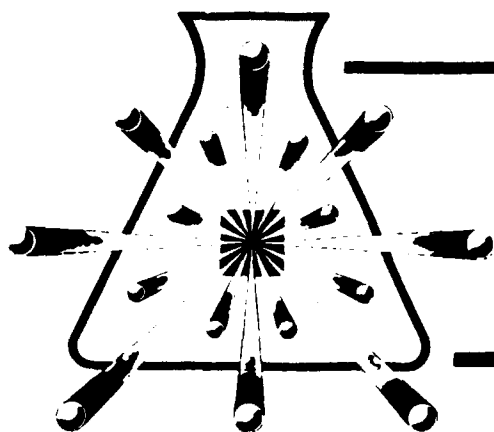
#### Typical Properties

Tensile Strength	2.5	GPa
Tensile Modulus	250	GPa
Density	2.5	g/cm <sup>3</sup>
Diameter	10	μm
Elongation	1.0	%
CTE	1.5	× 10 <sup>-6</sup> /°c
Thermal Conductivity	7.1	Kcal/mh°c
Specific Heat	0.185	cal/g°c
Electrical Resistivity	5.0	× 10 <sup>14</sup> Ωcm
Dielectric Constant at 1 MHz	4.5	
Composition	Si N O C	59.8 37.1 2.7 0.4 wt %
Crystal Structure	Amorphous	

#### Features

- ▶ High strength, high modulus
- ▶ Superior heat and oxidation resistivity
- ▶ High corrosion resistance to molten metal
- ▶ Electrical insulating
- ▶ Low dielectric constant





## DEVELOPMENTAL HIGH PERFORMANCE CERAMIC FIBERS

### DESCRIPTION

Silicon nitride and silicon-nitrogen-carbon fibers are made from ceramic precursors. Fibers are low in oxygen and are more thermally stable than commercially available ceramic fibers.

### TYPICAL FIBER PROPERTIES

PROPERTY	DEVELOPMENTAL FIBER TYPE		COMMERCIAL SILICON-BASED FIBERS	
	SI-C-N	Si <sub>3</sub> N <sub>4</sub>	I	II
Composition (Wt %)				
Silicon	55.8	58.8	55.5	NA
Nitrogen	27.8	40.9	-	NA
Carbon	14.8	0.4	28.4	NA
Oxygen	2.1	2.0	14.9	NA
Room Temperature Tensile Strength (ksi)				
Before Aging	460±150	210±110	340±100	400
After 50 Hours in Air at 1300°C	220±60	Poor	—Disintegrated—	
Modulus (Msi)	33±9	20	28	28
Diameter (Microns)	28±5	34±5	15	10
Density (g/cc)	2.5	2.2	2.6	2.4

#### NOTE:

Test specimens for tensile test are 1-in. long. Modulus is approximate and is determined from crosshead displacement and tensile strength.

### HANDLING AND STORAGE

Storage conditions have not been established, but no special conditions are anticipated.

### TOXICOLOGY

Not expected to produce any toxicological effects. Exercise ordinary care and personal cleanliness while handling.

The information presented herein is believed to be accurate and reliable, but is presented without guarantee or responsibility on the part of Ethyl Corporation. Further, nothing contained herein shall be taken as an inducement or recommendation to manufacture or use any of the herein described materials or processes in violation of existing or future patents.

Commercial Development Division  
Ethyl Corporation Telephone: 504/388-7803  
Ethyl Tower Telex 586441  
451 Florida Street  
Baton Rouge, Louisiana 70801

B-21



5/91

# Information About NICALON™ Ceramic Fiber

DOW CORNING

## DESCRIPTION

NICALON™ ceramic fiber is a silicon carbide ceramic fiber manufactured through a polymer pyrolysis process by Nippon Carbon Co., Ltd., of Japan. The fiber is homogeneously composed of ultrafine beta-SiC crystals with excess carbon and 9 to 11 percent oxygen (as SiO<sub>2</sub>). The fiber has excellent strength and modulus properties and retains its properties at high temperatures. NICALON ceramic fiber is highly resistant to oxidation and to chemical attack.

NICALON ceramic fiber is available in a variety of electrical grades, product forms, fiber denier options and surface treatment options, depending on its intended use.

## USES

NICALON ceramic fiber can be used as a reinforcement for plastic, ceramic and metal matrices to produce high-performance composite materials. Surface treatments or coatings are normally recommended to facilitate processing and to maximize composite performance. NICALON ceramic fiber can also be used to form fibrous products, such as high-temperature insulation, belting, gaskets and curtains. Its resistance to chemical attack allows it to be used in highly corrosive environments.

## PRODUCT AVAILABILITY

NICALON ceramic fiber products are available in a wide variety of grades, types and forms to accommodate a broad range of application requirements.

## NICALON™ CERAMIC FIBER (Ceramic Grade, HVR Grade, and LVR Grade)

Type	Multifilament, textile-grade silicon carbide fiber
Color	Black
Physical Forms	Continuous, multifilament tow; chopped fiber; woven cloth
Fiber Denier	600, 900, 1200 and 1800
Surface Sizings	Various
Special Properties	High strength and modulus; high-temperature stability; tailorable electrical properties; weaveable
Primary Uses	Reinforcement in plastic, ceramic and metal matrix composites; high-temperature insulation and materials handling

FIL. DIA. : 12, 15μ

## TYPICAL PROPERTIES

These values are not intended for use in preparing specifications.

	Ceramic Grade	HVR Grade	LVR Grade
Fiber Denier	600, 900, 1200 and 1800	1800	1800
Density, g/cm <sup>3</sup>	2.55	2.32	2.45 to 2.55
Tensile Strength, Ksi	430	425	430
Tensile Modulus, Msi	28	27	28
Strain to Failure, average percent	1.5	1.6	1.5
Volume Resistivity, ohm-cm.	10 <sup>9</sup>	>10 <sup>9</sup>	0.5 to 5.0
Dielectric Constant	9.2	6.4	—
Thermal Conductivity, Kcal/mhr °C, along fiber axis at room temperature	10	—	—
Coefficient of Thermal Expansion, °C <sup>-1</sup> , along fiber axis, 0 to 900 C (32 to 1652 F)	4.0 × 10 <sup>-6</sup>	—	—
Specific Heat, J/g °C	1.14	1.14	—
Thermal Conductivity, Kcal/mhr °C	10	—	—

Specification Writers: Please contact Dow Corning Corporation, Midland, Michigan, before writing specifications on these products.

™Trademark of Nippon Carbon Co., Ltd., of Japan.



## Product Grades

NICALON ceramic fiber is available in three different grades, differentiated primarily by their electrical properties:

**Ceramic grade (CG)** – The standard grade of the NICALON ceramic fiber product line; offers optimum mechanical properties and high-temperature performance.

**HVR grade** – A low dielectric fiber (high volume resistivity) that is designed to offer an optimum balance of mechanical and electrical properties in composite dielectric structures.

**LVR grade** – A higher conductivity fiber (low volume resistivity) that is designed to offer tailored levels of fiber conductivity. This grade is useful in the design of graded dielectric structures and for high voltage cable constructions. LVR NICALON ceramic fiber can be tailored to desired volume resistivity ranges. Contact Dow Corning Corporation to discuss specific product requirements.

## Product Forms

NICALON ceramic fiber is available in several physical forms, surface treatments and denier options to offer the user maximum application flexibility.

**Continuous fiber** – Supplied as multifilament tow, spooled on 3-inch I.D. bobbins to a minimum 500-meter length, unspliced. Spool quantity will vary depending on fiber denier, as in Table IV.

**Chopped fiber** – Available as chopped multifilament yarn in 1-, 3-, 6- and 9-millimeter lengths. Packaged in individual 0.5-kilogram containers.

**Woven cloth** – Available in three standard weave styles, as shown in Table II. Woven cloth is supplied nominally as 1-meter-square, individually packaged pieces. However, continuous rolls of specified lengths and widths are available on a special order basis. Other weave styles also can be made available on a special order or toll-weaving basis. Contact Dow Corning to discuss specific needs.

**TABLE I: FIBER DENIER OPTIONS**

<u>Fiber Denier (Nominal)</u>	<u>Filaments/Tow (Nominal)</u>	<u>Filament Diameter (Nominal)</u>
1800	500	15 $\mu\text{m}$
1200	500	12 $\mu\text{m}$
900	250	15 $\mu\text{m}$
600	250	12 $\mu\text{m}$

**TABLE II: STANDARD WEAVE STYLES**

<u>Weave Style</u>	<u>Yarn Count</u>	<u>Areal Weight (for CG)</u>
Plain Weave	16/inch (warp) 16/inch (fill)	280 g/m <sup>2</sup>
8 Harness Satin	22/inch (warp) 22/inch (fill)	380 g/m <sup>2</sup>
12 Harness Satin	26/inch (warp) 26/inch (fill)	450 g/m <sup>2</sup>

**TABLE III: SURFACE TREATMENT OPTIONS**

<u>Designation</u>	<u>Type</u>	<u>Intended Use<sup>1</sup></u>
M-Sizing	Polyvinylacetate	CMC, MMC
PVA-Sizing	Polyvinyl Alcohol (Water Soluble)	CMC, MMC
P-Sizing	Modified Epoxy	PMC
DCC-1 Surface Treatment	Dow Corning Proprietary	PMC, Low-Temperature TS
DCC-2 Surface Treatment	Dow Corning Proprietary	PMC, High-Temperature TS and TP

<sup>1</sup>PMC = plastic matrix composite; CMC = ceramic matrix composite; MMC = metal matrix composite; TS = thermosets; TP = thermoplastics.

**TABLE IV: PACKAGE SIZES**

	<u>Standard Packaging</u>
Continuous Fiber, 3-inch I.D.	
1800 denier	0.1-kg spools
1200 denier	0.067-kg spools
900 denier	0.05-kg spools
600 denier	0.035-kg spools
Chopped Fiber (1-, 3-, 6- and 9-mm)	0.5-kg bags
Woven Cloth, all forms	1-m <sup>2</sup> pieces (continuous rolls of specified length also available on request)

## HOW TO USE

### Plastic Matrix Composites

NICALON ceramic fiber is suitable for incorporation into standard resin prepreg types and compositions, using conventional prepregging techniques. Unidirectional or oriented prepreg can be produced using the continuous fiber or woven cloth, respectively. Special fiber surface treatments are normally recommended (see Table III) to effect maximum property translation into the composite and to afford superior retention of composite properties under hot-wet conditions. Resin systems can include the entire range of available thermosets or thermoplastics.

### Ceramic Matrix Composites

NICALON ceramic fiber can be incorporated as the reinforcing phase into a variety of ceramic composite systems. Standard composite processing techniques, such as sol-gel processing, chemical vapor infiltration, or polymer infiltration, can be applied, depending on the user's needs and capabilities. Matrix candidates include silicon nitride, silicon carbide, alumina, glass and others. The specific grade and type of NICALON ceramic fiber, as well as specific processing techniques, are best determined by the user.

### Metal Matrix Composites

Chopped, woven or continuous NICALON ceramic fiber can serve as a reinforcing phase in metal matrix composite systems. Specific fiber types, grades and processing conditions are best determined by the user.

### Weaving and Braiding

As a textile-grade yarn, NICALON ceramic fiber can be readily incorporated into a wide variety of woven tapes and broadgoods, as well as braid. A broad network of weaving and braiding houses exists in

the United States to respond to specific requirements of the user. Please contact Dow Corning to discuss specific woven goods or braiding requirements.

### Caution

Precautions normally associated with the handling of inorganic fibers should be followed. Use of gloves and eye protection is recommended while handling NICALON ceramic fiber.

### STORAGE AND SHELF LIFE

When properly stored under normal storage conditions, NICALON ceramic fiber has an indefinite shelf life.

### SHIPPING LIMITATIONS

None.

### PACKAGING

NICALON ceramic fiber is available as continuous yarn, chopped fiber or woven cloth in the package sizes shown in Table IV.

### PRODUCT AVAILABILITY

NICALON ceramic fiber products described herein are available exclusively in North America from Dow Corning Corporation, Midland, Michigan. Dow Corning's distribution rights are restricted to the United States and Canada.

### ORDERING

For information, please contact:  
Dow Corning Corporation  
Customer Service Department  
Midland, Michigan 48686-0994  
1-800-248-2481

### MSDS INFORMATION

ATTENTION: PRODUCT SAFETY INFORMATION REQUIRED FOR SAFE USE IS NOT INCLUDED. BEFORE HANDLING, READ PRODUCT AND MATERIAL SAFETY DATA SHEETS AND

CONTAINER LABELS FOR SAFE USE, PHYSICAL AND HEALTH HAZARD INFORMATION. THE MATERIAL SAFETY DATA SHEET IS AVAILABLE FROM YOUR DOW CORNING REPRESENTATIVE, OR DISTRIBUTOR, OR BY WRITING TO DOW CORNING CUSTOMER SERVICE, OR BY CALLING 1-517-496-6000.

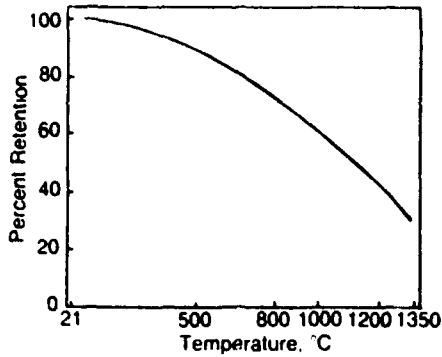
### WARRANTY INFORMATION - PLEASE READ CAREFULLY

Dow Corning believes that the information in this publication is an accurate description of the typical characteristics and/or uses of the product or products, but it is your responsibility to thoroughly test the product in your specific application to determine its performance, efficacy and safety.

Unless Dow Corning provides you with a specific written warranty of fitness for a particular use, Dow Corning's sole warranty is that the product or products will meet Dow Corning's then current sales specifications. **DOW CORNING SPECIFICALLY DISCLAIMS ANY OTHER EXPRESS OR IMPLIED WARRANTY, INCLUDING THE WARRANTIES OF MERCHANTABILITY AND OF FITNESS FOR USE.** Your exclusive remedy and Dow Corning's sole liability for breach of warranty is limited to refund of the purchase price or replacement of any product shown to be other than as warranted, and Dow Corning expressly disclaims any liability for incidental or consequential damages.

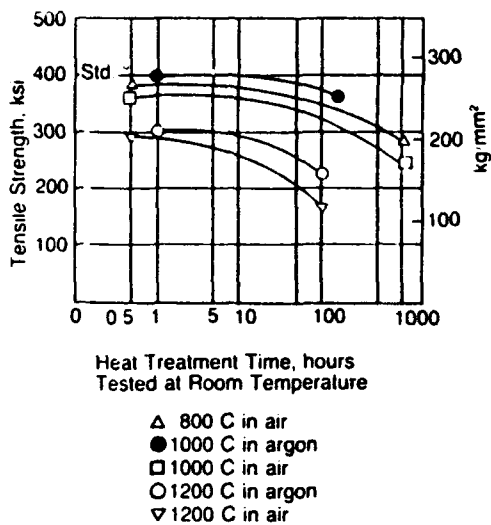
# FIGURE 1: THERMAL STABILITY

High Temperature Tensile Strength  
of NICALON Ceramic Fiber (per-  
cent retention of room temperature  
tensile strength)<sup>1</sup>



<sup>1</sup>Tensile strength measured at temperature in argon

## Tensile Strength of NICALON Ceramic Fiber After Heat Treatment



Heat Treatment Time, hours  
Tested at Room Temperature

- △ 800 C in air
- 1000 C in argon
- 1000 C in air
- 1200 C in argon
- ▽ 1200 C in air

BL37462

517/496-4000

**DOW CORNING CORPORATION**  
**MIDLAND, MICHIGAN 48686-0994**

"Dow Corning" is a registered trademark of Dow Corning Corporation.

Printed in U S A

Form No 19 073F-89

**DOW CORNING**

# new product information

5/91

## DOW CORNING® X9-6371 HPZ CERAMIC FIBER

### DESCRIPTION:

DOW CORNING® X9-6371 HPZ Ceramic Fiber is a textile grade inorganic silicon-carbonitride type fiber manufactured by Dow Corning Corporation in the U.S.A. by a polymer pyrolysis process. This fiber offers excellent tensile strength and modulus, as well as high volume resistivity. Related products with different combinations of modulus and electrical properties are being developed.

### INTENDED USES:

DOW CORNING X9-6371 HPZ Ceramic Fiber is intended as a reinforcement in high performance composites with plastic, ceramic, or metal matrices. It has a desirable combination of tensile, modulus, density and electrical properties, and retention of these properties at temperatures to 1400°C, which makes it suitable for a variety of applications in the aerospace industry.

### TYPICAL PROPERTIES:

These values are not intended for use in preparing specifications. This is a developmental product which is constantly undergoing improvement. Please contact Dow Corning for up-to-date information on properties.

Tow denier	1000/2000 g/9000 m
Filaments/tow	500/1000
Filament diameter	10 - 12 $\mu$ m
Density	2.3 - 2.5 g/cc
Tensile strength*	275 - 375 ksi
Tensile modulus*	22 - 30 Msi
Strain to failure	1 - 1.5%
Volume resistivity	$10^7 - 10^{13}$ ohm-cm
Dielectric constant	5.8 - 6.8
Coefficient of thermal expansion	$3 \times 10^{-6}$ per°C
Heat capacity	0.68 J/g C

\*Single filament testing at one inch gauge length, ASTM D-3379

**WARRANTY INFORMATION - PLEASE READ CAREFULLY.** Dow Corning believes that the information in this publication is an accurate description of the typical characteristics and/or uses of the product or products, but it is your responsibility to thoroughly test the product in your specific application to determine its performance, efficacy and safety.

**DOW CORNING CORPORATION, MIDLAND, MICHIGAN 48686-0994 TELEPHONE 517 496-4000**

NEW PRODUCT INFORMATION  
DOW CORNING X9-6371 HPZ CERAMIC FIBER  
Page 2

**FIBER CHARACTERISTICS:**

DOW CORNING X9-6371 HPZ Ceramic Fiber is prepared from hydridopolysilazane polymer by a pyrolytic process. The ceramic fiber is amorphous with a typical elemental composition of 57% silicon, 28% nitrogen, 10% carbon, and 4% oxygen, and has an oval cross-section.

A range of combinations of fiber properties can be produced. Most commonly available are a low modulus (~22 Msi tensile modulus, 2.3 g/cc density) and a standard modulus (~27 Msi tensile modulus, 2.4 g/cc density) grade.

This fiber is supplied with various surface treatments designed for optimum compatibility with various organic and inorganic matrix materials. The most commonly utilized sizing is polyvinyl alcohol (PVA) which has been found to be desirable to facilitate further handling such as weaving or braiding.

This textile grade fiber can also be supplied in woven cloth or braided forms; please inquire for specific details.

**STORAGE AND SHELF LIFE:**

DOW CORNING X9-6371 HPZ Ceramic Fiber does not deteriorate on storage and has an indefinite shelf life.

**SAFETY AND HANDLING PRECAUTIONS:**

Precautions normally associated with inorganic fibers of this type should be taken. The toxicological properties of fiber fragments or dusts produced during fiber (and composite) processing have not been thoroughly studied; hence exposure which might result in inhalation of such fibers or dusts should be eliminated by the use of appropriate ventilation or respirators. The fibers may be irritating to the skin, hence gloves are recommended. Safety glasses are also recommended.

**PACKAGING:**

DOW CORNING X9-6371 HPZ Ceramic Fiber is available as continuous yarn wound on 3" diameter bobbins. Typical weights per bobbin for various denier yarns are:

<u>Tow Denier</u>	<u>Bobbin Weight</u>	<u>Yarn Length Per Bobbin</u>	
1000	150 g	1350 m	(4430 ft.)
2000	300 g	1350 m	(4430 ft.)

NEW PRODUCT INFORMATION  
DOW CORNING X9-6371 HPZ CERAMIC FIBER  
Page 3

All bobbins are shipped in cardboard containers which protect the fiber from surface damage during shipping and storage. Fiber takeoff during use should be rolling rather than off-the-end to avoid damaging the ceramic fiber.

PRODUCT AVAILABILITY:

DOW CORNING X9-6371 HPZ Ceramic Fiber is an experimental product. It is available in pound quantities for evaluation purposes only in the United States at this time.

ADDITIONAL INFORMATION:

For additional information about this and related products, contact:

J. Donald Sheets  
Dow Corning Corporation  
Advanced Ceramics Program - Mail Stop 540  
Midland, Michigan 48686-0995  
Phone: 517-496-4814

WARRANTY INFORMATION  
PLEASE READ CAREFULLY:

Dow Corning believes that the information in this publication is an accurate description of the typical characteristics and/or uses of the product or products, but it is the user's responsibility to thoroughly test the product in specific applications to determine its performance, efficacy, and safety.

Unless Dow Corning provides a specific written warranty of fitness for a particular use, Dow Corning's sole warranty is that the product or products will meet Dow Corning's then current sales specifications. DOW CORNING SPECIFICALLY DISCLAIMS ANY OTHER EXPRESS OR IMPLIED WARRANTY, INCLUDING THE WARRANTIES OF MERCHANTABILITY AND OF FITNESS FOR USE. The exclusive remedy and Dow Corning's sole liability for breach of warranty is limited to refund of the purchase price or replacement of any product shown to be other than as warranted, and Dow Corning expressly disclaims any liability for incidental or consequential damages.

ACKNOWLEDGEMENT:

DOW CORNING X9-6371 HPZ Ceramic Fiber was developed with support from Air Force Contract F33615-83-C-5006, administered by the U.S. Air Force, Materials Laboratory, Processing and High Temperature Materials Branch, Wright Research and Development Center, funded by Defense Advanced Research Projects Agency, Materials Sciences Division.

X96371.RS:MISCFORMS

---

## **GLOSSARY**

---

### **NOMENCLATURE**

FURRAD	An Advanced Radiation Code Developed by MDSSC for ASR Analysis
AF	Air Force
APG	Advanced Power Group (formerly ASSG - Advanced Space Systems Group)
ASR	Advanced Survivable Radiator
BUCKL	An X-ray Deposition Code Developed by Sandia Laboratories
CDRL	Contract Data Requirement List
CRAD	Contracted Research and Development
CW	Continuous Wave
DoD	Department of Defense
E&TC	Engineering and Technology Center (formerly D&TC - Design and Technology Center)
IRAD	Independent Research and Development
KEW	Kinetic Energy Weapons
LANL	Los Alamos National Laboratory
MDSSC	McDonnell Douglas Space Systems Company
PCO	Program Contracting Officer
SDI	Strategic Defense Initiative
SOW	Satement of Work
STORMSL	An X-ray Deposition Code Developed by Sandia Laboratories
SUPER	Survivable Power
TCS	
WRDC	Wright Research and Development Center

### **English Symbols**

A	Surface Area of ASR or Base Radiator
A	
cal	Calories
cm	Centimeter
D	Fiber Diameter (mm) (lower case <u>d</u> also used)
F	
f	effective increase in heat transfer
G	
g	Gram
HF	High Frequency
I	Laser Intensity (W/cm <sup>2</sup> )
IR	Infrared
JCS	X-ray Hardness Level Mandated by the Joint Chiefs of Staff for Military Satellites
K	Degrees Kelvin
k	Fiber Thermal Conductivity (W/m-K)
kW-hr	Kilowatt Hours
L	Fiber Length (mm)
m	Meter
mg	Milligram

## **GLOSSARY**

mm	Milimeter
P	Fiber Separation (mm)
p	Insulation parameter between 0 and 1.
Q	Figure of Merit: Ratio of Heat Rejected by the ASR divided by the Heat Rejected by a Flat Plate Radiator; also Heat Flux (kW-hr)
R	Radius
s	
T	Temperature of Fiber or Base Material (K)
t	
Td	Optical Depth
W	Watts
z	Atomic Number
N	Conductance Parameter

### **Greek Symbols**

$\alpha$	Solar Absorptivity
$\Delta$	
$\delta T$	Effective Temperature Drop From the Radiator Surface to the Base of the Fibers
$\epsilon$	Emissivity
$\phi$	Incoming Ray Angle
$\eta$	Effective Fin Efficiency of the ASR Fibers
$\theta$	Angle of Incident Solar Radiation (degrees)
$\rho$	Reflectivity of Fiber or Base Material
$\sigma$	Stefan-Boltzmann Contant ( $5.667 \times 10^{-8} \text{ W/m}^2\text{-}^0\text{K}^4$ )
$\tau$	Transmissivity
$\omega$	Albedo

### **Subscripts**

0	
abs	Absolute
B	Base
base	Base Material
C	Conduction
cell	
e	
eff	Effective
i	
R	Radiation
s	Escape Path Length